BIOCHEMICAL CHARACTERIZATION OF HUMAN HEPARAN SULFATE 6-*O*-ENDOSULFATASE

Tanya Catherine Burch

A dissertation submitted to the faculty of the University of North Carolina at Chapel Hill in partial fulfillment of the requirements for the degree of Doctor of Philosophy in the School of Pharmacy (Medicinal Chemistry and Natural Products).

Chapel Hill
2008

Approved by:
Advisor: Jian Liu, Ph.D
Reader: Kenneth Bastow, Ph.D
Reader: Michael Jarstfer, Ph.D
Reader: Qisheng Zhang, Ph.D
Reader: Masahiko Negishi, Ph.D

ABSTRACT

TANYA BURCH: Biochemical Characterization of Human Heparan Sulfate 6-*O*-Endosulfatase

(Under the direction of Jian Liu)

Heparan sulfate (HS) is a complex and diverse polysaccharide abundantly found on the cell surface of cells from several different species. The HS biosynthetic machinery creates very heterogeneous structures that interact with a variety of proteins that result in important biological functions. In addition, HS can be remodeled in the extracellular matrix by a novel class of extracellular sulfatases (Sulfs) which selectively remove 6-*O*-sulfo groups from glucosamine residues within HS. The activities of Sulfs have been correlated with various biological activities relating to embryonic development and cancer. Therefore, understanding and utilizing Sulf activity can aid in understanding the structure-function relationship of HS as well as aid in developing and tailoring HS based therapies. The goals of this work were to investigate the substrate specificity of human 6-*O*-endosulfatase isoform 2 (HSulf-2) as well as to utilize HSulf-2 editing activity to tailor anticoagulant HS structures. The use of synthetic polysaccharides along with active HSulf-2 found in the conditioned medium of mammalian cells has allowed for the investigation of the substrate specificity of HSulf-2. Results demonstrated that HSulf-2 is selective toward 6-*O*-sulfo groups on glucosamine residues that are found in moderately and highly sulfated domains of HS. In addition, 2-*O*-sulfation of uronic acid and *N*-sulfation of glucosamine are necessary for serving as a substrate. Results also showed HSulf-2 can tailor HS anticoagulant structures and is capable of maintaining anticoagulant properties while reducing the binding of HS to

other proteins. The biochemical characterization of a human heparan sulfate 6-*O*-endosulfatase as described herein provides a novel method for determining the substrate specificity of HSulf-2. Because Sulf treated HS maintains excellent anticoagulant activity, results of my work open up a new approach to prepare anticoagulant HS with reduced side effects. The future development of this project could elucidate important structure-function relationships as well as become a valuable tool in drug discovery.

DEDICATION

To my parents, Ronald Wood and Alice Wood, and my in-laws, John A. Burch, Sr. and Josephine Burch, for giving me their love and support during my graduate school education.

To my husband, John A. Burch, Jr., who fully supported me through this arduous Ph.D process. If it had not been for you, the completion of this degree would not have been possible. You have been a consistent inspiration during the pursuit of my educational goals. Words cannot express how much I thank you.

ACKNOWLEDGEMENTS

I would like to express genuine gratitude to my advisor, Dr. Jian Liu, who has aided in my development as a scientist. He has provided me with excellent training, and I have learned a great deal during my graduate studies. Dr. Liu has gone the extra mile to provide me with advice and support during this process. He is also an excellent example of a scientist, and I hope to follow in his footsteps.

In addition, I would like to thank all of my lab mates (former and current) Dr. Suzanne Edavettal, Dr. Michael Duncan, Dr. Ronald Copeland, Dr. Jinghua Chen, Dr. Ding Xu, Danyin Song, Dr. Miao Chen, Renpeng Liu, and Ryan Bullis. Special thanks to lab mates Courtney Jones, Sherket Peterson, and Heather Bethea. Without your support and assistance, the completion of this degree would not have been possible.

TABLE OF CONTENTS

LIST OF FIGURES

Figure

LIST OF TABLES

Table

LIST OF ABBREVIATIONS

ACE	Affinity co-electrophoresis
AT	Antithrombin
BMP	Bone morphogenic protein
CDNS	Completely desulfated and *N*-sulfated
CHO	Chinese hamster ovary
CM	Conditioned medium
CS	Chondroitin sulfate
DEAE	Diethylaminoethyl
ECL	Enhanced chemiluminescent
ECM	Extracellular matrix
EXT	Exostosin
FGF	Fibroblast growth factor
GAG	Glycosaminoglycan
Gal	Galactose
GalNAc	*N*-acetyl galactosamine
GalT-I	Galactosyltransferase I
GalT-II	Galactosyltransferase II
GlcA	Glucuronic acid
GlcA2S	2-*O*-sulfated glucuronic acid
GlcAT-I	Glucuronyltransferase
GlcAT-II	Glucuronyltransferase II

GlcNAc	*N*-acetyl glucosamine
GlcNAcT-I	*N*-acetyl glucosaminyltransferase I
GlcNAcT-II	*N*-acetyl-glucosaminyltransferase II
GlcNS	*N*-sulfated glucosamine
G6S	Glucosamine 6-sulfate
GPI	Glycosylphosphatidylinositol
HA	Hyaluronic acid
HCl	Hydrochloric acid
HexA	Hexuronic acid
HIT	Heparin-induced thrombocytopenia
HP	Heparin
HPLC	High performance liquid chromatography
HS	Heparan sulfate
HSPG	Heparan sulfate proteoglycan
H_2SO_4	Sulfuric acid
HSulf	Human 6-*O*-endosulfatase
IdoA	Iduronic acid
IdoA2S	2-*O*-sulfated iduronic acid
IDS	Iduronate-2-sulfatase
IPTG	Isopropyl β-D-thiogalactopyranoside
K_d	Binding affinity
KH_2PO_4	Potassium phosphate
KS	Keratan sulfate

LMWH	Low molecular weight heparin
MBP	Maltose binding protein
MEF	murine embryonic fibroblast
MS	Mass spectroscopy
MSulf	Mouse 6-*O*-endosulfatase
NA	*N*-acetylated domain
NDST	*N*-deactylase/*N*-sulfotransferase
NS	*N*-sulfated domain
NST	*N*-sulfotransferase
PAMN HPLC	Polyamine high performance liquid chromatography
PAP	3'-phosphoadensine 5'-phosphate
PAPS	3'-phosphoadensine 5'-phosphosulfate
PF4	Platelet factor 4
PSB	5'-phosphate binding loop
QSulf	Quail 6-*O*-endosulfatase
RPIP	Reverse phase ion pairing
SDS-PAGE	Sodium dodecyl sulfate polyacrylamide gel electrophoresis
Ser	Serine
6-OST	6-*O*-sulfotransferase
Sulf	6-*O*-endosulfatase
3-OST	3-*O*-sulfotransferase
2-OST	2-*O*-sulfotransferase
UDP	Uridine diphosphate

UV	Ultraviolet
Wnt	Wingless
Xyl	Xylose
XylT	Xylosyltransferase

CHAPTER I

INTRODUCTION

Section I: Glycosaminoglycans

Macromolecules known as glycosaminoglycans (GAGs) are found in abundance on the cell surface and in the extracellular matrix (ECM). GAGs are predominately found on the cell surface attached to different core proteins in the form of proteoglycans. GAGs consist of linear, unbranched polysaccharides which bind to a variety of proteins such as growth factors, chemokines, and cytokines. These interactions lead to a wide range of biological events such as angiogenesis and lipoprotein metabolism in addition to viral entry and embryonic development (1-3). These polysaccharides consist of repeating disaccharide units. The repeating disaccharide units contain a uronic acid residue, which is either iduronic acid (IdoA) or glucuronic acid (GlcA), linked to either an *N*-acetyl galactosamine (GalNAc) or *N*-acetyl glucosamine (GlcNAc) residue. Hyaluronic acid, keratan sulfate, chondroitin sulfate, and heparin/heparan sulfate are four distinct classes of glycosaminoglycans (Figure 1). These GAGs are classified by their different repeating disaccharide units and arrangement of sulfations.

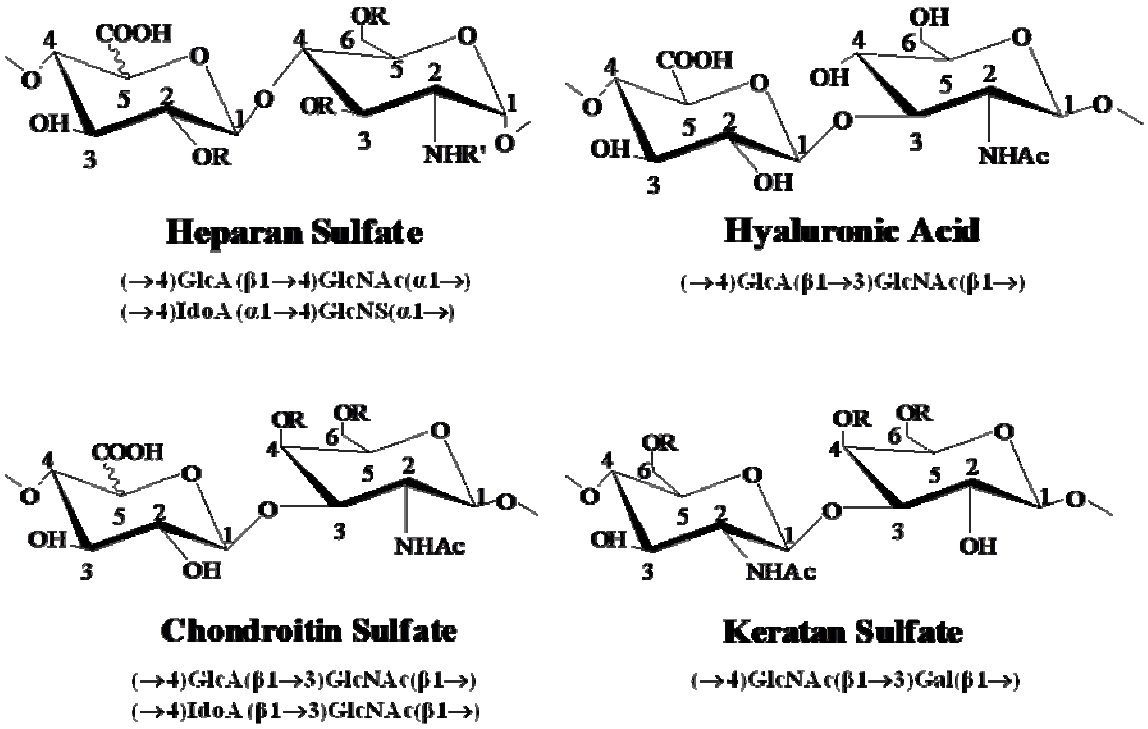

Figure 1. Repeating disaccharide units of glycosaminoglycans. R represents H or sulfate, and R' represents H, sulfate, or acetyl.

Hyaluronic Acid

Hyaluronic acid (HA), also known as hyaluronan or hyaluronate, is a highly viscous and compressible carbohydrate polymer widely known for its shock absorbing quality in synovial fluid, vitreous humor, and ECM loose connective tissues and joints (4). HA is a non-sulfated, non-epimerized GAG, which is neither covalently attached to a protein to form a proteoglycan nor is synthesized in the Golgi. It is a copolymer of glucuronic acid and glucosamine residues linked together via alternating β1, 3 and β1,4 linkages. It is synthesized directly into the ECM with an average molecular weight of 10^5 – 10^7 Da (5). In addition, HA has been approved for use in pre-operative and post-operative treatment in eye surgery, treatment of osteoarthritis of the knee, and is a common component of skin care products due to its wound healing and regenerative properties (*4, 6-8*). Studies suggest it plays a role in cell proliferation and migration as well as being an indicator for malignancy

and poor prognosis in prostate and breast cancer. HA has also been shown to aid in growth factor stimulation that facilitates angiogenesis (9).

Keratan Sulfate

Keratan sulfate (KS), also known as kertosulfate, is mainly found in cornea, cartilage, and bone (10). The main structure of KS consists of a copolymer of repeating galactose and *N*-acetyl glucosamine disaccharide units connected by alternating β1, 3 and β1, 4 linkages. KS is synthesized in the Golgi and is found in proteoglycan form. KS can vary in the degree of sulfation, and has a molecular weight ranging from 4×10^3 to 2×10^4 Da (10). In addition, it has been suggested that KS functions *in vivo* in embryogenesis, cartilage metabolism, and cancer invasion (11-13). Furthermore, it has been shown to have regenerative properties in wound healing and hydrating the cornea (10)

Chondroitin Sulfate

Chondroitin sulfate (CS) is found abundantly in the ECM of connective tissues and in the central nervous system (14). It is synthesized as a copolymer of repeating disaccharide residues of glucuronic or iduronic acid and *N*-acetyl galactosamine attached via alternating β1, 3 and β1, 4 linkages (Figure 1). Like heparan sulfate, CS is a structurally complex glycosaminoglycan. CS contains varying degrees of sulfation, and it can be divided into three distinct categories. Chondroitin sulfate A (CS-A) contains a galactosamine-4-*O*-sulfate, chondroitin sulfate B (CS-B), also known as dermatan sulfate (DS), contains a higher degree of IdoA residues, and chondroitin sulfate C (CS-C) contains galactosamine-6-*O*-sulfate (*14, 15*). They exist on the cell surface and in the extracellular matrix in the form of

proteoglycans, and can interact and modulate growth factors, cytokines, and chemokines (16). It has been implicated in the regulation and maintenance of cell proliferation, tissue morphogenesis, and displaying important roles in neural network formation in the developing mammalian brain (*14, 17*).

Section II: Structure and Biosynthesis of Heparin/Heparan Sulfate

Structure of Heparin vs. Heparan Sulfate

Heparan sulfate (HS) is a polysaccharide composed of 50 to 200 disaccharide units in length consisting of hexuronic acid (HexA) and *N*-acetyl glucosamine residues attached via alternating β1, 4 and α1, 4 linkages (Figure 1). The HexA can be either a GlcA or IdoA residue. HS is covalently attached to a core protein, and can be found on the cell surface and in the ECM. Studies of the past several decades have revealed that HS plays an important role in a variety of physiological processes.

Heparin (HP), a commonly administered anticoagulant drug, is a structural analog of HS. HP is a copolymer of repeating UA and GlcNAc residues. There are several noticeable differences between heparin and heparan sulfate. HS is common product of all mammalian cells while HP is an exclusive product of mast cells. Heparin contains a higher degree of sulfation and epimerization compared to HS, displaying extended repeating disaccharides of IdoA2S-GlcNS6S. On average 2.7 sulfate groups are present within disaccharide units of HP compared to an average of 0.6-1 sulfate groups present within the disaccharide units of HS (*18, 19*). HS displays a more diverse pattern of sulfation and epimerization, while containing heparin-like sequences within the polysaccharide chain. HS and HP isolated from natural sources contain monosaccharides present at various levels. Glucosamine residues commonly found in HS are either *N*-acetylated (GlcNAc) or *N*-sulfated (GlcNS). Only 1-7% of the glucosamine residues exist in the *N*-unsubstituted form ($GlcNH_2$) which allows HS to display primary amine groups (*18, 20*). 2-*O*-sulfated iduronic acid and 6-*O*-sulfated glucosamine are common monosaccharides found in HS, while 3-*O*-sulfated glucosamine and 2-*O*-sulfated glucuronic acid (GlcA2S) are rare monosaccharides found in HS (21).

NMR and molecular modeling studies reveal HP and HS display a helical-type structure with the various sulfo and carboxylate groups projected in an outward fashion (22). Structural variability, overall charge, and conformation affect interactions with target proteins. Therefore, the length of the HS chain and number of sulfo groups are important. In addition, changes in ring conformation and rotation around the glycosidic bond can affect the three dimensional arrangement of the sulfo groups. GlcA and GlcNAc residues are commonly found in the $^{1}C_{4}$ (chair) conformation. However, the IdoA residue can adopt either the $^{1}C_{4}$ or $^{2}S_{0}$ (skew boat) conformation (Figure 2) (23).

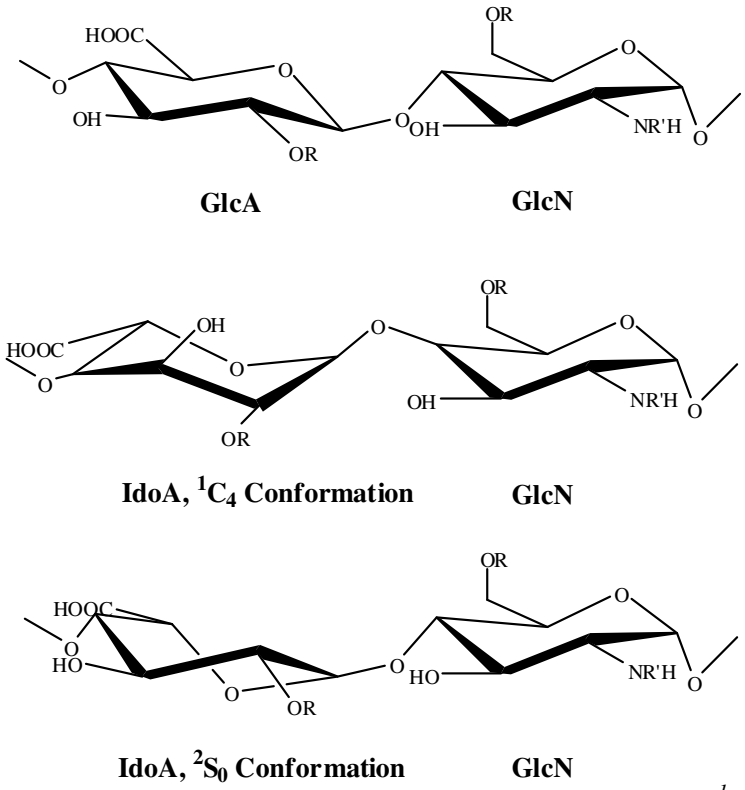

Figure 2. Disaccharide repeating units of HS. IdoA±2S is present in both $^{1}C_{4}$ and $^{2}S_{0}$ conformations. Both conformations are presented. R=-SO_3,-H; R'=-SO_3,-H, or –Ac.

Both chair and skew boat conformations of IdoA have been observed in co-crystal and NMR structural analysis of protein interactions (*24, 25*). The equilibrium between the two conformations for IdoA residues depends its own substitution with 2-*O*-sulfation and the

sulfation of the adjacent glucosamine residues (26). Moreover, it has been suggested that replacement of the *N*-sulfo groups to the reducing side of IdoA residues by an *N*-acetyl group has only a slight affect on the balance of IdoA conformational equilibrium. While it has also been suggested that 6-*O*-sulfo groups at the nonreducing end alters the balance of the IdoA2S equilibrium more toward the $^2S_0$ conformation (27). Therefore, there may be a cooperative effect between *N*- and 6-*O* sulfation. This information is important in elucidating conformational changes of HS and the potential regulatory role 6-*O*-sulfation may play within HS chains. Thus, the arrangement of IdoA residues can help optimize any structural, electrostatic, and van de Waals properties required for these protein interactions (*28, 29*).

Heparan Sulfate Proteoglycan Core Proteins

Heparan sulfate proteoglycans (HSPGs) are found abundantly on the cell surface and ECM of mammalian cells. HSPGs are comprised of a core protein covalently attached to one or more GAG chains. The core protein determines the localization and presentation of HS on the cell surface and in the ECM. The major HSPGs contain up to 5 conserved HS sites which consist of a SGXG or SG sequence, where X refers to any amino acid with this sequence commonly being preceded by various acidic residues (15). HS side chains modified by sulfotransferases, epimerase, and extracellular endosulfatases (Sulf1 and Sulf2) yield structurally diverse chains involved in various biological functions. Membrane bound and secreted proteoglycans are the two major classes of HSPGs. Syndecans and glypicans are the major membrane bound proteoglycans, while perlecans and agrins are the major secreted proteoglycans (Figure 3).

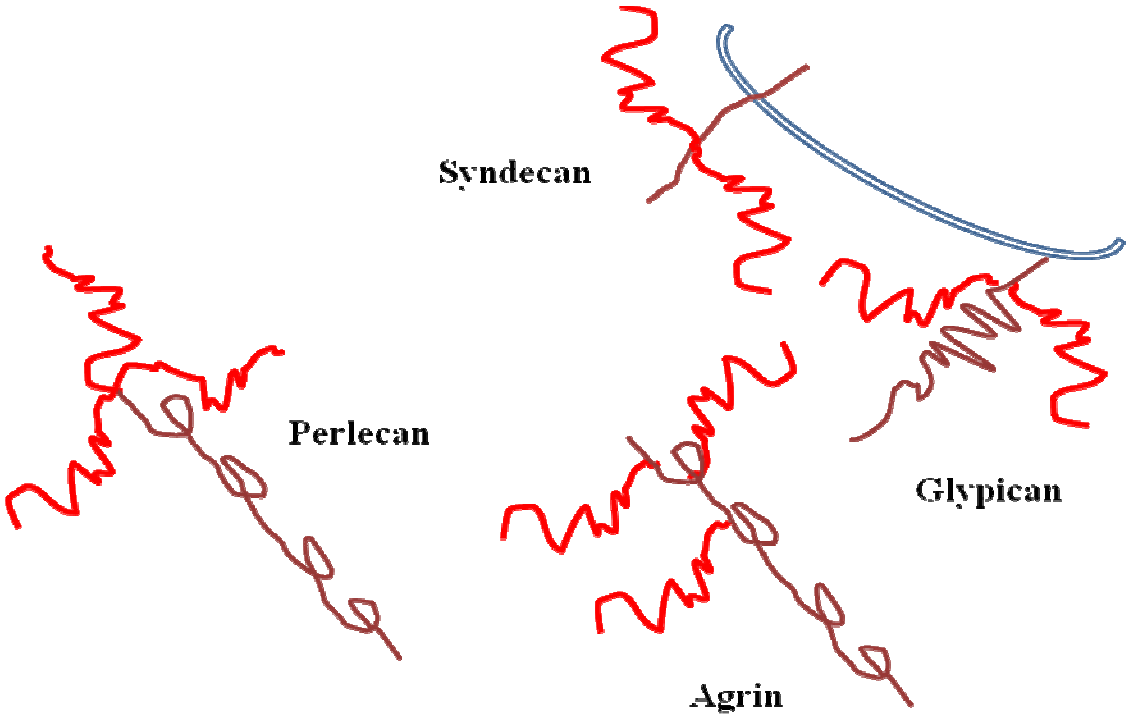

Figure 3. The family of HS proteoglycans. The core proteins are shown in *purple,* while the HS chains are shown in *orange* and *red*. Syndecan is a transmembrane protein and glypican is a glycosylphosphatidylinositol (GPI) anchored protein. Perlecan and agrin are not attached to the cell surface and are found in the ECM.

Syndecan

The syndecan core protein family is a single type I transmembrane protein. Syndecan-1, syndecan-2 (fibroglycan), syndecan-3 (N-syndecan), and syndecan-4 (amphiglycan or ryudocan) represent four human or mouse members as well as a *Drosophila* homologue having an average molecular weight of 20-45 kDa (30). Syndecan core proteins contain an *N*-terminal signal peptide sequence, an ectodomain, a homologous transmembrane domain, and a cytoplasmic *C*-terminal domain with four tyrosine residues at fixed positions. The ectodomain is somewhat divergent except for the several consensus sequences for GAG attachment and a protease dibasic cleavage sequence. This suggests the proteolytic cleavage sites can be cleaved allowing the shedding of the ectodomain to free the GAG from the cell surface. The shed HSPG is placed in the ECM to interact with biological targets in addition

to regulating the amount of HS on the cell surface and in the extracellular matrix (31). This protein core family is encoded by multiple genes expressed in a developmental and cell-type specific pattern by transcriptional and translational demands as well as tissue-specific proteases (*32, 33*). They carry three to five attachment sites for GAG side chains. The side chains for this core protein are HS and CS/DS.

Glypican

The glypican core protein family is another HSPG, but unlike syndecan it is anchored to the cell surface by a glycosylphosphatidylinositol (GPI) linkage at the hydrophobic *C*-terminal tail. The extracellular domain contains two or three GAG attachment sites. These GAG attachment sites carry HS exclusively and are found in close proximity to the cell membrane. There are 14 invariant cycteine residues in the extracellular domain that aid in the stabilization of a compact tertiary structure (30). Six isoforms have been identified in human and mouse which include glypican-1(glypican), glypican-2 (cerebroglycan), glypican-3 (OCI-5), glypican-4 (K-glypican), glypican-5, and glypican-6 as well as two *Drosophila* glypicans and one *C. elegans* glypican. The molecular weight of this core protein family has a range of 60-70 kD. Studies suggest that glypican regulate the activities of fibroblast growth factors (FGFs), bone morphogenic proteins (BMPs), wingless (Wnt), hedge hogs (Hhs), and insulin-like growth factors (IGFs) (34). In addition, glypicans have been implemented in the progression of several types of cancer (35). Mutations found in the gene that encodes glypican-3 leads to Simpson-Golabi-Behmel syndrome, which is a rare X-linked disorder characterized by pre- and postnatal overgrowth of multiple tissues, organs, and multiple visceral and skeletal abnormalities (34-38).

Agrin

Agrin is a 250 kDa protein which displays exclusively HS chains. It has at least six potential HS attachment sites and has five *N*-glycosylation sites (39). Agrin is found in the basement membrane of the neuromuscular junctions and renal tubular basement membranes of many species such as human, rat, and mouse (39-41). Agrin contains domains that have specific functions that have been shown to function in the aggregation of acetylcholine receptors during synapsis in the neuromuscular junctions. It is also participates in interactions with neural cell adhesion molecules involved in synaptogenesis during neural development, and is involved in lymphocyte activation contributing to immunological synapse formation (41-44).

Perlecan

Perlecan is one of the largest proteins found in mammals, *Drosophila melanogaster*, and *C. elegans*. Perlecan consists of approximately a 470 kD core protein which can display up to four HS chains (*45, 46*). However, it has been shown that perlecan can also display CS (47). This core protein contains five domains, each having a distinct function. It is mainly found in the basement membrane of most endothelial and epithelial cells where it can interact with fibroblast growth factor 2, vascular endothelial growth factor and platelet-derived growth factor (48). It is involved in vascular development and homeostasis in addition to the development of mature cartilage (49-51)

Biosynthesis of heparan sulfate

The biosynthesis of HS has been the subject of intense investigation since the biosynthesis of HS results in the generation of very heterogeneous and complex polysaccharide chains. HS ability to interact with different target proteins and/or ligands along with its involvement in various biological functions is correlated with the structural diversity of HS. Moreover, the combination of IdoA residues and sulfations patterns within the polysaccharide chain is vital for the structure-function relationship of HS in various biological contexts. The biosynthesis of HS is a non-template, enzymatic driven process resulting in the possibility of disaccharides units within the chains containing variable modifications. The HS biosynthetic pathway is separated into three stages: 1) biosynthesis of the tetrasaccharide linkage region, 2) chain initiation/chain elongation, and 3) chain modification. All enzymes participating in the HS biosynthesis have been cloned, allowing us to study and increase our knowledge of this critical biological pathway.

Step 1: Biosynthesis of the tetrasaccharide linkage region

The biosynthesis of HS occurs in the lumen of the Golgi apparatus and begins with the attachment of four monosaccharides known as the tetrasaccharide linkage region to the core protein. The tetrasaccharide linkage region of HS consists of a xylose-galactose-galactose-glucuronic acid (GlcA(β1→3)Gal(β1→3)Gal(β1→4)Xly(1→*O*-Ser) in which Xyl is covalently attached to a specific serine residue of the core protein. This tetrasaccharide sequence also serves as the linkage region for CS proteoglycans. Each sugar residue is added to the tetrasaccharide linkage sequence in a stepwise manner by four specific glycosyltransferases, namely xylosyltransferase (XylT), galactosyltransferase I (GalT-I),

galactosyltransferase II (GalT-II), and glucuronyltransferase I (GlcAT-I) (Figure 4). Sulfation was shown to be found on the C-4 and/or C-6 position of Gal1 and Gal2, and have been demonstrated for CS/DS but not for HS/HP biosynthesis suggesting that the sulfation at the linkage region directs the synthesis of CS or HS. C-2 phosphorylation of xylose has been demonstrated for HS/HP and CS/DS biosynthesis (52-54). It has been suggested that phosphorylation and sulfation play a critical role in regulating maturation and production of growing GAG chains (55-57).

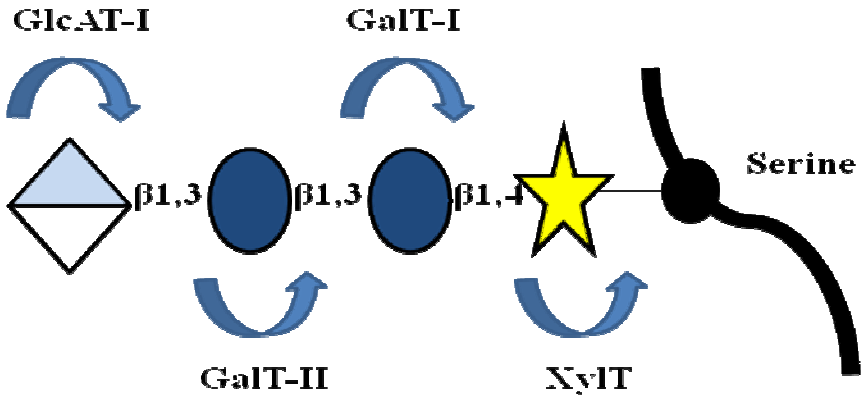

Figure 4. Generation of the tetrasaccharide linkage region. The synthesis of the tetrasaccharide linker region that attaches the GAG chains to a serine within the conserved attachment site of the core protein is shown. XylT attaches xylose the first residue of the tetrasacchride linkage region to the core protein. The activities of GalT-I, GalT-II, and GlcAT-I transfer two galactose residues and a glucuronic acid, respectively, to complete the tetrasaccharide linkage region. Xylose is depicted as the *yellow star*, galactose the *dark blue circle*, and glucuronic acid as the *light blue/white diamond*.

Xylosyltransferase (XylT)

Xylosyltranferase (XylT) is the first enzyme to proceed in the biosynthesis of the tetrasaccharide linkage region by using uridine diphosphate (UDP)-xylose as a donor substrate to transfer xylose to specific serine residues within the core protein. These serine residues are found in the SGXG peptide sequence within the protein, where X is any amino

acid. Not every SGXG sequence is involved in the formation of the tetrasaccharide linkage region suggesting additional signals for catalysis (*58, 59*). XylT is important in the formation of HS biosynthesis. It has been shown to be a rate–limiting step in the formation of GAGs (60). In addition, Chinese hamster ovary (CHO) cells deficient in XylT were unable to produce HS or CS, and re-expression of XylT restored GAG chain synthesis (*61, 62*). XylT-I and XylT-II have been identified and cloned with an overall sequence identity of 55 % (*63, 64*). They are type II transmembrane proteins located in the endoplasmic reticulum. Both XylT-I and XylT-II have been found in human, mouse, and rat, but only one isoform was found in *Drosophila melangaster* and *C. elegans* (63-65). These isoforms are differentially expressed in animal tissues (62). In addition, mutations in either XylT-I or XylT-II can be used as biochemical markers and genetic risk factors for diseases (*66, 67*).

Galactosyltransferase I (GalT-I) and Galactosyltransferase II (GalT-II)

Galactosyltranferase I (GalT-I) is the second enzyme used in the formation of the tetrasaccharide linkage region. This enzyme introduces the first Gal residue. Galactosyltransferase II (GalT-II) is the third enzyme involved in the formation of the tetrasaccharide linkage region. It attaches the second Gal residue to the linkage region. Both utilize UDP-galactose as a substrate donor. However, GalT-I adds the first Gal residue to the tetrasaccharide linkage region by generating a β1,4 linkage, whereas GalT-II generates a β1,3 linkage to the growing tetrasaccharide when adding the second Gal residue (68). Both enzymes show type II membrane topology and are located in the early-medial potion of the Golgi apparatus (*68, 69*). GalT-I can transfer a Gal onto a non-phosphorylated xlyoside, whereas the phosphorylated analog was not a substrate, suggesting phosphorylation at the C-

2 position of xylose inhibits the transfer of the first Gal residue to xylose (57). Re-expression of GalT-I into GalT-I deficient CHO cells restored GAG synthesis, demonstrating its importance in the biosynthesis of GAGs (70). In addition, siRNA-mediated inhibition in HeLa S3 cells demonstrated that GalT-II was essential for GAG formation (68). Two mutations in expressed GalT-I showing either absent or defective activity is responsible for the progeroid variant of Ehlers-Danlos syndrome, a connective tissue disorder manifesting in loose joints, fragile blood vessels, and abnormal wound healing (71). In addition, the GalT-I deficient form of Ehlers-Danlos syndrome produce altered HS which is associated with a delay in wound repair, altered cell migration, adhesion, and contractility (72).

Glucuronyltransferase I (GlcAT-I)

Glucuronyltranferase I (GlcAT-I) is final glycosyltransferase involved in the completion of the tetrasaccharide linkage region. It catalyzes the transfer of GlcA from UDP-GlcA to the terminal Gal residue. It plays a critical role in preparing for the initiation and elongation of the GAG chains. It has also been shown to regulate the overall GAG synthesis process and is rate-limiting in various cells since it positions the last monosaccharide at the branching point of GAG synthesis, which could direct the synthesis of CS or HS (73). The crystal structure was solved for GlcAT-I, and information from the crystallography and site-directed mutagenesis studies have aided in elucidating key residues associated with substrate binding and catalysis (*74, 75*). GlcAT-I has a greater reactivity toward compounds with sulfation of Gal1 and phosphorylation of Xyl at the C-2 position, which may contribute to the efficient completion and maturation of the tetrasaccharide linkage (*57, 76*). GlcAT-I has been expressed in mammalian cells and *E.coli* cells. However, the expression in yeast has led to a more soluble, properly folded, highly active

enzyme (77). In addition, there has been an increasing interest of glycosyltransferases as pharmacological targets, and the over expression of GlcAT-I by gene transfer is a promising strategy to overcome GAG depletion induced by pro-inflammatory cytokines that are major mediators of osteoarthritis (78).

Step 2: Chain Initiation/Chain Elongation

After the tetrasaccharide linkage region is generated, another group of enzymes are involved in the biosynthesis of HS to generate the HS backbone. The formation of the HS backbone can be divided into two sections: 1) chain initiation and 2) chain polymerization. The HS backbone is generated after the addition of a GlcNAc residue by *N*-acetyl-glucosaminyltransferase I (GlcNAcT-I) activity, and chain elongation proceeds by *N*-acetyl-glucosaminyltransferase II (GlcNAcT-II) and glucuronyltransferase II (GlcAT-II) activities which add α1,4 GlcNAc and β1,4 GlcA residues in alternating sequences to the nonreducing end of the growing polysaccharide (Figure 5) (79). These glycosyltransferases are encoded by the exostosin (EXT) gene family (17). Five members of the EXT family of glycosyltransferases are known: EXT1, EXT2, EXTL1 (EXT-Like 1), EXTL2, and EXTL3, which are type II transmembrane proteins found in the Golgi apparatus. The EXT gene family contains dual glycosyltransferase activity in HS biosynthesis in addition to functioning as tumor suppressor genes (*80, 81*). The actions of the EXT gene family produce HS polysaccharides that will later serve as substrates for modification by sulfotranferases in the biosynthesis of HS.

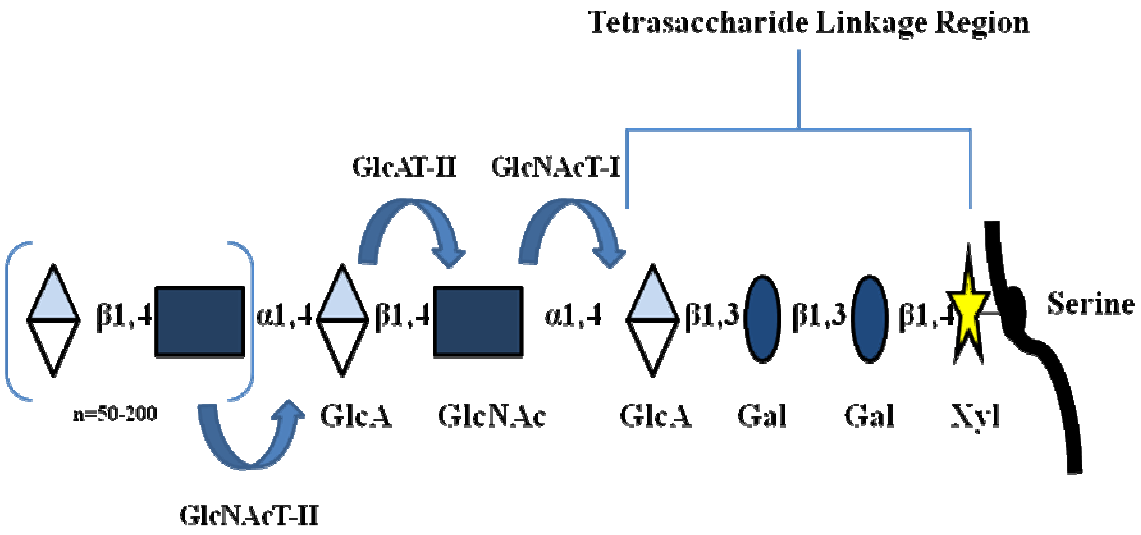

Figure 5. Initiation and polymerization of HS. Chain initiation is carried out by *N*-acetyl-glucosaminyltransferase I (GlcNAcT-I) which adds a GlcA residue to the tetrasaccharide linkage region. This directs the formation of HS backbone by the alternating activities of *N*-acetyl-glucosaminyltransferase II (GlcNAcT-II) and glucuronyltransferase II (GlcAT-II), which add GlcNAc and GlcA residues, respectively.

N-Acetyl-glucosaminyltransferase I (GlcNAcT-I)

N-acetyl-glucosaminyltranferase I (GlcNAcT-I) is a crucial enzyme involved in the initiation of the elongation of the HS polysaccharide chain. GlcNAcT-I catalyzes the transfer of a α1, 4 GlcNAc from UDP-GlcNAc to the nonreducing end of the tetrasaccharide linkage region (Figure 6). This step commits the resulting pentasaccharide to elongate into a HS chain rather than CS/DS chain (82). EXTL2 has been shown to exclusively exhibit GlcNAcT-I activity, where as EXTL3 has been shown to exhibit both GlcNAcT-I and GlcNAcT-II activities (*80, 83, 84*).

D-Glucuronyltransferase II (GlcAT-II)/*N*-Acetyl glucosaminyltransferase (GlcNAcT-II)

Chain elongation is accomplished by the alternating addition of GlcA and GlcNAc residues by EXT1 and EXT2, which can extend the chain up to 200 disaccharides in length. *N*-acetyl glucosaminyltransferase (GlcNAcT-II) catalyzes the transfer of GlcNAc residue

from UDP-GlcNAc, whereas D-glucuronyltranferase II (GlcAT-I) catalyzes the transfer of GlcA residue from UDP-GlcA in the production of the HS chain. The tumor suppressor genes, EXT1 and EXT2, encode for the two glycosyltransferases proteins. EXT1 and EXT2 both have dual GlcAT-II and GlcNAcT-II activities even though EXT2 activities are weaker than EXT1 (*85, 86*). It has been suggested that EXT1 and EXT2 form a heterocomplex *in vivo* to be a completely functional polymerization unit (*83, 85, 86*). In addition, EXTL1 and EXTL3 have been reported to have GlcNAcT-II (80).

Glycosyltransferase	Function
XylT	Transfer of xylose to a serine on the core protein
GalT-I	Transfer of first galactose to xylose.
GalT-II	Transfers of second galactose to linker
GlcAT-I	Transfer of glucuronic acid to complete linker region

Table 1. Summary of enzymes involved in the generation of the tetrasaccharide linkage region.

Step 3: Chain Modification

The HS chain contains disaccharide unit repeats of glucuronic acid and *N*-acetyl glucosamine (GlcA- GlcNAc)$_n$ generating an unepimerized, unsulfated HS backbone. The biosynthesis of HS is not complete until the HS chain is further subjected to modifications. The enzymes that produce these modifications are *N*-deactylase/*N*-sulfotransferase (NDST), C_5 epimerase (C_5-Epi), 2-*O*-sulfotransferase (2-OST), 6-*O*-sulfotransferase (6-OST), and 3-*O*-sulfotransferase (3-OST), respectively. These sulfotransferases and C_5 epimerase are membrane bound and found in the Golgi apparatus and therefore available to produce the necessary modifications to the HS chain. HS sulfotransferases utilizes 3'-phosphoadensine 5'-phosphosulfate (PAPS), a common sulfo donor, to transfer a sulfo group to different acceptor sites on the polysaccharide (Figure 6).

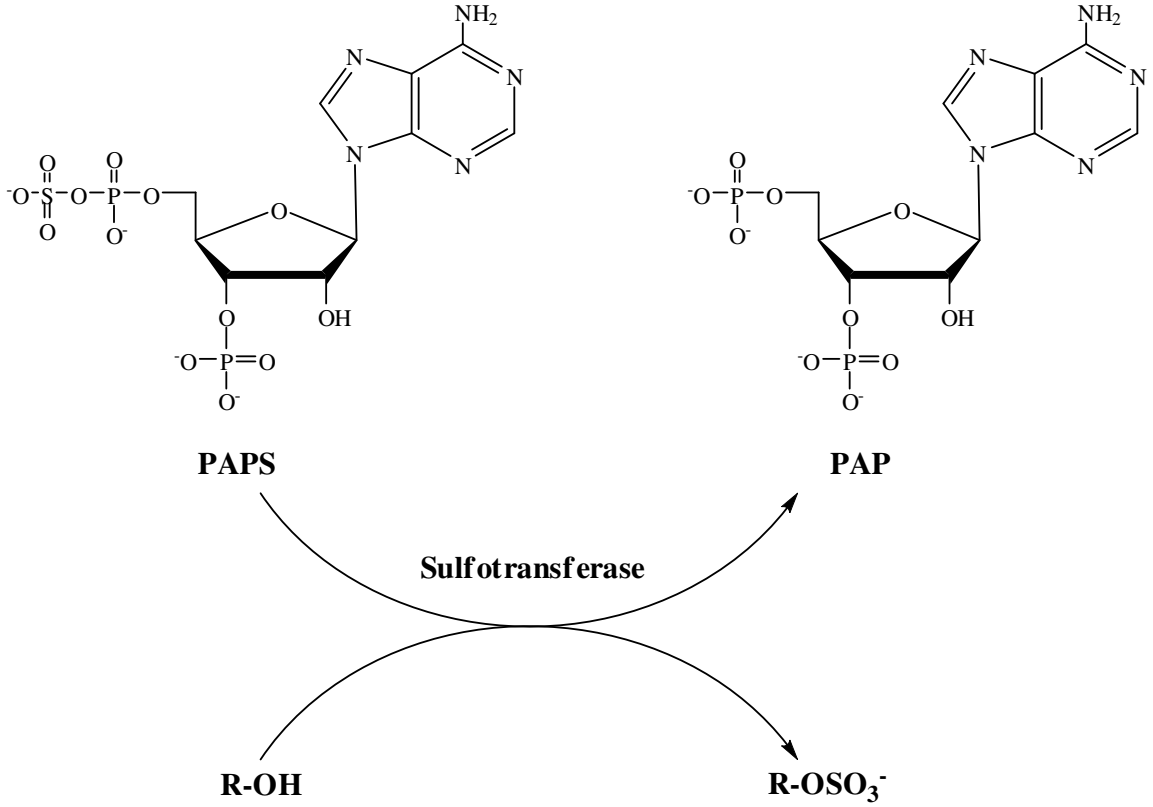

Figure 6. The general scheme of the catalyzed reaction by sulfotransferases. R-OH represents the acceptor substrate for the sulfo group catalyzed by sulfotransferases from PAPS. Sulfotransferases included NDST, 2-OST, 6-OST, or 3-OST. The $R\text{-}OSO_3^-$ represents the sulfated product.

These enzymes catalyze the modifications which include *N*-deacetylation and *N*-sulfation of the *N*-acetyl position of glucosamine, C_5 epimerization to convert GlcA to IdoA, 2-*O*-sulfation at the 2-OH position of GlcA or IdoA, along with 6-*O*-sulfation and 3-*O*-sulfation at the 6-OH and 3-OH position of glucosamine. The majority of these isoforms have been cloned and expressed (87). Incomplete sulfation at specific sites on the polysaccharide chain results in heterogeneity and diversity within HS. To further complicate the biosynthesis of HS, HS sulfotransferases with the exception of 2-OST have multiple

isoforms, which include four isoforms for NDST, three isoforms for 6-OST, and seven isoforms for 3-OST. The different isoforms have somewhat distinct substrate specificities. These isoforms have different expression patterns in tissue, and can be regulated by specific tissues to yield specific saccharide sequences related to the structure-function relationship associated with various biological interactions (29)

N-Deacetylase/N-Sulfotransferase (NDST)

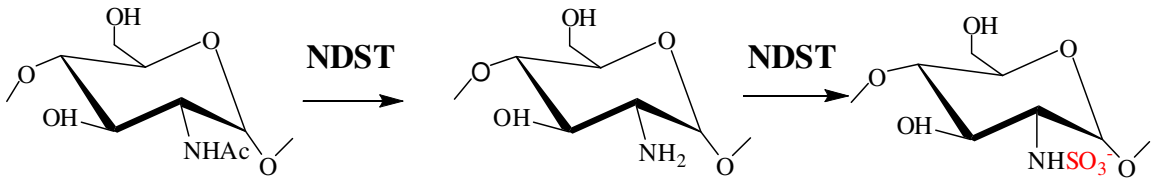

Figure 7. The bifunctional activity of NDST. The removal of the acetyl group from GlcNAc is catalyzed by the *N*-deacetylase activity of NDST creating an unsubstituted glucosamine with a free amino group ($GlcNH_2$). The *N*-sulfotransferase activity of the enzyme catalyzes the transfer of a sulfo group from PAPS to generated GlcNS. The transferred sulfo group is colored *red*.

NDST is a dual functioning enzyme that catalyzes the removal of the acetyl group from GlcNAc residues and the addition of a sulfo group to the free amino group ($GlcNH_2$) that was deacetylated (Figure 7). NDST has four isoforms, which are NDST1, NDST2, NDST3, and NDST4. All isoforms have type II membrane topology and consist of a cytoplasmic region, transmembrane region, stem region, and catalytic domain encompassing distinct and independent *N*-deacetylase and *N*-sulfotransferase activities. NDST isoforms have shown differences in their levels of *N*-deacetylase and *N*-sulfotransferase activities along with exhibiting different tissue expression patterns, and NDST1 and NDST2 have largely overlapping expression in tissues, whereas NDST3 and NDST4 expression patterns in tissue seem to be more restricted (88). NDST1-deficient mice show a reduction of *N*- and *O*-

sulfation and C_5-epimerization of HS, and die shortly after birth due to defects of the developing lungs (89). However, NDST2-deficient mice have a less severe phenotype containing a defect in mass cell HP and having an inability to produce HS (90).

NDST activity acts upon approximately 40-50% of the polysaccharide chain. *N*-sulfation has been suggested to be a prerequisite or a strong modulator of subsequent sulfotransferase modifications to the polysaccharide chain. It has been demonstrated that NDST1 and NDST2 activities can be regulated by varying the amount of PAPS, or the expression levels of EXT1 and EXT2 can affected the amount of NDST1 present in the cell, which, in turn, can greatly influence HS structure during biosynthesis (*91, 92*). *N*-sulfation occurs inconsistently along the chain creating blocks of highly sulfated NS domains flanked by shorter, moderately sulfated NS/NA domains separated by longer stretches of unsulfated NA domains.

The crystal structure for the *N*-sulfotransferase domain (NST1) of human NDST1 has been solved in complex with 3'-phosphoadensine 5'-phosphate (PAP) shown in Figure 8 (93). NST1 is spherical overall with an open cleft containing five-stranded parallel β-sheet with α sheet on both sides. Between the 5'-phosphoate binding loop (PSB-loop) and α6 there is a cavity where the PAP binding site is located. Perpendicular to the PAP binding cavity is an open clef that is large enough to fit a hexasaccharide. A cleft near the 5'-phosphate of PAP consisting of the α6 and a random coil between β2 and α2 may be involved in the substrate binding site.

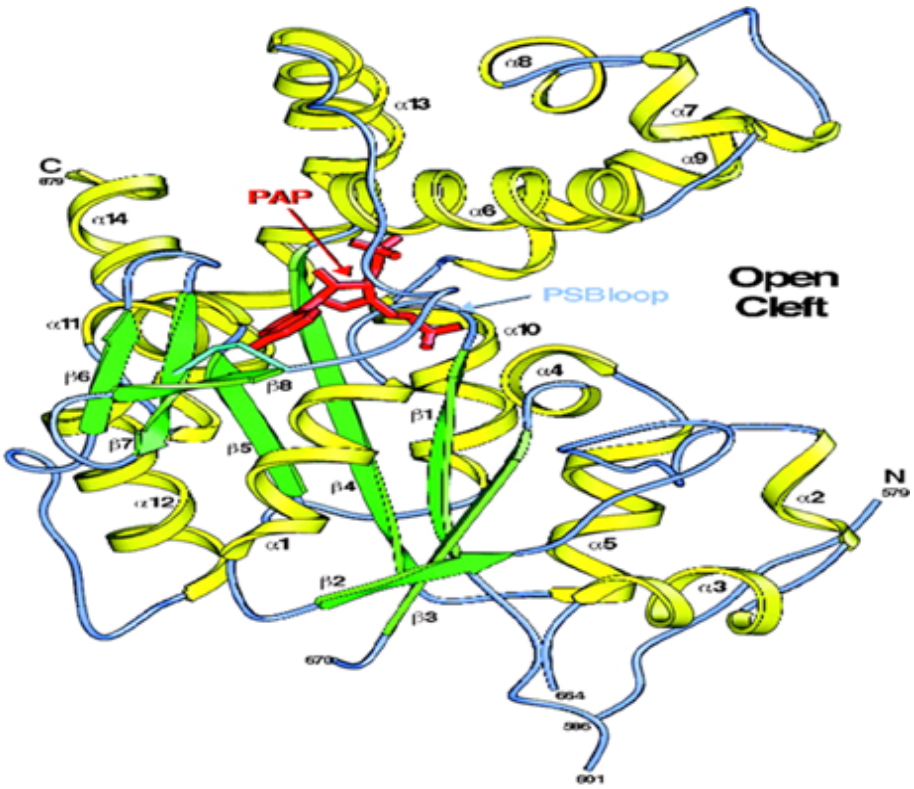

Figure 8. Overall structure of NST1 (93). Ribbon representation of NST1 in complex with PAP. Helices are in *yellow*, β-strands in *green*, random coil in *blue*, disulfide bond in *light blue*, and PAP molecule in *red.*

Lys-614 of NST1 has been shown to be conserved in other heparan sulfate sulfotransferases along with all cytosolic sulfotransferase through site-directed mutagenesis and crystallography studies (*94, 95*). Superimposition of the crystal structure of estrogen sulfatase in complex with PAP-vandate and the crystal structure of NST1 has suggested that Lys-614 is a proton donor during catalysis (93). The crystal structure of NST1 has led to the modeling of NST domains of additional isoforms of NDST, which has shown that their binding sites show variable charge distributions that may equate to their varying levels of NDST activity (88).

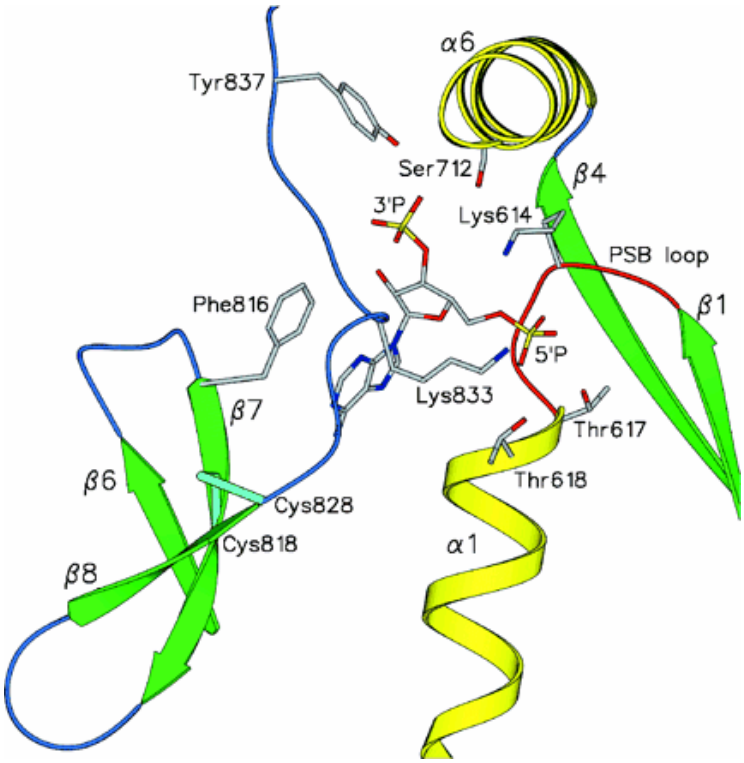

Figure 9. Ribbon diagram of the PAP binding site of NST1 (93). The side chains of key residues are shown that can interact with PAP. The disulfide bond is shown in *blue*.

Glucuronyl C_5 Epimerase (C_5-Epi)

During the HS biosynthesis, C_5-epi catalyzes the converts D-glucuronic acid residues to L-iduronic acid residues by changing the configuration at the C_5 position. This enzyme has type two membrane topology and is found in the Golgi apparatus. Figure 10 shows the activity of this enzyme proceeds in two stages beginning with the abstraction of a proton at the C_5 position on GlcA producing a carbanion intermediate. The second step involves the introduction of a proton from the medium at the C_5 position that results in inversion of configuration of the stereocenter that shifts the carboxyl group across the plane of the structure (96).

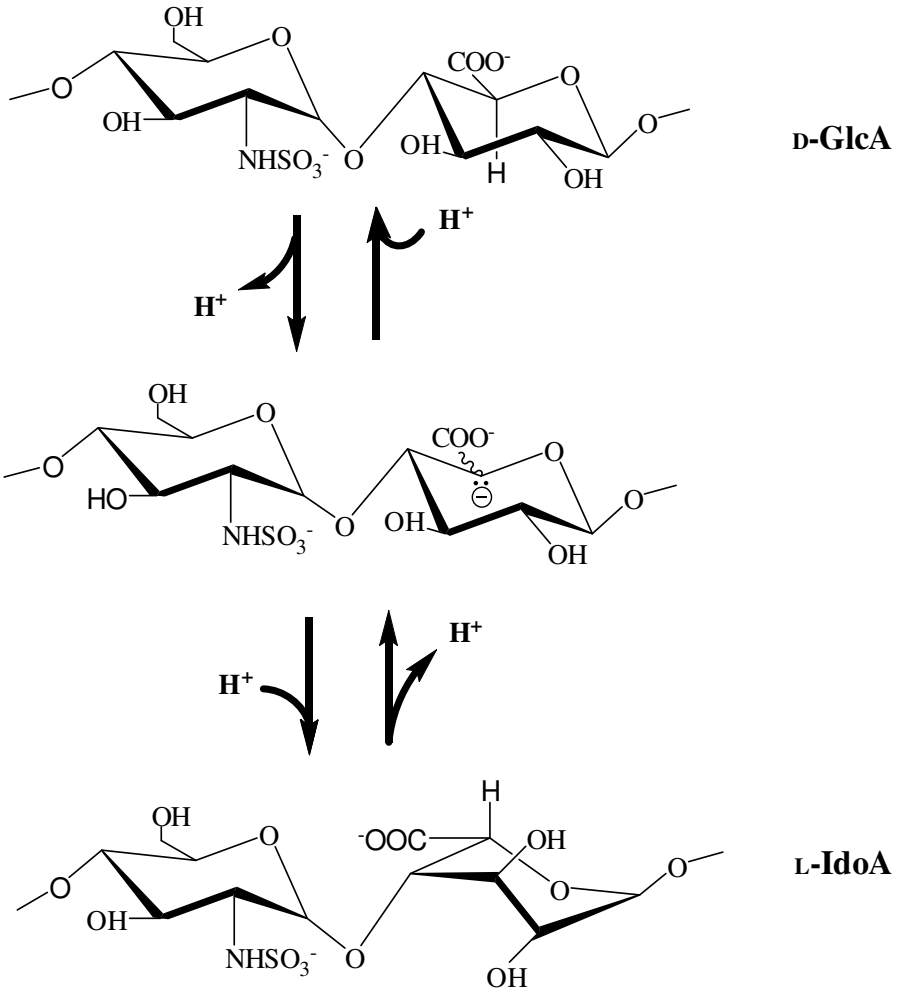

Figure 10. General mechanism for C_5 epimerization reaction. C_5-epi catalyzes the abstraction of the C_5 proton from GlcA (top) followed by re-addition of a proton from the medium to produce a carbanion (middle) resulting in the formation of IdoA (botton).

The requirement for substrate recognition by C_5-epi is an adjacent GlcNS residue to a GlcA residue at the non-reducing end of the polysaccharide within the structural context of GlcNS-GlcA (97). Therefore, the enzyme would not have activity against GlcA residues containing an adjacent GlcNAc residue (GlcNAc-GlcA). This reaction has been shown to be reversible with an *in vitro* system, but *in vivo* it has been suggested that it is locked into place with the introduction of 2-*O*-sulfation of the IdoA residue (98). Activities *in vivo* may be due to C_5-epi forming a stable complex with 2-OST (99). The equilibrium of the reaction favors

the formation of the GlcA residue *in vitro*. However, the formation of C_5-epi/2-OST complex increases epimerase activity, and aids in the shift of equilibrium to the IdoA residue (97). Epimerization is important in biological functions of HS since the flexible conformation of IdoA residues play an essential role in orienting the sulfo groups that interact with numerous proteins. In addition, this enzyme is important in the production of HP, since C_5-epi deficient mast cells failed to epimerize GlcA to IdoA residues, and the C_5-epi deficient mast cells containing HP have an altered *O*-sulfation pattern (100).

Uronosyl 2-*O*-Sulfotransferase (2-OST)

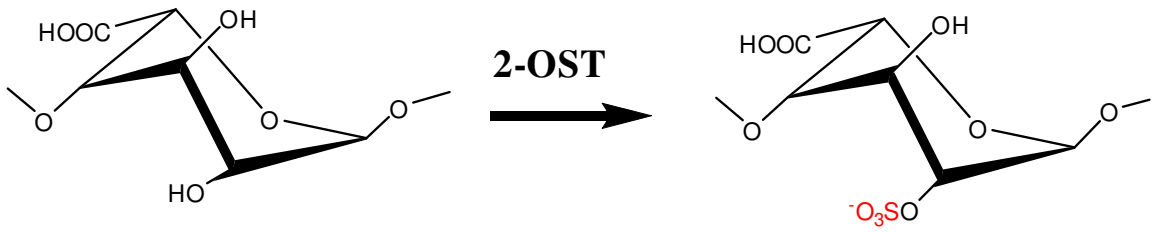

Figure 11. 2-OST catalyzed reaction. A sulfo group from PAPS is transferred to the 2-OH position of IdoA by 2-OST to generated IdoA2S. GlcA is also a sulfated by 2-OST, but the enzyme favors the sulfation of IdoA. The transferred sulfo group is in *red*.

2-*O*-sulfation of IdoA residues in the HS polysaccharide chain is very important for many biological functions via binding to fibroblast growth factor (FGF) signaling such as cell migration, developmental patterning, and organ and nervous system development (101-106). 2-OST is also a type II transmembrane protein and found in the Golgi apparatus. 2-OST catalyzes the transfer of a sulfo group to the 2-OH position to either GlcA or IdoA residues (Figure 11). However, it has a preference for IdoA residues. To date, only one isoform is identified and it is highly conserved across species. In addition, the crystal structure of 2-OST has not been solved. However, mutational studies have shown that 2-

OST is vital for biological activities. Mice deficient in 2-OST die in the neonatal period and have developmental defects in the kidneys, eyes, and bones (103).

Glucosaminyl 6-*O*-Sulfotransferase (6-OST)

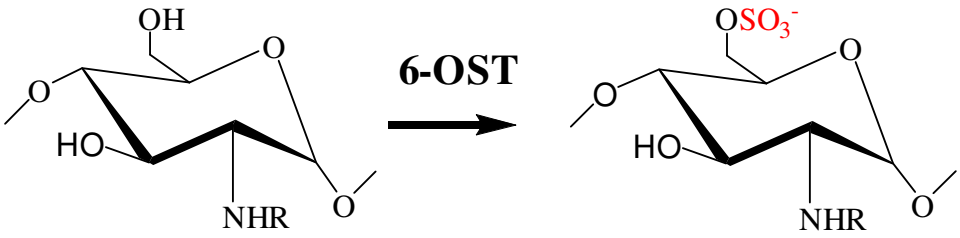

Figure 12. Reaction catalyzed by 6-OST. A sulfo group from PAPS is transferred to the 6-OH position of glucosamine. The transferred sulfo group is shown in *red*. R represents a proton, acetyl, or sulfate.

6-OST is responsible for transferring a sulfo group to the 6-OH position on glucosamine as shown in Figure 12. 6-OST has three isoforms (6-OST-1,-2, and -3) and one alternatively spliced variant (6-OST-2 S, where S refers to Short) (*107, 108*). Each isoform has overlapping substrate specificities, but each has a preference to a particular substrate adjacent to a GlcNS or IdoA residue. 6-OST-1 has a preference for -IdoA-GlcNS- disaccharide residues, 6-OST-3 acts equally on -IdoA-GlcNS- or -GlcA-GlcNS- disaccharide residues, and 6-OST-2 preference depends on the availability of either disaccharide residue. In addition, their preference of disaccharide substrate can be with or without 2-*O*-sulfation present, and GlcNAc residues are capable of being a substrate for all isoforms (*107, 109*). Therefore, it can be concluded that each isoform has similar substrate specificities. These enzymes are type II membrane proteins found in the Golgi apparatus. 6-OST-1 is expressed strongly in liver, 6-OST-2 is expressed mainly in brain and spleen, and 6-OST-3 is expressed throughout the body. Studies suggest that isoforms of 6-OST may be regulated in tissue-specific manner and modulate HS with tissue-specific structures and functions (*110, 111*).

The majority of 6-OST-1 null mice was neolethal or exhibited a smaller size than their wild-type counterparts. In addition, these mice had developmental abnormalities and distorted HS biosynthesis (112). Furthermore, 6-*O*-sulfation is necessary for binding to a variety of ligands such as FGF-2 and Wnt (*113, 114*). This suggests that 6-OST is an important enzyme in the biosynthesis of HS that has essential function for embryonic development.

Glucosaminyl 3-*O*-Sulfotransferase (3-OST)

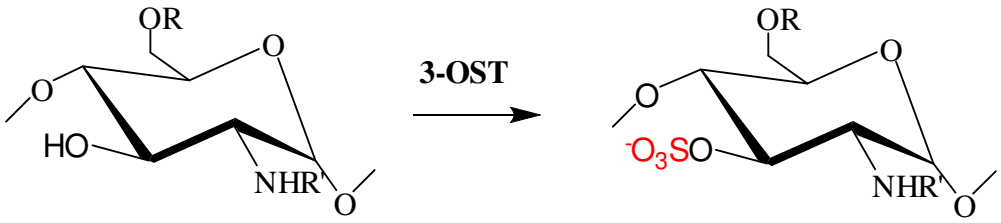

Figure 13. General scheme of the catalyzed reaction of 3-OST. A sulfo group is transferred from PAPS to the 3-OH position on glucosamine by 3-OST. R represents a proton or sulfo group. R' represents a proton, acetyl, or sulfo group. The transferred sulfo group is colored *red*.

The transfer of sulfo groups to the 3-OH position of glucosamine residues on the HS polysaccharide chain is achieved by 3-OST (Figure 13). 3-OST modification is very rare and the final step in HS biosynthesis. 3-OST has seven isoforms which are 3-OST-1, 3-OST-2, 3-OST-3A, 3-OST-3B, 3-OST-4, 3-OST-5, and 3-OST-6 (115-117). 3-OST-3A and 3-OST-3B have nearly identical amino acid sequences in the sulfotransferase domain. Therefore, both 3-OST-3A and 3-OST-3B can be represented as 3-OST-3. The sulfotransferase domains of the 3-OSTs have greater than 60% sequence homology (118). The substrate specificities of all 3-OSTs have been thoroughly examined (*119, 120*). 3-OST-1 catalyzes the transfer of a sulfo group to the 3-OH position of a glucosamine residue adjacently linked to GlcA or IdoA. 3-OST-2, 3-OST-3, 3-OST-4, and 3-OST-6 catalyze the transfer of a sulfo

group to the 3-OH position of a glucosamine residue adjacently linked to a 2-*O*-sulfo iduronic acid (IdoA2S). Lastly, 3-OST-5 catalyzes the transfer of a sulfo group to the 3-OH position of a glucosamine residue next to a GlcA, IdoA, and IdoA2S.

Isoform	Tissue Type
3-OST-1	Brain, Heart, Kidney, Lung
3-OST-2	Brain
3-OST-3A	Heart, Lung, Kidney, Placenta
3-OST-3B	Brain, Lung, Heart, Kidney
3-OST-4	Brain
3-OST-5	Brain, Skeletal muscle, Spinal cord
3-OST-6	Kidney, Liver

Table 2. Expression of 3-OST isoforms in human tissue.

With the exception of 3-OST-5, all other isoforms of 3-OST have more specific substrate specificities (Figure 14). The substrate specificities of 3-OST isoforms produce specific biological functions for HS. 3-OST-2, -3, -4, and -6 generate modified HS that serve as entry receptors for herpes simplex virus type 1 (HSV-1). 3-OST-1 generates HS that binds to AT and produces anticoagulant activity. 3-OST-5 is more promiscuous and can produce both anticoagulant HS as well as produce HS that can serve as an entry receptor for HSV-1.

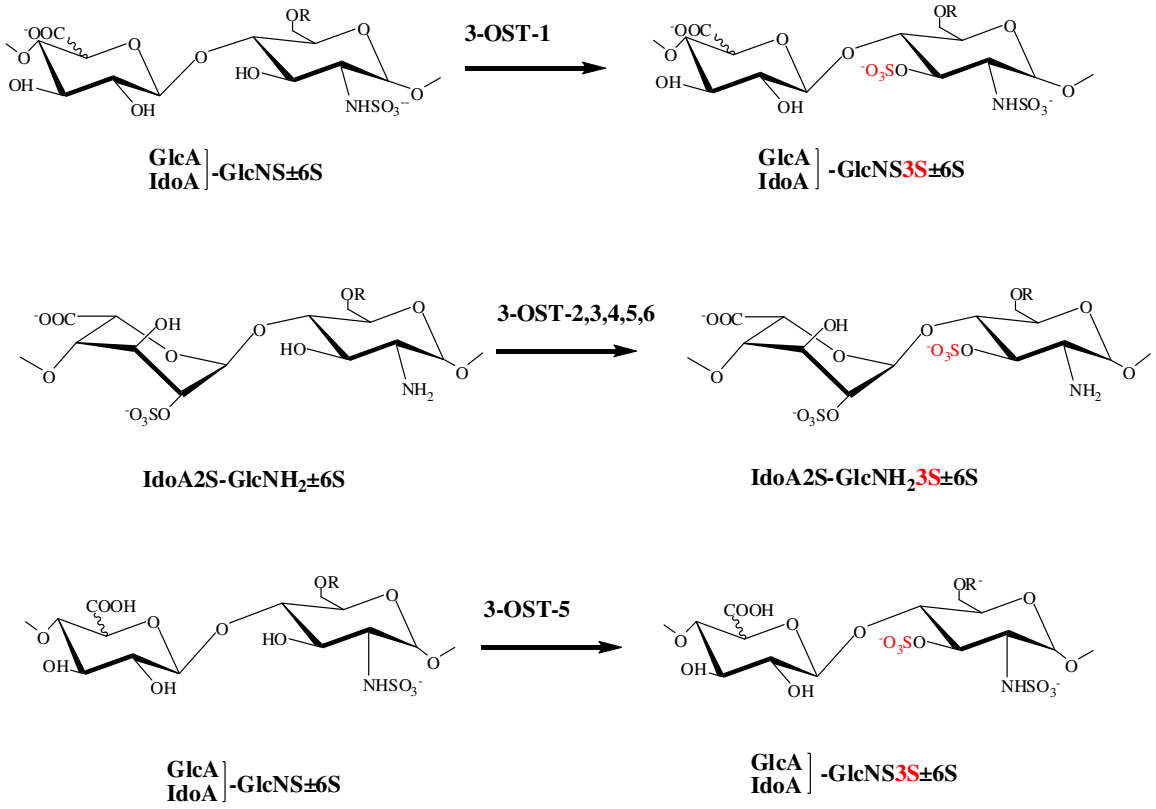

Figure 14. Substrate specificities of 3-OSTs (117). 3-OST-1 transfers a sulfo group to the 3-OH position of *N*-sulfated glucosamine (GlcNS±6S) linked to a GlcA or IdoA residues. 3-OST-3,-4,-6 transfers a sulfo group to the 3-OH position of an *N*-unsubstituted glucosamine ($GlcNH_2$±6S) linked to an IdoA2S residue. 3-OST-5 transfers a sulfo group to the 3-OH position of a glucosamine residue ($GlcNH_2$±6S or GlcNS±6S) linked to GlcA or IdoA/IdoA2S residues. The 3-*O*-sulfation by 3-OSTs is shaded and indicated in bold. R represents a sulfo group ($-SO_3$) or proton (-H).

The isoforms of 3-OST are distributed differently in tissue (Table 2). Except for 3-OST-1, all other isoforms contain a type II membrane topology and can be found in the Golgi apparatus. 3-OST-1 does not contain a transmembrane region, which suggests it may localize in the membrane through another type of interaction. However, 3-OST-1 has been detected in the serum and medium of cell lines (121). The crystal structure of 3-OST-1 in complex with PAP has been solved at 2.5-Å resolution (122). The crystal structure of 3-OST-1 and PAP is somewhat spherical with a large open cleft, and contains a α/β motif found to be

conserved in all sulfotransferases (Figure 15). The crystal structure aided in providing information about the mechanisms involved in the biosynthetic pathway.

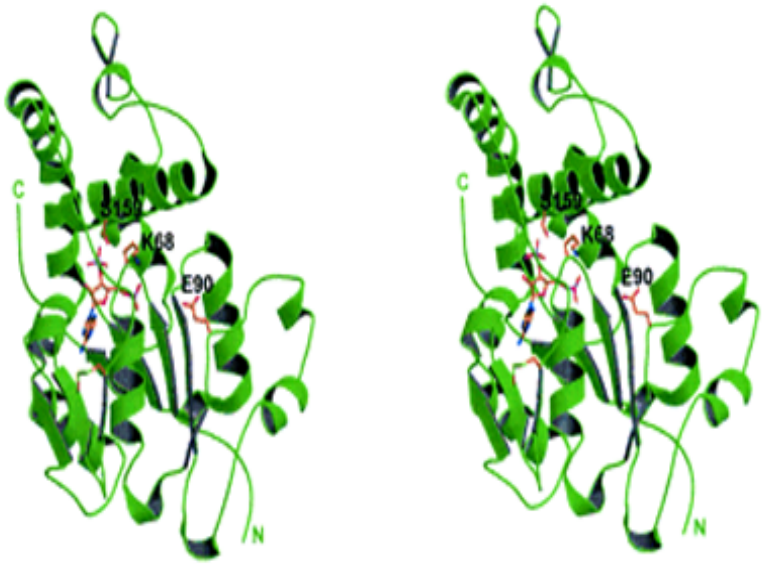

Figure 15. The crystal structure of 3-OST-1 in complex with PAP (122). The stereo ribbon diagram of the crystal structure of 3-OST-1 is shown with PAP and conserved residues Ser-159 and Lys-68 that interact with the 3'- and 5'-phosphates of PAP. In addition, Glu-90 is proposed to be involved in catalysis.

Along with site-directed mutagenesis analysis, the results suggested that Arg-67, Lys-68, Arg-72, Glu-90, His-92, Asp-95, Lys-123, and Arg-276 are essential for PAPS binding and enzymatic activity. In addition, Arg-67, Arg-72, His-92, and Asp-95 are conserved in 3-OSTs but not in NDST1, showing that these residues are important for substrate specificity. The crystal structure of the ternary complex 3-OST-3/PAP/tetrasaccharide has been solved at 1.9- Å resolution (Figure 16). The overall structure of 3-OST-1 and 3-OST-3 are very similar. The tetrasaccharide binds to the positively charged cleft of 3-OST-3. The *N*-sulfo group of the G1 residue and the carboxylate along with the 3-OH group of the I2 residue interact with the protein. The G3 residue contains the 3-OH group where a sulfo group would be accepted from PAPS. Here, it is positioned closely to PAP and can hydrogen bond

with Glu-184. The U4 residue hydrogen bonds with residues that have been determined to be responsible for substrate specificity, and these residues were confirmed by mutational studies. However, for 3-OST-1, the U4 residue would adopt a different confirmation and interact in a different manner with these residues.

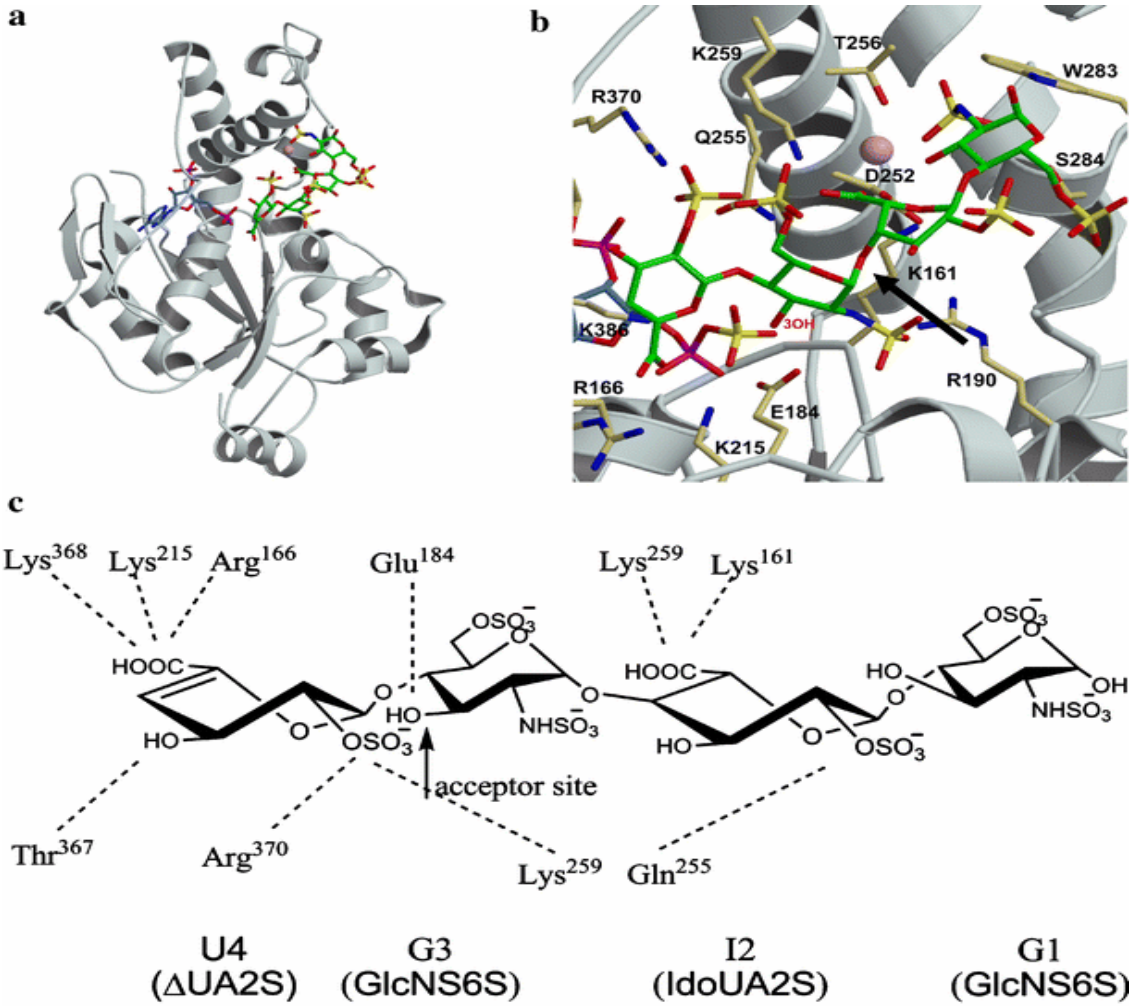

Figure 16. **The crystal structure of 3-OST-3/PAP/tetrasaccharide complex (29)** A) The crystal structure shown for the 3OST-3 in complex with PAP (*blue*) and a tetrasaccharide HS molecule (*green*). B) Superposition of PAPS onto PAP in the active site of the 3OST-3 crystal structure. This figure displays the relative orientation of the acceptor 3-hydroxyl to the sulfo group being transferred from PAPS. Side chains that are involved in binding the tetrasaccharide are shown. A sodium ion involved in binding is pictured in *pink*. C) Side chain with specific functional groups of the bound tetrasaccharide. Hydrogen bonds are indicated by *dashed lines*.

Remodeling of heparan sulfate

6-O-enodsulfatase

Once biosynthesis of HS within the cell is completed, mature HS is released from the cell in proteoglycan form, and can be found on the cell surface or in the ECM where it can interact with growth factors, cytokines, and chemokines to modulate biological activities. It was thought that no further modification to HS occurred that would alter the heterogeneous and complex nature of this GAG. However, a novel class of sulfatase enzymes called Sulfs emerged, which have endosulfatase activity and are capable of removing 6-*O*-sulfo groups from within HS (Figure 17) (*123, 124*). Before the discovery of Sulfs, HS sulfatases were found intracellularly in the lysosomal compartments. Here, lysosomal sulfatases worked as exosulfatases aiding in the catabolism of HS. Sulfatases in general are a class of enzymes that are highly conserved sequentially, structurally, and mechanistically across eukaryotic and prokaryotic species (125). Sulfatases catalyze the hydrolytic cleavage of sulfate esters (CO-S) or sulfamates (CN-S). All known sulfatase contain a conserved amino acid motif, C/S-X-P-S/X-R-X-X-X-L/X-T/X-G/X-R/X, found within the catalytic domain, which is essential for directing the post-translational modification of the initial cysteine or serine residue into a catalytically active C_{α}-formylglycine residue (126).

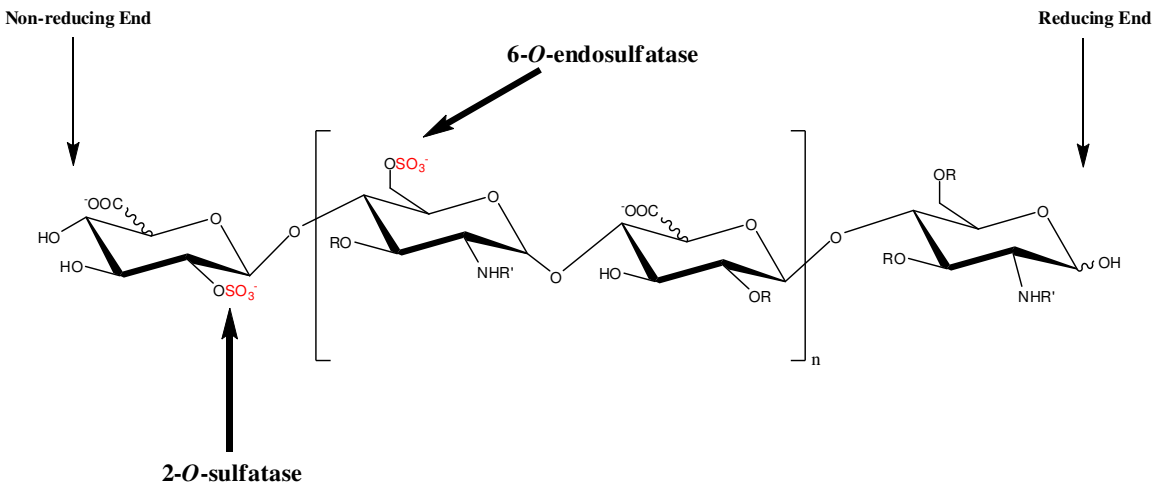

Figure 17. General scheme of exolytic and endolytic sulfatase activity. Exolytic sulfatase activity refers to the removal of sulfo groups from the terminal end of the polysaccharide. For example, 2-*O*-sulfatase from *Flavobacterium heparinum* removes sulfo groups from the 2-OH position on uronic acid at the end of the chain. Endolytic sulfatase activity refers to the removal of sulfo groups from within the polysaccharide chain. For example, 6-*O*-endosulfatase removes sulfo groups from the 6-OH position on glucosamine within the chain. Sulfo groups colored *red* would be removed by sulfatases.

Structural Features

HS 6-*O*-endosulfatase has been identified in quail, human, mouse, rat, chicken, Zebra fish, *Drosophila*, *Xenopus*, and *C. elegans*. Two isoforms, Sulf-1 and Sulf-2, have been identified in several species, and have been cloned and expressed in several different cell lines (*123, 124, 127-129*). Sulf-1 and Sulf-2 have been reported to be found on the cell surface or in the conditioned medium of cells, where it removes 6-*O*-sulfo groups from glucosamine (*123, 127, 130*). Mammalian Sulfs are approximately 870 amino acids in length. The structure of Sulfs can be divided into three domains, the *N*-terminal sulfatase domain, the hydrophilic domain, and the *C*-terminal domain. The *N*-terminal sulfatase domain contains the catalytic amino acids necessary for activity. It also contains a signal sequence approximately 24 amino acids in length. The hydrophilic domain follows the

sulfatase domain and is approximately 300-320 amino acids in length. It contains approximately 40% charged amino acids of which 27% are basic and 13% are acidic residues. It has been suggested that the hydrophilic domain is needed for cell surface localization through cell surface components and/or HS, endosulfatase activity, and potentially oligomerization (*123, 124, 127*). The *C*-terminal domain is approximately 100 amino acids in length and has significant homology to glucosamine 6-sulfatase (G6S). It has been suggested the *C*-terminal domain for G6S and Sulfs determine specificity toward glucosamine. The 130 kDa full length protein contains about 10 *N*-glycan sites. In addition, the full length protein can be processed further into a smaller protein, which can be found in the ECM of over-expressing cell lines (124). Additional, multiple aspargine-linked glycoslyation sites in the *N*-terminal sulfatase domain and *C*-terminal domain were identified in quail sulf isoform one (QSulf1). It has been revealed that glycosylation of QSulf1 is critical for enzymatic activity, membrane targeting, and secretion (131). To date, a crystal structure of Sulf is not available.

Substrate Specificity

It has been suggested that QSulf-1 has a high substrate specificity toward trisulfated IdoA2S-GlcNS6S disaccharides and a slight substrate specificity toward disulfated GlcA-GlcNS6S disaccharides (132). However, other studies showed that QSulf-1 was selective only toward disaccharide motifs found in highly sulfated NS-domains (i.e. $[IdoA2S\text{-}GlcNS6S]_n$), and enzymatic activity had no effect on disaccharide motifs found in moderately sulfated NA/NS domains (i.e.IdoA-GlcNS or GlcA-GlcNS6S) (133). In addition, QSulf1 and QSulf-2 have been shown to have the same substrate specificity toward trisulfated

IdoA2S-GlcNS6S disaccharides located within highly sulfated NS-domains of HS *in vitro* (127). In addition, human sulf isoform one (HSulf-1) and HSulf-2 were shown to have high selectivity toward trisulfated disaccharides, IdoA2S-GlcNS6S, within the appropriate context of heparin, and did not show any activity toward disulfated glucosamine residues when IdoA residues lacking 2-*O*-sulfation were adjacent to glucosamine-6-suflate (IdoA-GlcNS6S). A mass spectrometry study of HP suggested that HSulf-1 may have to a lesser extent activity toward another disaccharide motif within HP, the 6-, *N*-sulfated disaccharide (134). This study also showed that the smallest substrate for the HSulf-2 was a fully sulfated tetrasaccharide. All *in vitro* studies showed that this novel class of enzymes definitely had the greatest substrate specificity toward trisulfated IdoA2S-GlcNS6S disaccharides found within highly sulfated NS-domains. The consensus for whether Sulf have substrate specificity for other disaccharide motifs found in HP/HS is unclear.

To complicate the issue of Sulf substrate specificity, murine embryonic fibroblast (MEF) cells from Sulf knockout mice were used to evaluate the activities of Sulfs on the disaccharide level. Analysis of HS from MEFs showed that there was an increase in 6-*O*-sulfation for UA-GlcNAc6S disaccharides found in transition zone domains (NA domains), UA2S-GlcNS6S disaccharides found in highly sulfated NS-domains, and UA-GlcNS-6S disaccharides found in moderately sulfated NA/NS domains (135). In addition, loss of either one or both Sulfs resulted in an increase in the 6-*O*-sulfation of a different composition of these disaccharide even though *in vitro* studies have suggested that Sulf-1 and Sulf-2 have functional redundancy (*127, 136*). A combination of *in vitro* and *in vivo* studies showed that changes in 6-*O*-sulfation by loss of Sulfs produce a moderate change in *N*- and 2-*O*-sulation of HS that influence the HS biosynthetic pathway for regulating biological functions (*135,*

137). This suggests that Sulfs along with sulfotransferases have a dynamic relationship that results in the complexity of HS and challenges the current model of HS biosynthesis which suggests that biosynthetic enzymes and Sulfs function independently of each other (138).

Role in development

Their ability to regulate the amount of 6-*O*-sulfation within HS chains has the ability to alter the structure-function relationship with proteins in mature as well as developing bodies of different species. It has been shown that Sulfs can modulate Wnt ability to associate with its receptor Frizzled (*123, 132, 137, 139*). It also has a positive effect on BMP releasing it from its inhibitor Noggin and allowing it to interact with its receptor (133). However, Sulfs have the ability to inhibit FGF signaling by disrupting the formation of FGF2-HS-FGFR ternary complex (140). They can additionally have positive or negative effects on growth factors such as vascular endothelial growth factor (VEGF), FGF1, cytokines, and chemokines (141).

Moreover, Sulf-1 and Sulf-2 were expressed in normal and osteoarthritic (OA) human articular cartilage in addition to joints from normal and aging mice. Sulfs expression level was significantly raised in human OA cartilage and aging mouse joints compared to their normal counterparts (142). Moreover, it has been demonstrated that TGF-β1 can induce the expression of HSulf-1 *in vitro* and *in vivo*, and HSulf-1 may provide negative feedback in order to regulate TGFβ1 in pulmonary fibrosis (143). Studies show that Sulfs modulate growth factor signaling that is essential in the digital development of the quail autopod and the differentiation of satellite cells during muscle regeneration in mice (*144, 145*) In developing quail, Sulf-1 expression and activity are found in somites, axial structures, and

differential stages of cartilage and joint formation (146). In addition, RSulfFP1 found in rat oligodendrocyte progenitor cells (OPCs) was down-regulated by TGFα, and further investigation led to the expression of this Sulf in OPC regulated cell migration and Wnt activity was correlated with tyrosine phosphorylation of β-catenin (147). The regulator effects of Sulf activity suggest they are important modulators of variety of developmental and physiological processes.

Furthermore, mouse studies were conducted to understand the function of Sulfs *in vivo*. In the developing skeleton of mice, Sulf-1 and Sulf-2 are reported to have a redundant function but displayed specific malformations with premature bone ossification and fusion in the sternum, lumbar and tail vertebrae, and reduced bone length(148). In addition, Sulf-1 and Sulf-2 play an important role in esophageal innervation by reducing GDNF binding to HS and allowing it to interact with its receptor to produce GDNF signaling and neurite sprouting in the developing esophagus of mice (149). Results showed that Sulf-1 knockout mice did not show any obvious phenotype except for an increase in the mortality rate within the first couple of months (135). Sulf-2 knockout mice had a reduction in litter size and body weight as compared to their wild-type counterparts. Sulf-1 and Sulf-2 double knockout mice had a decreased litter size, decreased body weight, and were hard to obtain due to a short live span. Sulf-2 gene trap experiments, an approach that is used to introduce insertional mutations into the Sulf gene, revealed strain-specific non-penetrant defects, which adversely effected lung growth and development along with overall viability (150). The results suggest that Sulfs have distinct activities *in vivo* and are necessary for development and viability.

Role in cancer

In addition, changes in Sulfs expression in certain types of cancers can have either beneficial or adverse affects. HSulf-1 mRNA is detected in normal ovarian, breast, renal, pancreatic, and liver. However, it is undetectable in 5 of 7 ovarian carcinoma cells, and HSulf-1 was significantly diminished in or undetectable in approximately 75% of ovarian cancers (151). Down-regulation of HSulf-1 was detected in some breast, renal, pancreatic, and hepatocellular carcinoma cell lines. Re-expression of HSulf-1 in ovarian cell lines reduced heparin-binding growth factor signaling, reduced cell proliferation, and made cells more susceptible to apoptosis via a kinase inhibitor and a chemotherapeutic agent (151). HSulf-1 is down-regulated in squamous cell carcinoma of the head and neck. Re-expression of HSulf-1 inhibited hepatocyte growth factor (HGF) signaling, cell growth, and cell motility and invasion (152). Additionally, in breast cells HSulf-1 can reduce proliferation *in vitro* and reduce tumor size and angiogenesis *in vivo* (153). Conversely, HSulf-2 mRNA was significantly higher in breast carcinomas as well as brain tumors, and colon carcinomas compared to their normal counterparts (*154, 155*). In hepatocellular carcinoma HSulf-2 re-expression promoted histone H4 acetylation, increased the effectiveness of histone deacetylase inhibitors, and inhibited tumorigenesis (156). Nevertheless, HSulf-2 was shown to up-regulate glypican-3, increased FGF signaling, and lowered survival in hepatocellular carcinoma (157). In addition, in subsets of cancers including breast cancer, pancreatic cancer, lung adenocarcinoma, and hepatocellular carcinoma HSulf-1 is significantly upregulated (158-162). HSulf-2 is additionally upregulated in some subsets of breast cancers especially estrogen-receptor positive tumors as well as CNS cancer and multiple myeloma (*136, 154, 155*). Both HSulf-1 and HSulf-2 are upregulated in Wnt-dependent pancreatic

adenocarcinoma tumors. Producing mutations in HSulf-2 or siRNA silencing of HSulf-2 has led to reduced Wnt signaling which subsequently reducing cell growth *in vitro* and tumor growth *in vivo* (139). Over-expression of both HSulf-1 and HSulf-2 in myeloma tumors suggested that Sulfs present within the tumor microenvironment are able to inhibit growth factor signaling and other factors that attribute to tumor growth *in vivo* (136).

Loss of HSul-1 expression increases both autocrine and paracrine proliferation signaling by amphiregulin and heparin binding epethelilial growth factor (HB-EGF), HB-growth factors of the EGF superfamily, and re-expression of HSulf-1 in breast cancer is shown to decrease cyclin D1 levels leading to decreased S-phase fraction and increased G2-M fraction and cell death (163). Furthermore, down-regulation of HSulf-1 via DNA methylation and histone H3 methylation can lead to chemoreistance, and treatment with demethylating agent and/or deacytelase inhibitor can reactivate HSulf-1 expression in ovarian cancer cell lines leading to increased sensitivity to chemotherapeutic drugs (164). DNA methylation was also demonstrated in the silencing of 3-OST-2 in human breast, colon, lung, and pancreatic cancers (165). Taken together, the silencing enzymes involved in HS biosynthesis and remodeling such as Sulfs can raise the level of sulfation within HS. As a result, altered HSPGs are involved in cancer development and progression.

Heparanase

Heparanase is a mammalian endo-β-glycosidase derived from normal and malignant cells and tissues including placenta, liver, endothelial cells, platelets, mast cells, neutrophils, macrophages, and T and B lymphocytes that can be secreted into the ECM (166-169). The cloning and expression along with biochemical studies on heparanase suggest it has no

isoforms (168). Heparanase is a 65 kD proenzyme that is processed by cleavage to form a heterodimeric protein, which contains a 50 kDa and 8 kDa subunits connected by a linker region (*170, 171*). Proteolytic cleavage of the linker promotes a conformational change that produces an enzymatically active protein. This allows heparanase to cleave the glycoside bond of HS via a hydrolase mechanism. The mode of action of heparanase separates it from bacterial heparinases that deploymerize HS chains by eliminative cleavage. Heparanase activity only digests HS at a few sites producing approximately fragments 10-20 residues in length. It has been suggested that heparanase requires *O*-sulfation, but *N*-sulfation or IdoA residues are not necessary for cleavage to occur, but 2-*O*-sulfation on a hexuronic acid residue near the cleavage site may be critical for substrate recognition (172). The degradation of HS into smaller fragments produces normal and pathological changes that involve a variety of HS binding proteins such as growth factors, chemokines, and morphogens (*15, 33*). In addition, heparanase is significantly elevated in many types of cancer, and is linked to cancer progression and poor prognosis (*173, 174*). The development of therapeutic agents to inhibit heparanase activity led to the synthesis of PI-88, which is mixture of highly sulfated mannan penta- and tetrasaccharides isolated from yeast *pichia pastoris*. It is a HS mimic, which has been proven to inhibit heparanase activity and compete with HS in binding to growth factors that result in the decrease in tumor angiogenesis and metastasis *in vivo* (*175, 176*). To date, PI-88 is the only heparanase inhibitor to reach clinical trials for its effectiveness in several types of cancers.

Section III: Structural Analysis of Heparan Sulfate

The heterogeneity and diversity of HS has made it a very challenging macromolecule to analyze and decode it chemical structure. With all of the emerging data involving HS in numerous physiological interactions, it is critical to elucidate the structure-function relationship. Unfortunately, there is no available method such as DNA sequencing to analyze the sequence of HS. In addition, structural analysis of HS would require a pure sequence, but this would be difficult since HS is not a template driven process and produces a mixture of different lengths and sulfation pattern of HS. Currently, only HS oligosaccharides less than tetradecasaccharide can be completely sequenced (177). Therefore, it is not possible to structurally characterize HS on the polysaccharide level.

Heparin Lyase Degradation

Structural analysis of HS can be accomplished at the disaccharide level. This requires depolymerization of the polysaccharide chain to generate disaccharides to determine their identity and relative compositions by separation techniques such as reverse-phase-ion-pairing (RPIP) HPLC or mass spectrometry. There are two methods for depolymerizing HS polysaccharides. The first technique is an enzymatic method that utilizes heparin lyases. Heparin lyases are expressed and purified from *Flavobacterium heparium* (178). There are three isoforms of the enzyme that have specific substrate cleavage sites as depicted in Figure 18. Heparin lyase I breaks the glycosidic linkage between *N*-sulfated glucosamine (GlcNS) and 2-*O*-sulfated iduronic acid (IdoA2S). Heparin lyase III cleaves the glycosidic linkage between either *N*-acetyl glucosamine (GlcNAc) or GlcNS and nonsulfated glucuronic acid (GlcA). Heparin lyase II contains broad substrate specificity. It cleaves the linkage between

GlcNAc/GlcNS and GlcA/IdoA residues. A mixture of heparin lyases are usually used together to generate a high degree of polymerization. The cleavage of the glycosidic bonds of HS create disaccharides containing a $\Delta^{4,5}$-unstaturated uronic acid at the non-reducing end, which can be detected by UV absorption at 232nm. However, the depolymerization using a mixture of these enzymes does not go to completion and some disaccharide species may be underestimated (177).

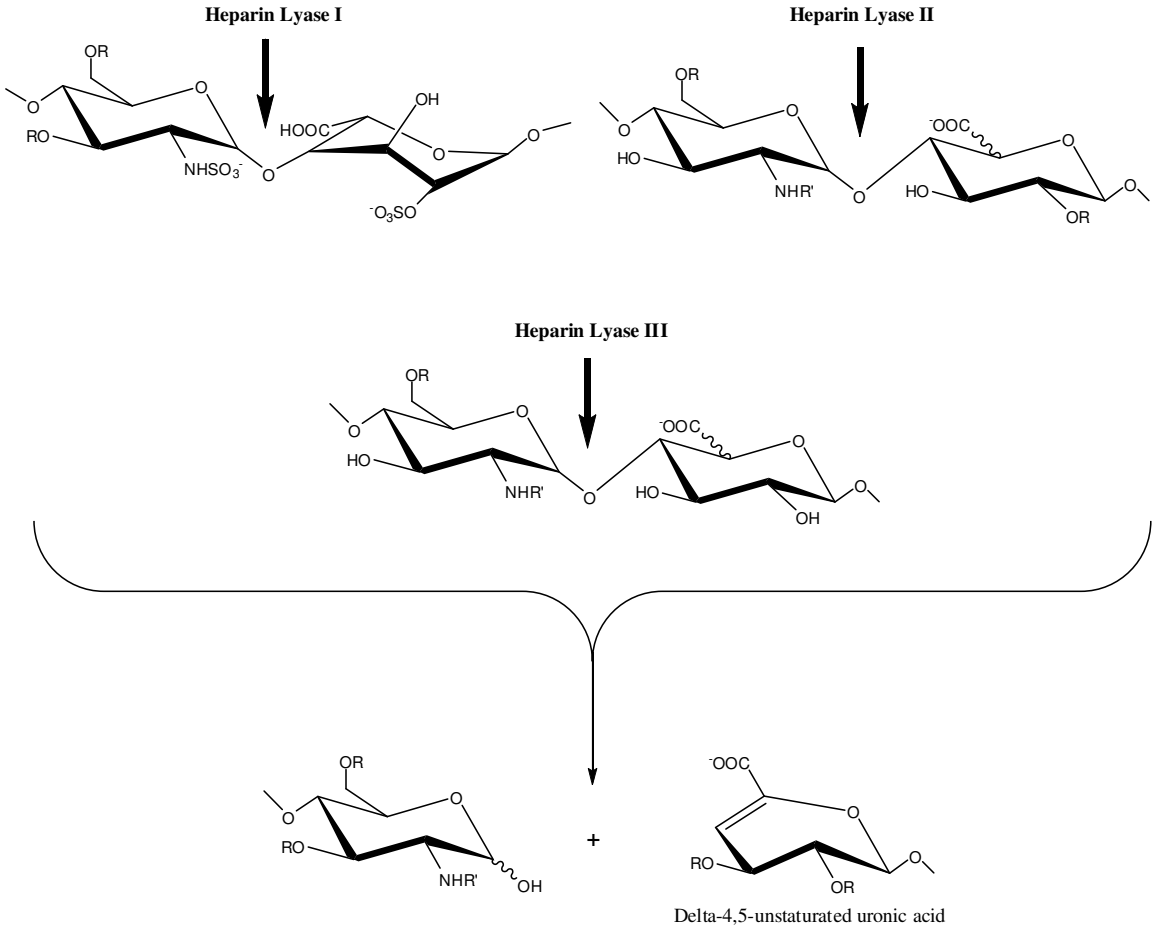

Figure 18. Heparin lyases substrate specificity. R represents a sulfate or proton. R' represents a sulfate, acetyl, or proton.

Nitrous Acid Degradation

The second method for generating disaccharides is a chemical method employing nitrous acid. This is a common method that breaks the glycosidic linkage of either *N*-sulfated glucsoamine (GlcNS) or *N*-unsubstituted glucosamine ($GlcNH_2$) at the reducing end as shown in Figure 19. At low pH nitrous acid degradation (pH 1.5), the nitrous acid prefers to react with GlcNS residues (179). At high pH (pH4.5-5.5), the nitrous acid predominately reacts with $GlcNH_2$ residues (180). The advantage of this technique is that configuration of the uronic acid (GlcA or IdoA) is retained, but the disaccharide must contain a fluorescent or radioactive tag for detection (180). The detection of the resultant disaccharides can also be achieved by mass spectrometry.

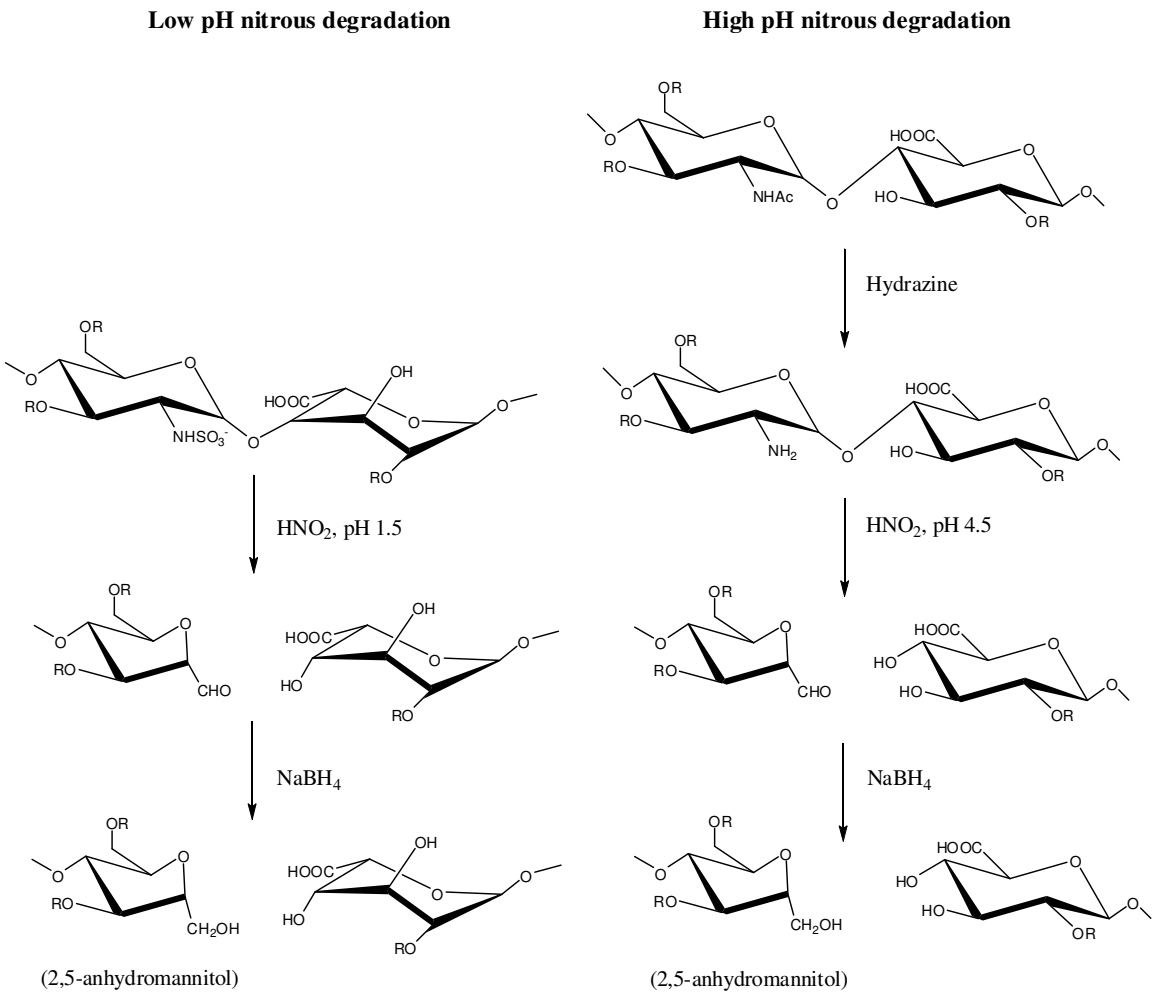

Figure 19. Nitrous acid degradation of HS. The linkage between *N*-sulfated glucosamine and uronic acid is cleaved at pH 1.5 by nitrous acid. For nitrous acid degradation at pH 4.5-5.5, *N*-acetylated glucosamine is first converted to *N*-unsubstituted glucosamine, since high pH nitrous acid degradation only cleaves the linkage between *N*-unsubstituted glucosamine and uronic acid.

A common method to resolve a mixture of disaccharide is by RPIP-HPLC. The advantage of this method is that it can identify many combinations of disaccharides containing either GlcA or IdoA with different numbers of sulfo groups present. Unfortunately, this method can only produce information on a disaccharide level and cannot provide how the disaccharides are linked together to form the oligo- or polysaccharide.

However, it is a powerful tool in determining substrate specificity of enzymes involved in modifying HS and determining different disaccharide motifs within a structure.

Sequencing Strategy

In addition, another strategy for elucidating the structural sequence of HS oligosaccharides can be accomplished in two steps. The first step would introduce either a mass, radiolabel, or fluorescent tag at the reducing end of the oligosaccharide (181-183). The tagged oligosaccharide would be subjected to partial or exhausted digestion by either heparin lyases or nitrous acid, and the tag would aid in determining if the resulting product originated from the reducing end once compared to standards. The second step involves treatment of the non-reducing end with exoenzymes such as sulfatases, hexauronidases, and α-hexaminidases. These exoenzymes would aid in the identification of each residue after each treatment once compared to standards. The disadvantage of this strategy is that it would require a sufficient amount of material and time to complete each step.

Furthermore, another strategy would be the employ mass spectroscopy (MS) for structural analysis of HS. Recent advances in this technology have permitted a more direct sequencing method that can deduce relatively large oligosaccharide sequences by depolymerizing the oligosaccharide and then identifying overlapping sequences. Matrix-assisted laser desorption/ionization MS (MALDI-MS), electrospray ionization (ESI-MS), and a combination of RPIP-HPLC/ESI-MS are MS techniques have helped determine the sequence of HS oligosaccharides (184-186). Nonetheless, these MS methods need to be improved, because they cannot obtain data for oligosaccharides larger than a tetradecasaccharide.

Section IV: Important Protein Interactions

Antithrombin

Antithrombin (AT) is a critical mediator in blood coagulation. It is a 58kDa serine protease inhibitor that deactivates factor Xa and thrombin (IIa) activities involved in the cleavage of fibrinogen to fibrin (blood clot). AT is activated by its binding to HS/HP. The mechanism of action for active AT involves an amino acid P1 loop which serves as a substrate for the serine protease. AT undergoes a conformational change once the P1 loop is cleaved, which results in the protease being covalently attached as a inactive, acyl-enzyme intermediate to AT (*187, 188*). Many studies have examined the correlation of HP/HS and AT in anticoagulant activity in the blood coagulation cascade. It has been shown that once AT binds to HS it increases the affinity of AT about 1,000-fold for Factor Xa and thrombin (189). Through extensive study of HS and AT structure-function relationship, an AT binding pentasaccharide, -GlcNS(or Ac)6S-GlcA-GlcN3S±6S-IdoA2S-GlcNS6S-, was identified which has a 10-50nM binding affinity to AT. Upon further structural analysis, the 3-*O*-sulfated glucosamine residue is critical for binding and increases the binding affinity by 20,000-fold (190). The discovery of the AT binding pentasaccharide has lead to the clinical development of Low Molecular Weight Heparin (LMWH), such as Lovenox®, and the synthetic HS pentasaccharide Arixtra®. The crystal structure of AT complexed with the pentasaccharide has been solved, and has shown extensive hydrogen bonding with the carboxylate groups on hexuronic acid and 3-*O*- and 6-*O*-sulfo groups of glucosamine (191).

In addition, the crystal structure does not show the interaction of AT with 2-*O*-sulfo groups of the IdoA residue, and studies have shown that it is not crucial for AT binding (192). Furthermore, it has been shown using a chemoenzymatic approach that an

anticoagulant structure devoid of IdoA2S residues are not essential for AT binding and anticoagulant activity (193). Moreover, in order for clinical anticoagulant drugs to be effective, they need to inhibit Factor Xa and thrombin. Arixtra can inhibit Factor Xa but not thrombin. In order to inhibit thrombin, anticoagulant heparin needs to be at least 14-20 residues in length to generate a bridge between AT and thrombin to create a ternary complex (194).

The administration of anticoagulant heparin has many beneficial effects in treating arterial and venous thrombic disorders as well as in surgery (195). However, heparin-induced thrombocytopenia (HIT) can occur during treatment. Platelet factor 4 (PF4) is a chemokine secreted form platelets. HIT develops when PF4 binds and forms a complex with heparin. Antibodies are generated to attack this complex and create a severe immunological response. It has been demonstrated that 2-*O*-sulfo groups on IdoA residues are important for PF4 binding, and 6-*O*-sulfo groups on glucosamine residues may have some requirement for binding to PF4 (196). However, *N*-sulfo groups are not necessary for binding. Moreover, PF4 can inhibit AT mediated inactivation of Factor Xa (197). Thus, side effects such as PF4 can lower the efficacy and predictability of anticoagulant heparin. Therefore, anticoagulant research has focused on developing a better heparin, and trying to understand the underlying mechanisms that cause unfavorable outcomes with the usage of anticoagulant therapies.

Fibroblast Growth Factor

Fibroblast growth factors (FGFs) are involved in many cell signaling events that are implicated in angiogenesis, tumor progression, embryonic development, and even wound healing (198-200). The FGF family contains 22 members, which bind ligand dependent FGF

receptor tyrosine kinases (FGFR1-4). Once FGF binds to its receptor, receptor dimerization occurs, which leads to phosphorylation and activation of downstream molecules that initiate the signaling cascade. Cell based studies have demonstrated that HP/HS binding to FGF allows it to bind to its receptor and promote FGF signaling (*201, 202*). Both mouse and *Drosophila* genetic studies have shown that HS is vital for FGF signaling (*203, 204*). In addition, along with the length of the polysaccharide, IdoA2S and GlcNS residues are important for signaling by FGF-1 and FGF-2. However, 6-*O*-sulfation is necessary for FGF-1 signaling but not for FGF-2 signaling (205).

Two models have emerged from two crystal structures solved for the FGF/HP/FGFR ternary complex are shown in Figure 20 (*207, 208*). For the ternary complex containing FGF-2, the 2:2:2 stoichiometry is referred to as the "two end model", where two HP molecules make contact with one FGF and one FGFR in addition to each HP making contact with another FGFR. For the ternary complex containing FGF-1, an "asymmetric" 2:2:1 stoichiometry is shown, where one HP molecule comes into contract with two FGFs and one FGFR. Each model gives a different depiction of how each FGF subtype and HP interacts with FGFR. However, in order for the receptor tyrosine kinases to undergo *trans* autophosphorylation, they need to be in close proximity to each other. Mutational studies confirm the physiological relevance of this model. Therefore, the "two end model" meets this requirement and would seem more feasible in a biological context (206).

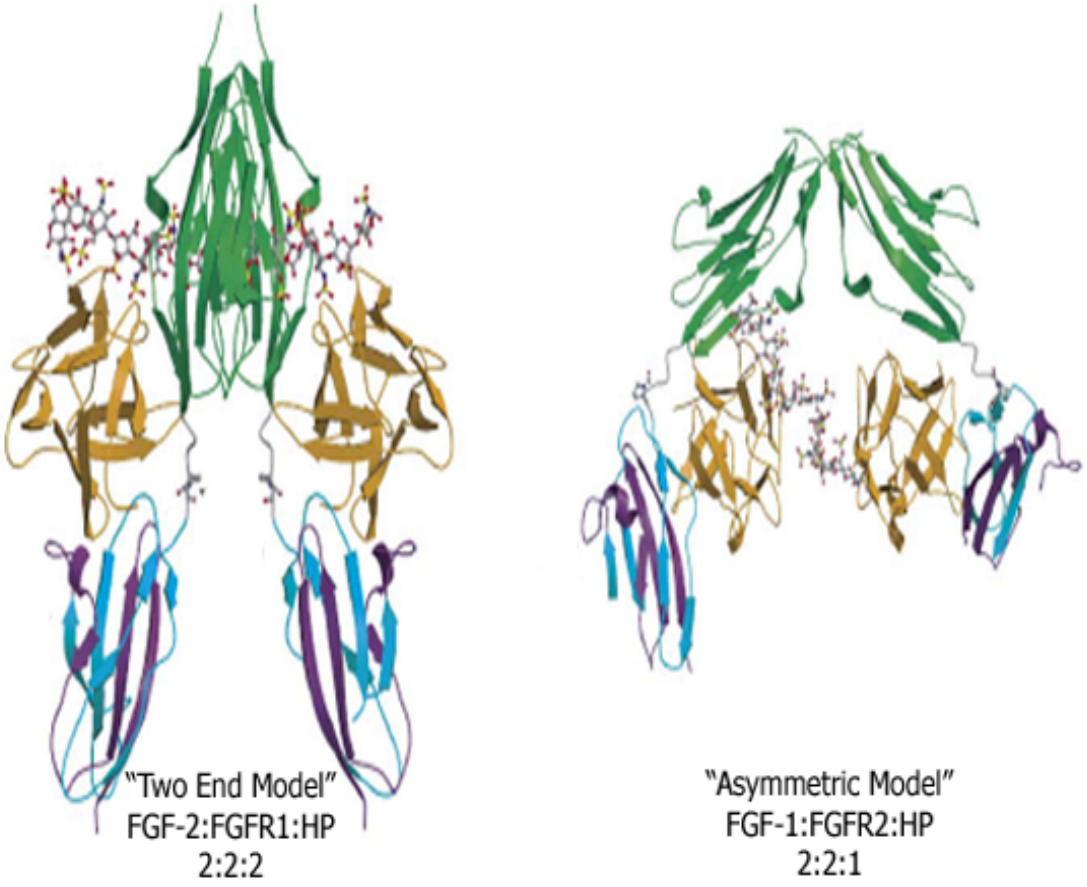

Figure 20. Two crystal structures of FGF:FGFR:HP ternary complex (206). Each crystal structures show the two different binding interactions. FGF is represented in *green* and FGFR in *orange*. HP atom coloring is *red* for oxygens, *yellow* for sulfurs, *blue* for nitrogens, and *gray* for carbons.

Statement of Problem

Heparan sulfate (HS) is a highly sulfated GAG present in significant quantities on the cell surface. The biosynthesis of HS is a complex process leading to structurally heterogeneous structures. To further complicate this process, HS can be remodeled in the extracellular environment by a novel class of Sulf enzymes. Previous studies have shown the extracellular remodeling by Sulfs has been involved in Wnt signaling in addition to the progression of certain types of cancers. Effects on biological functions due to Sulf tailoring of the fine structure of HS may provide new insights into understanding and modulating these activities.

Utilizing the substrate specificity of Sulfs along with its HS tailoring abilities, Sulfs can provide us with additional information about the structure-function relationship of HS and other biological molecules. In addition, harnessing Sulf editing activities may aid in developing or improving therapeutic drugs. The goals of this dissertation are to provide additional information about the substrate specificity of a human Sulf in regard to activity against different disaccharide motifs within HS polysaccharides other than IdoA2S-GlcNS6S such as GlcA-GlcNS6S or GlcA2S-GlcNS6S. In addition, we want to demonstrate that Sulfs can be used as a tool for editing HS polysaccharide based drugs.

CHAPTER II

MATERIALS AND METHODS

Mammalian Cell Culture

Maintenance of CHO cells was performed according to an established protocol. Cells were grown in a T75 flask with F12 medium supplemented with 10% fetal bovine serum (FBS, JRH Bioscience) and antibiotics penicillin/streptomycin. Cells were passaged using a standard protocol after cells reached 90% confluence. Briefly, the cells were washed three times with 1 × phosphate buffered saline (Gibco), and detached from the flask with 2ml of buffered trypsin (Gibco) at 37ºC. Once detached, the cells were diluted to 10ml with supplemented F12 medium and the concentration (cells/ml) was determined by using a hemocytometer under a microscope. Cells were seeded into a new flask at approximately 10^5 cells per flask. For long term storage, cells were passaged as described above and then centrifuged at 500×g for 15min. The cells (10^7 cells/ml) were then resuspended in F12 medium containing 10%FBS and 10% dimethyl sulfoxide and frozen slowly at -80ºC by placing them in a double insulated container.

Agarose Gel Electrophoresis

PCR products and DNA plasmid construct quality were assessed by agarose gel electrophoresis. Briefly, a 1% agarose solution was made by microwaving 0.4 g agarose with 40 ml 10 mM Tris-acetate 1 mM EDTA (TAE) buffer. Once the solution cooled to approximately 70 °C, 1 µl of 5 mg/ml solution of ethidium bromide was added and the

agarose was poured into a standard gel casting box with a well comb. After the gel set, 1x TAE buffer was added to the gel box and samples were diluted 2 fold with loading buffer (50% glycerol, 0.0125% bromophenol blue) and added to separate wells. The gel was run at 120 volts and analyzed under UV light.

Preparation of [^{35}S] HS

Wild-type CHO and HSulf-2/CHO were grown to 90% confluence in F12 media containing 10% FBS and 100 Units/mil Penicillin/Streptomycin. Cells were grown in the growth media containing 1 mCi/ml of sodium [^{35}S] sulfate (ICN) for 10 h. [^{35}S]HSPGs were harvested and purified on a DEAE column and subjected to β-elimination under alkaline conditions followed by phenol extraction to remove polypeptides. [^{35}S]HS was then isolated by ethanol precipitation. The estimated specific ^{35}S-radioactivity of the [^{35}S] HS was 4 x 10^7cpm/μg. We observed that the yield of [^{35}S] HS from HSulf-2/CHO cells was comparable to that from wild type CHO cells.

Western Blotting Analysis

Protein was run on an SDS-PAGE gel. The protein from the SDS-PAGE gel was transferred onto a nitrocellulose membrane (Amersham). The membrane was soaked in PBSTM (PBS, 0.1% Tween 20, 5% w/v nonfat dry milk) for 1 hour at room temperature to block nonspecific binding of the antibody. The membrane was washed with PBST (PBS, 0.1% Tween 20) for 15 minutes then 5 minutes at room temperature. The membrane was probed with anti-*myc* antibody (1:3000) in PBSTM overnight at 4ºC. The membrane was washed with PBST for 15 minutes then 5 minutes at room temperature, and then incubated

with horseradish peroxidase-conjugated anti-mouse IgG secondary antibody (1:5000) in PBST for one hour at room temperature. The membrane was subsequently washed briefly two times with PBST, and then washed with PBST for 30 minutes. The membrane was then washed three times for five minutes with PBST, and the signals were detected by ECL detection system that employs chemiluminescence.

Quantification of Purified Lovenox-Alcian Blue Assay

The amount of lovenox was quantified using an alcian blue assay previously described (209). Briefly, the alcian blue dye stock solution was made by dissolving 1mg of the dye with 100ml of 18mM H_2SO_4, a 1/100 dilution of the resulting dye stock solution should have an A_{600nm} of approximately 1.4. Additional dye was added if the appropriate absorbance was not reached. This was followed by centrifugation at 10,000rpm for 30min. to remove insoluble dye particles. Standards and unknown samples were prepared in duplicate with standards of lovenox ranging from 0-2.0µg. All samples were brought up to 10µl with distilled water, followed by the addition of 10µl of reagent A. Reagent A contained a 1:1 ratio of 8M guanidine-HCl and 54mM H_2SO_4, 0.75% Triton X-100, this solution was prepared fresh with each use. Then 100µl of working dye was added to all samples bringing the final volume of the samples to 120µl. The working dye solution contained 18mM H_2SO_4, 0.25% Triton-X100, and 5% dye stock solution, which was filtered through a 0.2µm filter and the resultant solution was centrifuged at 10,000rpm for 10min. to remove any insoluble material. The samples were mixed thoroughly and centrifuged at 14,000rpm for 30min. The pellet was dissolved with 500µl of 8M guanidine-HCl after the supernatant was removed. The samples were analyzed at A_{600nm}.

SDS-PAGE Electrophoresis

Protein purity was determined using SDS-PAGE using precasted Tris-Tricine SDS-PAGE (16.5% resolving gel, 4% stacking gel, 8.6 × 6.8cm (W × L), BioRad). Samples (10µl) were diluted with an equal volume of sample buffer (200mM Tris-HCl, pH 6.8, 2% SDS (BioRad). Gels were run at 100V for 45min., and then stained with coomassie blue (0.4%) for 1hr. Gels were destained with 10% acetic acid.

Affinity Co-Electrophoresis (ACE)

To quantitatively determine the binding affinity between 3-OST-1 and 3-OST-5 modified polysaccharide from Chinese hamster ovary cells and AT, an affinity co-electrophoresis approach was used in a similar manner as previously described (*210, 211*). Purified AT was cast in 1% low melting point agarose (GIBCO) separation zones in a degassed gel buffer containing 125mM sodium acetate and 50mM 3-(*N*-morpholino)-2-hydroxhypropane-sufonic acid, pH 7, at nine final concentrations ranging from 0-60nM of AT in each zone. In separate experiments, nonradioactive labeled 3-*O*-sulfated [^{35}S] HS polysaccharide from Chinese hamster ovary cells was loaded into each separation zone and the gel was subjected to electrophoresis at 350mA for 2 hr. 30min. in circulated cold gel buffer. The gel was dried using a Bio-Rad Gel Air dryer, and analyzed on a Phosphor Imager (Amersham Biosciences, Storm 860). The binding affinity between the nonradioactive labeled 3-*O*-sulfated [^{35}S] HS polysaccharide and AT was calculated as a K_d value by plotting R/gD verses R, where the retardation coefficient $R = (M_0\text{-}M)/M_0$. M_0 is representative of the migration of the free nonradioactive labeled 3-*O*-sulfated [^{35}S] HS polysaccharide, and M is the observed migration of the nonradioactive labeled 3-*O*-sulfated

[^{35}S] HS polysaccharide in the presence of a specific concentration of AT located in a separation zone. Based on the Scatchard equation, the calculation of the slope from the resulting plot yields -1/K_d.

Heparin Lyase Digestion

The digestion of unmodified and modified polysaccharides were carried out as previously described (212). Digestions were carried out in 250µl of 50mM ammonium acetate (pH 7) containing limited amounts of heparin lyase I, II, and III, which are expressed and purified using a bacterial expression system. The reactions were incubated at 37ºC overnight, and the reactions are terminated by heating at 100ºC for 2min. The resultant material was centrifuged for 5min. at 13,000rpm to remove any insoluble material and was subsequently ready for HPLC analysis, or placed on a Bio Rad P-2 column for further further purification of oligosaccharides. Oligosaccharides were collected, dried down in a speed vacuum, and then resuspended in water and ready for HPLC analysis.

Polyamine-High Performance Liquid Chromatography (PAMN-HPLC)

Samples were analyzed using PAMN chromatography. The elution profile was monitored as the [^{35}S] labeled sample was applied to a silica-based polyamine (PAMN) HPLC column (0.46 × 25cm, Waters) (213) The column was equilibrated with filtered distilled water, and the radioactive material was eluted with a linear gradient of KH_2PO_4 from 0 to 1M in 60min. at a flow rate of 0.5ml/min., followed by a continuous state of washing at 1M for up to 100min. The [^{35}S] elution profile was monitored using an online radioactive detector.

Preparation of HSulf-2 Transiently Expressed CHO Cells (HSulf-2/CHO)

The expression plasmid pcDNA3.1A-*myc*/His-HSulf-2 was transiently transfected into wild type CHO cells using LipofectAMINE 2000 (Invitrogen, Inc.) following the manufacturer's protocol in 6 well plates. After 48 hrs., conditioned medium (CM) was collected, dialyzed against 50mM HEPES, pH 8.0, concentrated 20×, and stored at -80ºC until needed. Cells were washed 3×1ml cold 1×PBS, and then harvested by scraping cells from plate. Cells were centrifuged at 2,000rpm for 10min., and the cell pellet was subjected to mixture of 1.5M sucrose, 1% triton X-100 for 1hr. on ice. The mixture was centrifuged at 14,000rpm at 4ºC for 20min to separate the cellular debris. The supernatant (cell extract) was stored at -80ºC until needed.

Reverse Phase Ion Pairing-High Performance Liquid Chromatography (RPIP-HPLC)

The disaccharides were analyzed by reverse phase ion pairing RPIP-HPLC. Briefly, a C18 reverse phase column (Vydac or ThermoFischer) was equilibrated with 38 mM ammonium dihydrogen phosphate, 2 mM phosphoric acid and 1 mM TBA dihydrogenphosphate and eluted with acetonitrile at 8% for 45 minutes, at 15% for 15 minutes, and at 19.5% for 30 minutes in a solution containing 38 mM ammonium dihydrogen phosphate, 2mM phosphoric acid, 1 mM TBA dihydrogen phosphate at a flow rate of 0.5 ml/min. The identities of the disaccharides were confirmed by co-elution of ^{35}S-labeled and disaccharide standards (Sigma-Aldrich).

AT Affinity Assay

[^{35}S]HS was incubated with 5 µg AT in 50 µl of reaction buffer containing 10 mM Tris-HCl (pH 7.5), 150 mM sodium chloride, 1 mM Mn^{2+}, 1 mM Mg^{2+}, 1 mM Ca^{2+}, 10 µM dextran sulfate, 0.02 % sodium azide and 0.0004 % Triton X-100 for 30 minutes at room temperature. 100 µl of 1:1 slurry of aged ConA-Sepharose was added, and the reaction was agitated for one hour at room temperature on an orbital shaker. The beads were washed three times with the reaction buffer and eluted with buffer containing 10 mM Tris-HCl (pH 7.5), 1000 mM sodium chloride, 1 mM Mn^{2+}, 1 mM Mg^{2+}, 1 mM Ca^{2+}, 10 µM dextran sulfate, 0.02% sodium azide, and 0.0004% Triton X-100.

Assay for the AT-Mediated Deactivation of Factor Xa by Lovenox

Briefly, factor Xa (Enzyme Research Laboratories, South Bend, IN) was diluted to 10U/ml with PBS containing 1 mg/ml BSA. The chromogenic substrates S-2765 (for factor Xa assay) was purchased from Diapharma and prepared at 1 mM with PBS. Lovenox was dissolved in PBS containing 1mg/ml BSA at various concentrations (1–400 ng/ml). The reaction mixture, which consisted of 1µl AT(2mg/ml) and various concentrations of lovenox was incubated at 37°C for 2 min. Factor Xa (1µl) was added. After incubating at 37°C for 4 min, 15µl S-2765 was added to a final volume of 100µl. The absorbance of the reaction mixture was measured at 405 nm continuously for 2 min. The absorbance values were plotted against the reaction time. The initial reaction rates as a function of concentration were used to calculate the IC_{50} values.

DEAE Chromatography

Heparan sulfate polysaccharides were purified by DEAE -Sephacel ion exchange chromatography. Briefly, the reaction was diluted with 3× the reaction volume of UPAS buffer (20mM sodium acetate, 150mM sodium chloride, 3M urea, 0,02% Triton X, pH 5) and applied to a 0.2ml DEAE column. The column was washed four times with 1ml UPAS buffer and then washed two times with 1ml of wash buffer (250mM sodium chloride, 0.001% Triton X). The column was eluted with 1ml of 1M sodium chloride. For modifications with sulfotransferase reactions, the amount of ^{35}S-labeled polysaccharide was determined by scintillation counting (10% of the total eluent volume). The remainder of the eluent was dialyzed against 20mM ammonium bicarbonate for four hours at 4ºC. The dialyzed polysaccharide was dried by centrifugal evaporation and resuspended in water for further use. For analysis of Sulf activity, the radioactivity of the eluent volume of the ^{35}S-labeled polysaccharide was determined by scintillation counting.

Modification of Polysaccharides

The starting material (heparosan, *N*-sulfo heparosan, bovine kidney HS, and CDNS heparin) were modified by 5-10µg of NST-1, C_5-Epi, 2-OST, 6-OST-1/3, 3-OST-1, and 3-OST-5, 0.5 to 1 $\times 10^6$ cpm [^{35}S] PAPS, 10nmols unlabeled PAPS to produce the desired polysaccharide. Reactions were incubated at 37ºC for 1hr. The reaction was heat deactivated in a 100 °C for two minutes. The polysaccharides were purified by DEAE ion exchange chromatography. The amount of [^{35}S] sulfo groups per chain and pmols of [^{35}S] sulfation of ^{35}S-labeled disaccharide was measured based on the specific ^{35}S radioactivity.

Spin Column Assay

The G-25 sephadex spin column (Roche) was centrifuged at 2000 rpm to remove storage buffer. The reaction was applied to the spin column and centrifuged at 2000 rpm for 4 min. The eluent was collected and the amount of ^{35}S-labeled polysaccharide was determined by scintillation counting.

HSulf-2 Enzymatic Assay

Substrates were mixed with 50µl of concentrated (20×) HSulf-2 conditioned medium from Chinese hamster ovary cells, 50mM HEPES pH8.0, 10mM $MgCl_2$ in a 100µl reaction volume. The reaction mixture was incubated overnight at 37ºC.

FGF BaF3 Cell Assay

The BaF3 FGFR1c cells were maintained in RPMI 1640 media (Sigma, St. Louis, MO) supplemented with 10% fetal bovine serum, 0.5 ng/ml IL-3 (PeproTech, Inc., Rocky Hill, NJ), 2 mM l-glutamine, penicillin (50 IU/ml), and streptomycin (50 µg/ml), and 50 µM β-mercaptoethanol. For mitogenic assays, BaF3 FGFR1c cells were washed three times with RPMI 1640 media to remove IL-3 and resuspended in the growth media lacking IL-3. About 30,000 cells were plated per well in a 48-well plate in media containing various concentrations of heparin, lovenox, and 2 nM FGF2 (PeproTech, Inc.) in a total volume of 200 µl. The cells were then incubated at 37°C for 40 hr. To each well, an additional 50 µl growth media containing 1 µCi [^{3}H] thymidine was added. Cells were harvested after 4–5 hr by centrifugation. The incorporation of [^{3}H] thymidine into the DNA was determined by scintillation counting.

Cloning of MBP-Sulfs

EST clones were obtained from Open Biosystems for human and mouse isoforms (accession numbers AF112227, AF097544, AF181684). For the cloning of the full length HSulf-2 construct forward primer 5'-AAAGGGATAGGATCCATGGGCCCCCCGAGC-3' and reverse primer 5'-AAAGGGATAAAGCTTTTAACCTTCCCAGCC-3' were used. For the truncated HSulf-2 construct in which the signal sequence was removed forward and reverse primers 5'-AAAGGGATAGGATCCTTCCTGTCGCACCACCGCCTG-3' and 5'-AAAGGGATAAAGCTTTTAACCTTCCCAGCC-3' were used. For the full length MSulf-2 construct forward and reverse primers 5'-AAAGGGATAGGATCCATGGCACCCCCTGGC-3' and 5'-AAAGGGATAAAGCTTTTAGCCTTCCCAACC-3' were used. For the full length MSulf-1 construct forward and reverse primers 5'-AAAGGGATAGTCGACATGAAGTATTCCCTC-3' and5'-AAAGGGATAAAGCTTCTAACCTTCCCATCC-3' were used. The purified genes from human and mouse were amplified with polymerase chain reaction and primers and cloned into pMAL-c2X vector (New England Biolabs) using BamHI/HindIII (human and mouse Sulf 2) and SalI/HindIII (mouse Sulf 1) sites to generate a maltose-binding protein (MBP)-Sulf fusion protein. Expression of Sulfs was achieved in OriB containing GroEL/ES. The bacteria were grown in LB medium supplemented with 12.5 μg/ml tetracycline, 15 μg/ml kanamycin, 35 μg/ml chloramphenicol, and 50 μg/ml carbenicillin at 37 °C. When the $OD_{600\ nm}$ reached 0.6–0.8 the temperature was lower to 22ºC, and expression was induced by the addition of IPTG and L-arabinose at a final concentration of 0.1 mM and 1 mg/ml, respectively.

PF4 Neutralization Assay

For a 100µl reaction volume, various amounts of PF4 (0-100ug) were pre-incubated with 400ng/ml of lovenox for 2min at 37ºC in a 48 well plate. The mixture of PF4 and lovenox was incubated for 2 min at 37ºC with 1µl AT (2mg/ml). 1µl of Factor Xa (10U/ml) was introduced and incubated at 37ºC for 4 min. 15µl of chromogenic substrate S-2765 (2mg/ml) (Diapharma) was added to the wells, and the plate was read at 405nm for 2min. to determine Factor Xa activity.

PF4 Filter Binding Assay

For a 100µl reaction volume, 10,000cpm of HSulf-2 treated and untreated [^{35}S] HS from CHO cells, increasing amounts of PF4 (1-10µg), and reaction buffer containing 50mM Tris, 130mM NaCl, pH 7.3 were incubated together at 37ºC for 10 min. 200µl of reaction buffer was added to the reaction. The 300µl total volume samples was applied to a buffer equilibrated nitrocellulose membrane (Amersham), and the samples were drawn through the membrane by a vacuum manifold. The membrane was washed 2×500µl with reaction buffer, and then allowed to dry. The remaining radioactivity was detected by a scintillation counter.

CHAPTER III

SUBSTRATE SPECIFICITY OF HUMAN HEPARAN SULFATE 6-*O*-ENDOSULFATASE

Introduction

The biosynthesis of HS has been the subject of various studies that have been previously reported. The discovery of the novel class of enzymes called Sulfs has generated a new perspective on the role of HS once synthesized in the Golgi and released into the extracellular environment. In this chapter the substrate specificity of human heparan sulfate 6-*O*-endosulfatase isoform 2 (HSulf-2) is described. The focus of this chapter is to determine the substrate specificity using synthetic polysaccharide substrates. By using a mammalian expression approach, a sufficient amount of crude HSulf-2 was obtained from transient transfection for this project. HSulf-2 from the conditioned medium of mammalian cells was employed to investigate whether HSulf-2 had a broader substrate specificity than previously reported (124). The method described in this chapter allows for the ability to determine substrate specificity more directly by being able to evaluate the removal of specific sulfo groups from the polysaccharide.

Developing a Method to Measure HSulf-2 Activity

We wanted to develop a rapid and easy method for determining HSulf-2 activity against HS *in vivo*. The strategy was to utilize a method to determine the amount of

radioactivity remaining on the HS polysaccharide. Therefore, DEAE chromatography was chosen. If active HSulf-2 was expressed by CHO cells, the DEAE chromatography method would allow us to rapidly determine whether there was any removal of sulfo groups on the polysaccharide. HSulf-2 was cloned into the pcDNA3.1A/*myc*-His vector, and the transient transfection of the CHO cells was carried out by using a standard procedure. CHO cells expressing HSulf-2 and empty vector separately were metabolically labeled with [^{35}S] Na_2SO_4 and the resultant [^{35}S] HS was isolated from the cells. The [^{35}S] HS was subjected to DEAE anion exchange chromatography as described in Chapter II. ^{35}S-labeled polysaccharide was eluted from the DEAE column, and the amount of radioactivity was determined using a scintillation counter. Results were inconclusive and could not provide evidence of sulfatase activity. It was possible that HSulf-2 was not removing enough sulfo groups on the polysaccharide chain to be accurately determined by this method.

Therefore, disaccharide analysis was utilized as an alternative method to determine the *in vivo* activity of HSulf-2 expressed in CHO cells. This common method is more sensitive and provides structural information about the material being analyzed. Unfortunately, this method requires more time for analysis. If sulfatase activity can be detected by this method, then the digestion of [^{35}S] HS from CHO cells expressing HSulf-2 with a mixture of heparin lyases should yield a decrease in a [^{35}S]-labeled disaccharide with a structure of ΔUA2S-GlcNS6S. As a result of the removal of 6-*O* sulfo groups from the ΔUA2S-GlcNS6S disaccharide motif, the subsequent increase in a [^{35}S]-labeled disaccharide with a structure of ΔUA2S-GlcNS would be observed in the elution profile as shown in Figure 21. This hypothesis was based on a previous study in which HSulf-2 enzyme removed 6-*O* sulfo groups from ΔUA2S-GlcNS6S disaccharide motifs found in heparin

(124). The strategy for the determination of sulfatase activity by disaccharide analysis is described in figure 21.

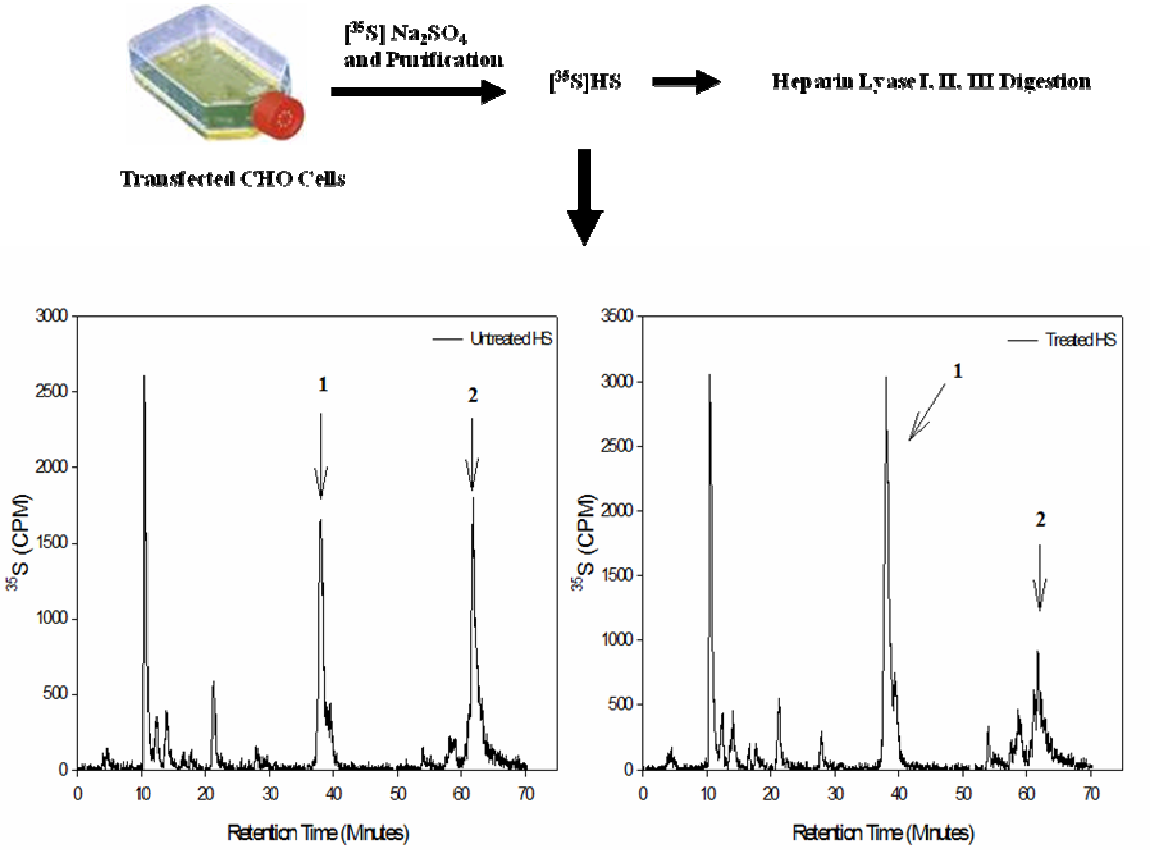

Figure 21. Strategy for the determination of *in vivo* sulfatase activity. If HSulf-2 is present peak 2, ΔUA2S-GlcNS6S, would decrease and peak 1, ΔUA2S-GlcNS, would increase in the elution profile of treated versus untreated material. The removal of 6-*O*-sulfo groups from the polysaccharide would indicate CHO cells were expressing active enzyme.

Disaccharide Analysis of HSulf-2 Treated Heparan Sulfate Confirmed Sulfatase Activity

[^{35}S]-labeled disaccharides were resolved on the RPIP column as shown in figure 22. Along with radioactive detection of the [^{35}S] label, nonradioactive standards with an absorbance of 232nm were co-injected to monitor the elution position of the disaccharides. The separation of the ^{35}S-labeled disaccharides on the RPIP column was based on their negative charge densities. [^{35}S] HS isolated from the mock transfected cells yielded ΔUA2S-GlcNS and ΔUA2S-GlcNS6S disaccharide peaks at 42 min. and 68 min. (Figure 22, panel

A). [^{35}S]-labeled disaccharides isolated from the HSulf-2 transfected CHO cells (Figure 22, panel B) eluted at the same positions. In panel B, the 2-fold reduction of the ΔUA2S-GlcNS6S disaccharide peak along with approximately a 1.5-fold increase in the ΔUA2S-GlcNS disaccharide peak was observed. The summary of the disaccharide analysis is shown in table 3. Overall, these results showed CHO cells were expressing active HSulf-2 enzyme.

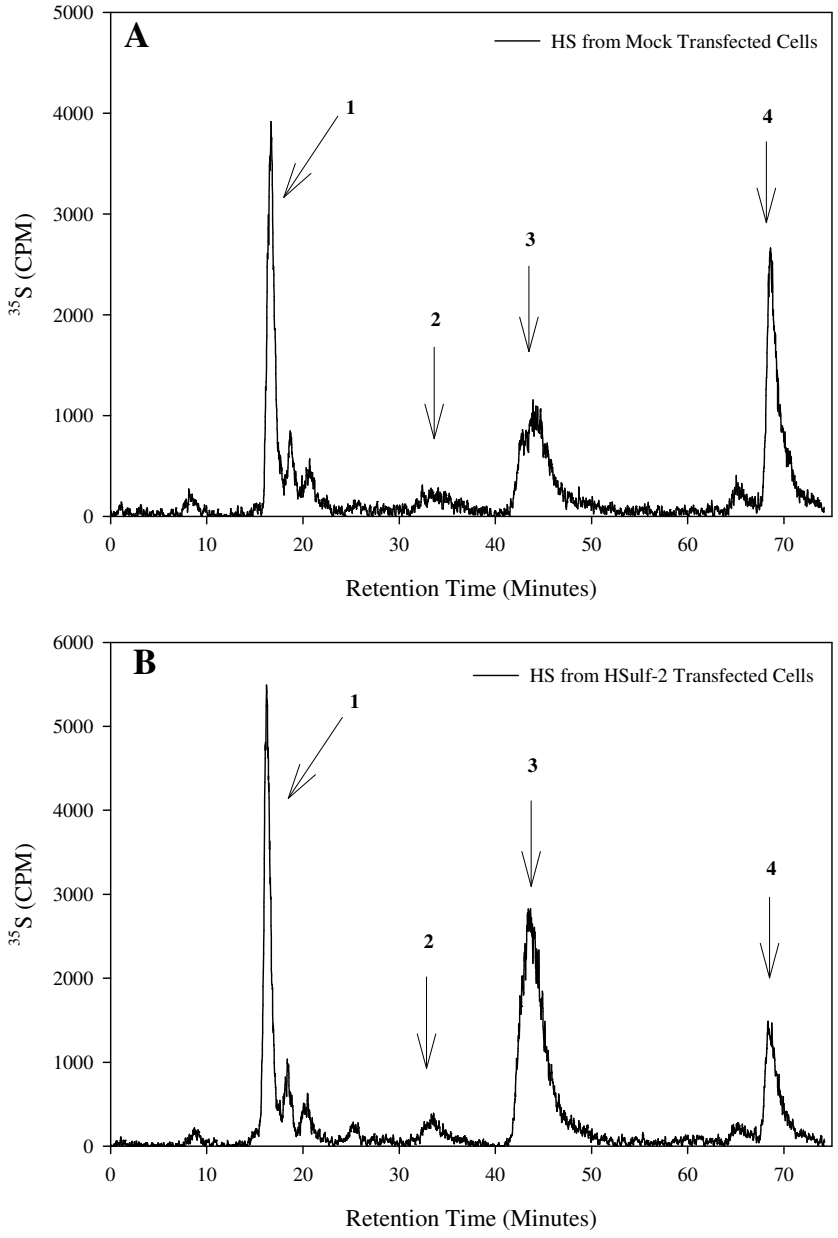

Figure 22. RPIP-HPLC chromatogram of ^{35}S-labeled disaccharide analysis of transfected CHO cells. The cells were transfected with empty vector and HSulf-2/pcDNA2.1A/*myc*-His vector, and were metabolically labeled as described in Chapter II. Approximately 200,000 cpm of the ^{35}S-labeled disaccharides were subjected to chromatography. The x-axis shows the retention time in minutes, the y-axis monitors [^{35}S] using online detection.

	(1) ΔUA-GlcNS (mol %)	(2) ΔUA-GlcNS6S (mol %)	(3) ΔUA2S-GlcNS (mol %)	(4) ΔUA2S-GlcNS6S (mol %)
pcDNA3.1A/CHO	30.4±2.4	5.7±0.6	32.5±2.0	31.4±3.8
HSulf-2/CHO	30.5±2.4	6.5±2.5	45.6±7.9	17.4±3.0

Table 3. Summary of HS disaccharide analysis of HSulf-2 activity *in vivo*. CHO cells expressing HSulf-2 were metabolically labeled to generate [^{35}S] HS. [^{35}S] HS was isolated, purified, and subjected to heparin lyase I, II, III degradation to generate ^{35}S-labeled disaccharides. Disaccharides were resolved on RPIP-HPLC for analysis. Nonradioactive standards were run to determine the elution positions of the disaccharides. Results represented as mol-percent of specific disaccharide products from two independent experiments.

Detection of HSulf-2 in Mammalian Cells

The cloning of HSulf-2 is described in chapter II. The resultant protein contains a *myc* epitope tag and a 6× Histidine (His_6) tag on its *C*-terminus in which either tag could be used to facilitate the detection of the protein by Western blotting. The Western blotting procedure is described in chapter II. Figure 23 represents the standard curve of the molecular weight of the protein standards and their migration distance used to calculate the molecular weight of the band observed in figure 23, lane 2. As expected, HSulf-2 was detected in the cell extract of the CHO cells (Figure 24, lane 2) compared to empty vector used as a control (Figure 24, lane 1).

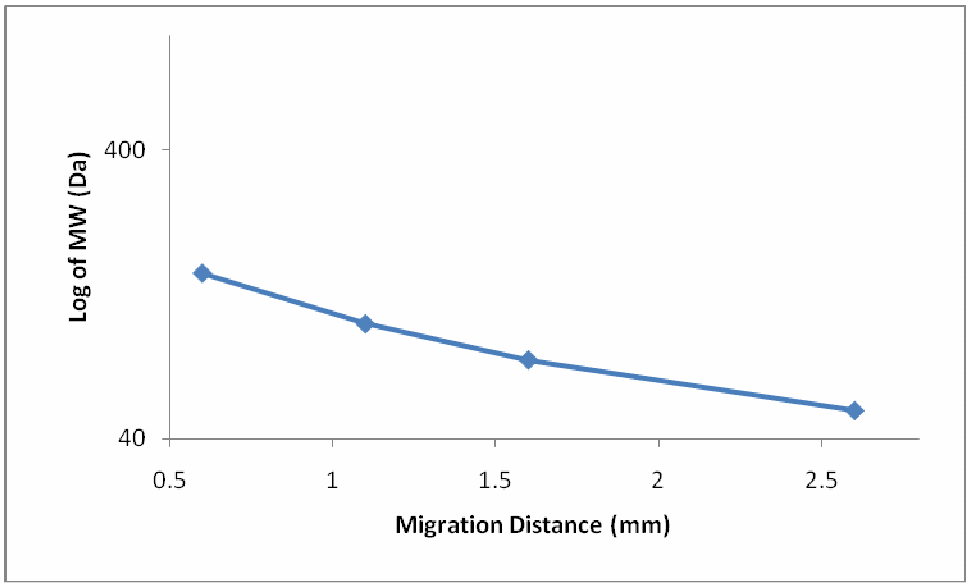

Figure 23. Molecular weight standard curve of HSulf-2. The standard curve was prepared by comparing the molecular weight markers within the molecular weight ladder with their migration distances within the Western blot. The migration distance of the band of interest was measured and the resultant molecular weight was determined from the standard curve. The calculated molecular weight of the band representing HSulf-2 was 135 kDa.

This band was consistent with the size of the full length, glycosylated protein containing a *myc*-His tag but no signal sequence. The Western blotting technique was used to detect HSulf-2 secreted in the conditioned medium (CM), but no bands were detected (data not shown). Overall, HSulf-2 was successfully expressed in CHO cells.

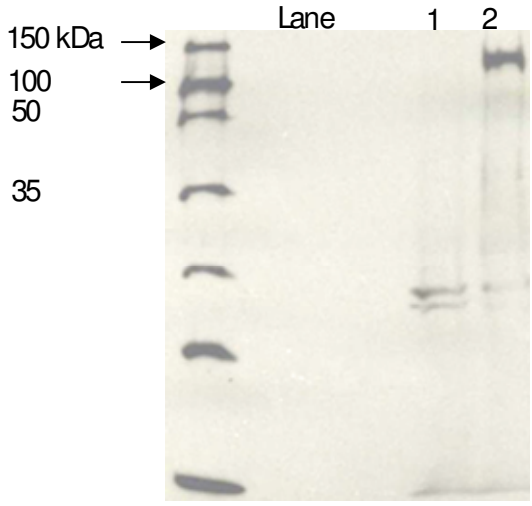

Figure 24. Western blotting analysis of HSulf-2/CHO cell extract. The Western blotting technique was used on the empty vector and HSulf-2 cell extract as described in chapter II. Lane 1, cells transfected with pcDNA3.1A/*myc*-His; Lane 2, cells transfected with HSulf-2/pcDNA3.1A/ *myc*-His. HSulf-2 had a calculated molecular weight of 135 kD.

Determination of in vitro Hsulf-2 Activity

To carry out the experimental design, we needed to make sure that HSulf-2 is also active in an *in vitro* format. To determine the *in vitro* enzymatic activity of HSulf-2, the enzyme was extracted from the cell lysate of CHO cells, and the activity evaluated by disaccharide analysis by RPIP chromatography. The procedures for the extraction of HSulf-2 from the CHO cell lysate are described in chapter II. Initially, [^{35}S] HS was prepared from CHO cell culture that was metabolically labeled with Na_2 [^{35}S] SO_4. The [^{35}S] HS was treated with HSulf-2 cell extract was followed by a disaccharide analysis by subjecting HS to the digestion with a mixture of heparin lyases. The CM from CHO cells expressing HSulf-2 was collected and evaluated for enzymatic activity using the same method. The ^{35}S-labeled disaccharides were resolved on the RPIP column. If activity were present, the elution profiles of the untreated and the treated [^{35}S] HS should yield similar results as the *in vivo* disaccharide analysis for the determination of enzymatic activity. It was shown that the CM

of HSulf-2 expressing CHO cells contained enzymatic activity by the observance of a 5-fold decrease in the ΔUA2S-GlcNS6S disaccharide peak and the subsequent 2-fold increase in the ΔUA2S-GlcNS disaccharide peak at elution positions 35 min. and 65 min. (Figure 25, panel B) compared to the untreated [^{35}S]HS (Figure 25, panel A). In addition, a peak at 12 min. was concluded to be a free [^{35}S] sulfate peak, which was a result of the de-sulfation of [^{35}S] HS by HSulf-2 in the CM. The discrepancy in the amount of ΔUA2S-GlcNS disaccharide peak could be due to HSulf-2 removing sulfo groups from other disaccharide peaks which have been identified in the elution profile. Interestingly, the HSulf-2 CM yielded enzymatic activity even though it was not detected by Western blotting. This may be due to the cleavage of the C-terminal *myc*-His tag from the protein by a post-translational protease previously reported (124), rendering an undetectable protein by Western blotting.

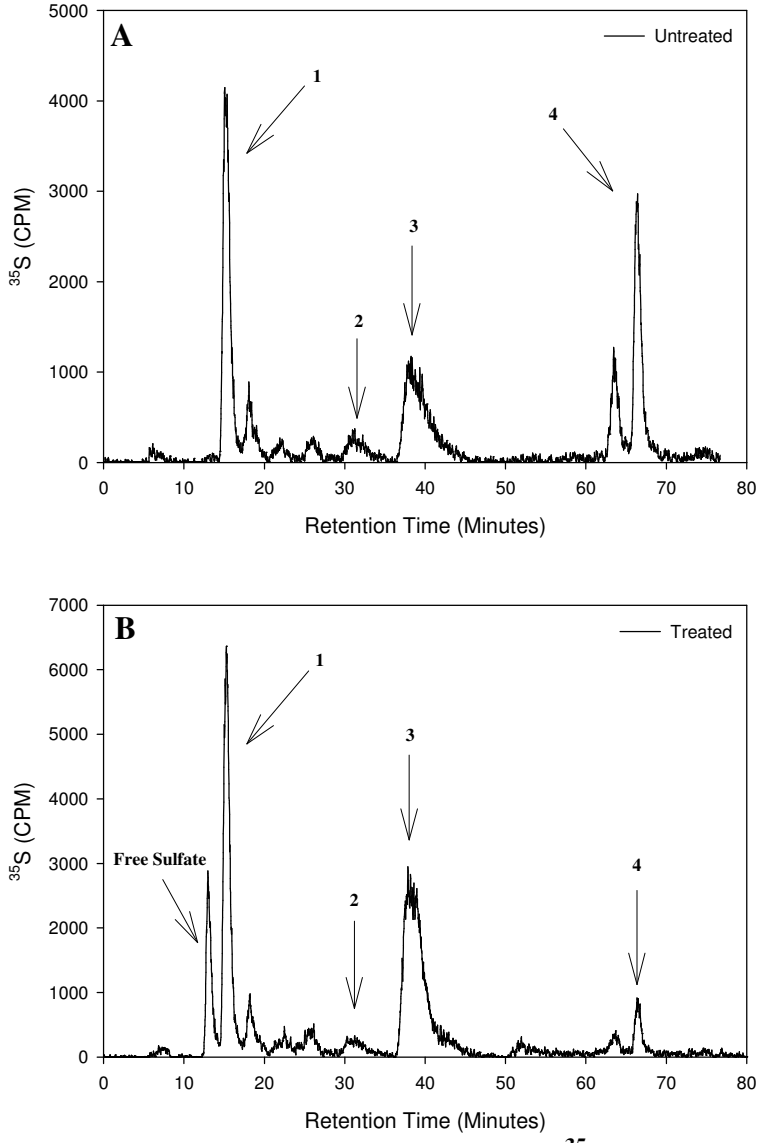

Figure 25. Comparison of RPIP-HPLC chromatograms of ^{35}S-labeled disaccharide analysis of HSulf-2 CM activity *in vitro*. Nontransfected CHO cells were metabolically labeled to generate [^{35}S] HS. [^{35}S] HS was isolated, purified, and subjected to HSulf-2 treatment. [^{35}S] HS was degraded with heparin lyase I, II, III to generate ^{35}S-labeled disaccharides. Approximately 200,000 cpm of the ^{35}S-labeled disaccharides were subjected to RPIP chromatography. Nonradioactive standards were run to determine the elution positions of the disaccharides. Panel A represents mock CM treatment of [^{35}S] HS. Panel B represents HSulf-2 CM treatment of [^{35}S] HS. (1) represents ΔUA-GlcNS; (2) represents ΔUA-GlcNS6S; (3) represents ΔUA2S-GlcNS; (4) represents ΔUA2S-GlcNS6S. The *x-axis* shows the retention time in minutes, the *y axis* monitors [^{35}S] using online detection.

For the cell extract containing HSulf-2, to a lesser extent there was a decrease in the ΔUA2S-GlcNS6S disaccharide peak followed by a in small increase in the ΔUA2S-GlcNS disaccharide peak at elution positions 35 min. and 65 min. (Figure 26, panel B) after HSulf-2 cell extract treatment compared to the untreated [^{35}S] HS (Figure26, panel A). In addition, at 12 min. there is a peak concluded to be a free [^{35}S] sulfate peak, which was a result of the de-sulfation of [^{35}S] HS by HSulf-2 in the cell extract. The summary of the disaccharide analysis is shown in Table 4. These results showed enzymatic activity present in the cell extract.

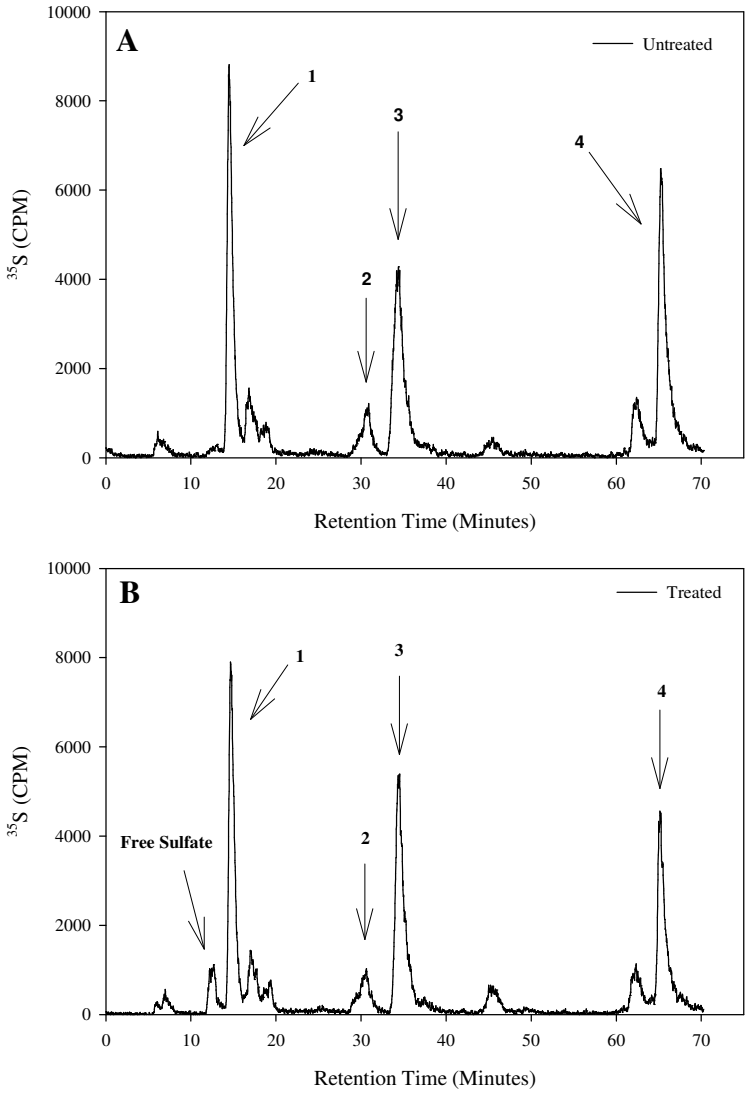

Figure 26. RPIP-HPLC chromatograms of ^{35}S-labeled disaccharide analysis of HSulf-2 *in vitro* activity from cell extract. Nontransfected CHO cells were metabolically labeled to generate [^{35}S] HS. [^{35}S] HS was isolated, purified, and subjected to HSulf-2 treatment. [^{35}S] HS was degraded with heparin lyase I, II, III to generate ^{35}S-labeled disaccharides. Approximately 200,000 cpm of the ^{35}S-labeled disaccharides were subjected to RPIP chromatography. Nonradioactive standards were run to determine the elution positions of the disaccharides. Panel A represents mock treatment of [^{35}S] HS. Panel B represents HSulf-2 CM treatment of [^{35}S] HS. (1) represents ΔUA-GlcNS; (2) represents ΔUA-GlcNS6S; (3) represents ΔUA2S-GlcNS; (4) represents ΔUA2S-GlcNS6S. The *x-axis* shows the retention time in minutes, the *y axis* monitors [^{35}S] using online detection.

	(1) ΔUA-GlcNS (mol %)	(2) ΔUA-GlcNS6S (mol %)	(3) ΔUA2S-GlcNS (mol %)	(4) ΔUA2-GlcNS6S (mol %)
Untreated cell lysate	32.0±0.5	6.9±0.9	28.1±0.4	33±0.1
HSulf-2 cell lysate	33.5±1.8	6.4±2.2	34.0±0.4	26.1±0.8
Untreated CM	34.4	5.5	31.5	28.6
HSulf-2 CM	37.5	4.6	52.4	5.5

Table 4. Summary of HS disaccharide analysis of *in vitro* HSulf-2 activity. Nontransfected CHO cells were metabolically labeled to generate [^{35}S] HS. [^{35}S] HS was isolated, purified, and subjected to HSulf-2 treatment. [^{35}S] HS was degraded with heparin lyase I, II, III to generate ^{35}S-labled disaccharides. Nonradioactive standards were run to determine the elution positions of the disaccharides. Results represented as mol-percent of specific disaccharide products from two independent experiments for the cell extract and one determinant for the CM.

Evaluation of [^{35}S] HS Polysaccharides

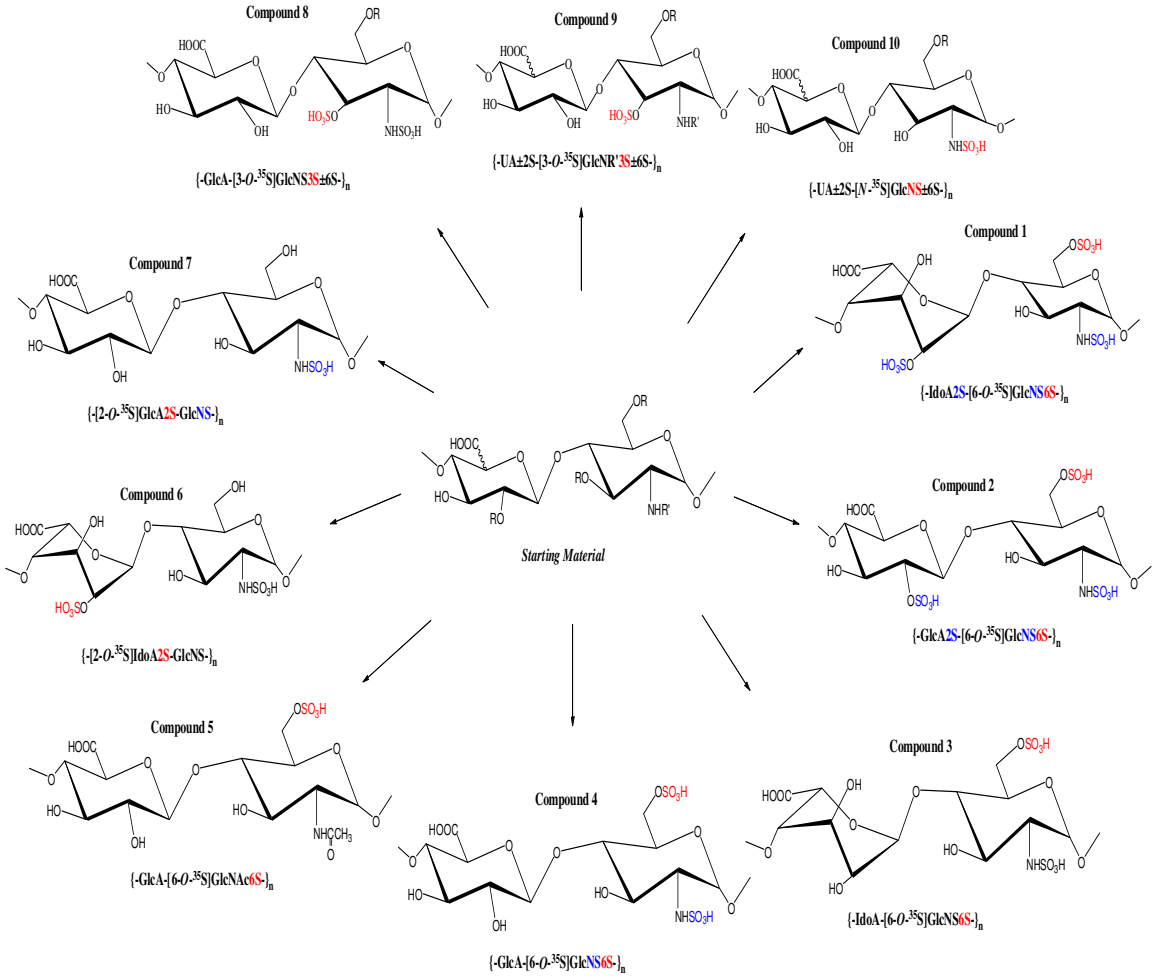

Figure 27. Strategy for the development of synthetic HS polysaccharides. The steps involved in generating synthetic substrates to evaluate HSulf-2 activity. The sulfo groups colored in *blue* are nonradioactive modifications, and sulfo groups colored in *red* depict radioactive modifications that aid in tracking enzymatic activity. R represents a proton or sulfate. R' represents a proton, acetyl, or sulfate.

In this section, we wanted to investigate the issue of HSulf-2 substrate specificity by generating polysaccharides that would aid in determining which disaccharide structures within the polysaccharide were necessary and could produce enzymatic activity. Therefore, with the use of different starting materials, we were able to synthesize polysaccharides with different [^{35}S] labeled positions on structures carrying specific structural motifs within these

polysaccharides as depicted in Figure 27. In order to produce these polysaccharides all HS biosynthetic enzymes were expressed in *E. coli* in large quantities. To generate [^{35}S] labels at specific sites on the polysaccharide, the polysaccharide was incubated with a specific sulfotransferase in the presence of [^{35}S] PAPS. The resultant structures are not completely sulfated at the desired positions due to incomplete enzymatic activity of the sulfotransferases. The overall sulfation level among the products was between 0.78-1.85 nmoles of *O*-sulfo groups per microgram of polysaccharide (Table 5). In addition, there was between 1-10 sulfo groups per chain of ^{35}S-labeled polysaccharide, which was measured based on the specific ^{35}S radioactivity.

Compound Name	Proposed Repeating Units	*O*-^{35}S-Labeled Sulfation Level (nmoles /µg Polysaccharide)
1	**[-IdoA2S-[6-*O*-^{35}S]GlcNS6S-]$_n$**	**0.8**
2	**[-GlcA2S-[6-*O*-^{35}S]GlcNS6S-]$_n$**	**0.6**
3	**[-IdoA-[6-*O*-^{35}S]GlcNS6S-]$_n$**	**1.9**
4	**[-GlcA-[6-*O*-^{35}S]GlcNS6S-]$_n$**	**1.4**
5	**[-GlcA-[6-*O*-^{35}S]GlcNAc6S-]$_n$**	**0.1**
6	**[-[2-*O*-^{35}S]IdoA2S-GlcNS-]$_n$**	**1.1**
7	**[-2-*O*-^{35}S]GlcA2S-GlcNS-]$_n$**	**1.3**
8	**[-GlcA-[3-*O*-^{35}S]GlcNS3S±6S-]$_n$**	**1.1**
9	**[-UA±2S-[3-*O*-^{35}S]GlcNR3S±6S-]$_n$**	**0.8**
10	**[-UA±2S-[*N*-^{35}S]GlcNS±6S-]$_n$**	**1.6**

Table 5. Summary of the sulfation level of the synthetic polysaccharides. Synthetic polysaccharides were generated from heparosan, *N*-heparosan, CDNS heparin, and ICN HS as starting material. The starting material was modified by HS sulfotransferases to produce the desired product. ^{35}S-labeled sulfation level in nmoles of ^{35}S-labeled sulfate per microgram of polysaccharide was measured by the specific ^{35}S radioactivity.

Development of a method using a spin column has allowed us to assay for HSulf-2 activity against the synthesized polysaccharides quickly and more efficiently than HPLC chromatography. The separation by spin column was based on the molecular size of the

analytes. Once the [^{35}S] modified polysaccharides were synthesized, each was subjected to HSulf-2 digestion to determine whether the enzyme would remove the [^{35}S] sulfo groups from the polysaccharide. The release of [^{35}S] sulfo groups would be quantified by how much ^{35}S-radioactive counts were trapped in the spin column. Controls for [^{35}S] sulfate and [^{35}S] HS were performed. This spin column method traps small molecules such as free sulfate within the resin and excludes larger molecules (size exclusion limit: approximately 6,500 daltons) such as polysaccharides which run through the column during centrifugation. The amount of pmols of [^{35}S] sulfate can be quantified by this method.

Evaluation of 2-O-sulfated Uronic acid

It is well documented that Sulfs have activity against IdoA2S-GlcNS6S disaccharide motifs within HP/HS removing 6-*O*-sulfo groups from these structures. Studies show that IdoA2S residues are important in Sulf activity. Therefore, we wanted to determine whether HSulf-2 had activity against GlcA2S residues also. However, we needed to synthesize structures containing either IdoA2S- or GlcA2S-[6-*O*-^{35}S] GlcNS6S to evaluate whether enzymatic activity was specific toward either 2-*O*-sulfated hexuronic acid. Therefore, Compound 1 was synthesized from *N*-sulfo heparosan. Before the generation of compound 1 could occur, heparosan was first subjected to deacetylation by sodium hydroxide. After deacetylation, heparosan contained $GlcNH_2$ residues which could be converted to GlcNS residues by NST-1 to produce *N*-sulfo heparosan. *N*-sulfo heparosan was then subjected to epimerization of the C_5 position of D-glucuronic acid to convert the residue to L-iduronic acid. Next, 2-OST was used to place 2-*O*-sulfo groups on IdoA residues to create IdoA2S

residues on the chain. Finally, 6-OSTs were used to place [^{35}S] sulfo groups on the 6-OH position on the GlcNS residues to produce IdoA2S-[6-*O*-^{35}S] GlcNS6S disaccharide motifs within the polysaccharide. Even though this structure originated from heparosan, its content is more "heparin-like" since the resulting product of the enzymatic modifications contained a content of 80% IdoA2S-GlcNS before the addition of [^{35}S] 6-*O*-sulfo groups on this structure. Compound 2 was also generated from *N*-sulfo heparosan. Therefore, 2-*O*-sulfo groups were placed on 2-OH position of GlcA residues to generate GlcA2S residues by 2-OST. 6-OSTs were used to place [^{35}S] sulfo groups on the 6-OH position of GlcNS residues to produce GlcA2S-[6-*O*-^{35}S] GlcNS6S disaccharide motifs within the polysaccharide.

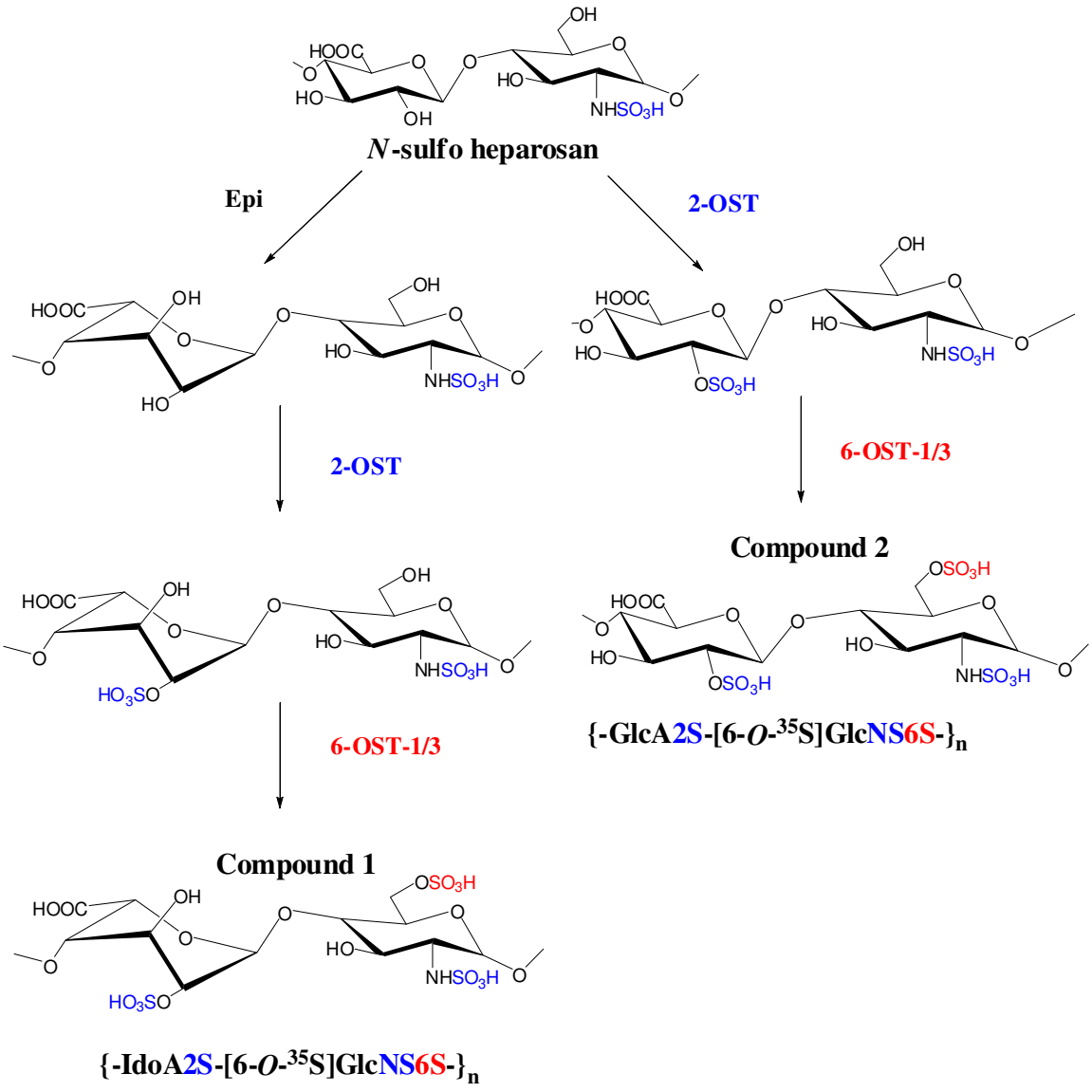

Figure 28. Generation of compound 1 and 2. For compound 1 and 2, *N*-sulfo heparosan is used as the starting material. After subsequent modifications using sulfotrasnferases, sulfo groups were placed on the polysaccharide to produce the desired product. Sulfotransferases depicted in *blue* add sulfo groups colored *blue*. Sulfotransferases depicted in *red* add sulfo groups colored in *red*. The color *blue* represents modification using nonradioactive PAPS, while the color *red* represents modifications using radioactive PAPS.

After treating compound 1 with HSulf-2 , results showed a very high [^{35}S] sulfate release with approximately 97.5 % removal of [^{35}S] 6-*O*-sulfo groups from the polysaccharide compared to control (2.7%). This showed the spin column was capable of

determining sulfatase activity. To further prove the spin column method is able to screen potential substrates, a disaccharide analysis was employed to demonstrate the enzyme was active against this substrate. After degrading the polysaccharide with a mixture of heparin lyases, only 6-*O*-[^{35}S] labeled disaccharides were able to be resolved on the RPIP column. The elution profile for the untreated material revealed a major peak at 32 min, which was identified as an IdoA2S-GlcNS6S disaccharide (Figure 29, panel A). Additional peaks at 16min. and 18min. were apparent, but were not identified. In the Figure 29, panel B, the elution profile for the HSulf-2 treated material contained a large free [^{35}S] sulfate peak (approximately 94%) in addition to trace amounts of both the IdoA2S-GlcNS6S disaccharide peak (4.3%) and the unidentified peaks (1.9%). The summary of the disaccharide analysis is shown in table 6.

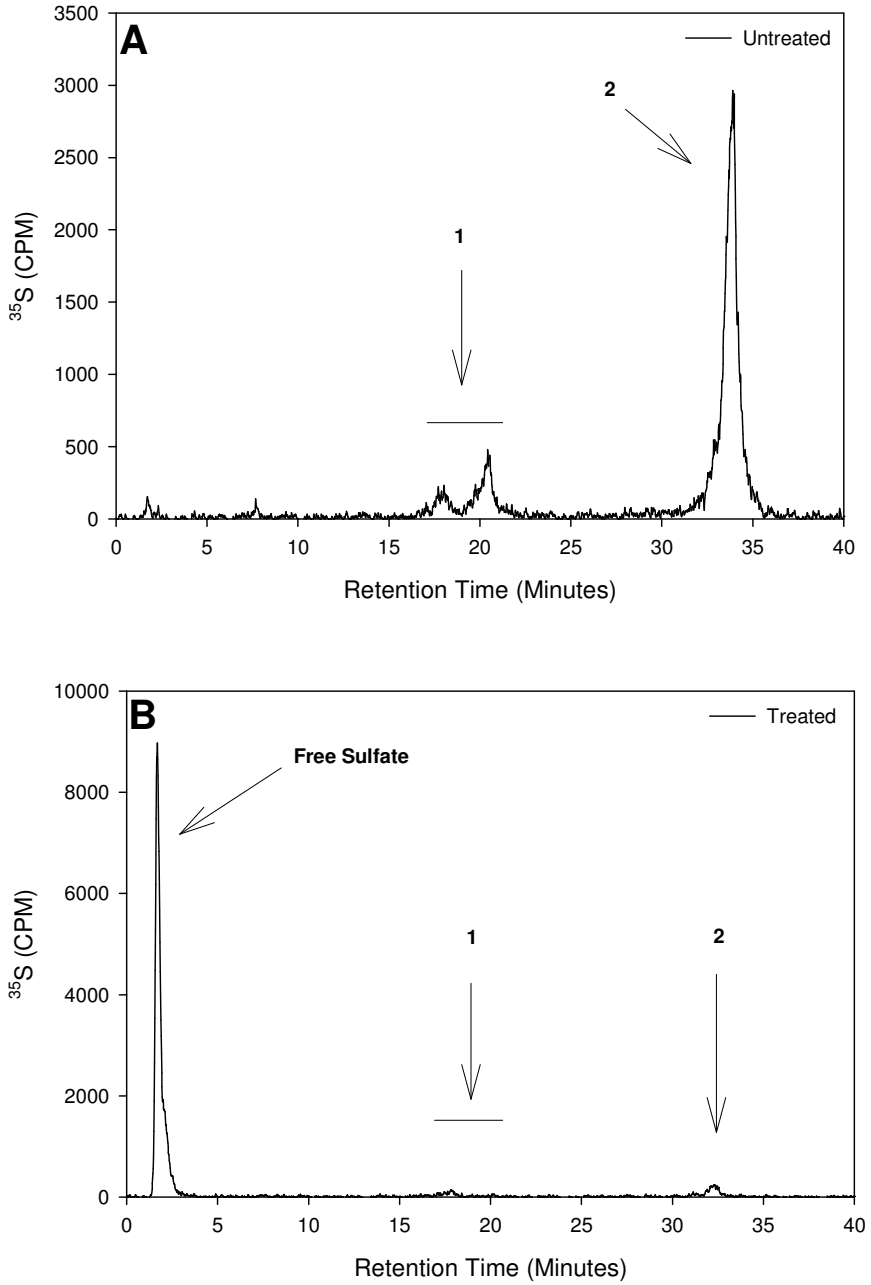

Figure 29. HSulf-2 activity against compound 1. Treated and untreated compound 1 was subjected to heparin lyase degradation to produce ^{35}S-disaccharides. Approximately 50,000 cpm of the digested material was subjected to RPIP chromatography. (1) represents a mixture of unidentified disaccharides; (2) represents IdoA2S-GlcNS6S disaccharide. The *x-axis* shows the retention time in minutes, and the *y-axis* monitors [^{35}S] using online detection.

	Free Sulfate (mol%)	(1) ΔUA-GlcNS6S (mol %)	(2) IdoA2S-GlcNS6S (mol %)
Untreated	0.0	18.3	81.7
Treated	93.8	1.9	4.3

Table 6. Summary of the disaccharide analysis of compound 1. Untreated and treated polysaccharide was degraded with heparin lyase I, II, and III to generate ^{35}S-labeled disaccharides. Disaccharides were resolved on RPIP-HPLC for analysis. Results represented as mol-percent of specific disaccharide products.

HSulf-2 activity against compound 2 could not be determined by the spin column method due to the incomplete formation of a majority of GlcA2S-[6-*O*-^{35}S] GlcNS6S disaccharide motifs, which was determined by disaccharide analysis of this structure. Disaccharide analysis of the product revealed the synthesized polysaccharide contained a majority of GlcA-GlcNS6S disaccharide motifs and a minority of GlcA2S-GlcNS6S disaccharide motifs within this structure. This discovery would make it difficult to determine whether sulfo groups were actually being removed from the target product. Therefore, HSulf-2 activity against compound 2 was determined by disaccharide analysis on the HPLC. We wanted to observe whether the minor GlcA2S-GlcNS6S disaccharide peak could be digested by HSulf-2, which would result in a decrease or a complete disappearance of this peak in the elution profile. This compound was degraded by a mixture of heparin lyases to generate only 6-*O*-[^{35}S] labeled disaccharides. The ^{35}S-labeled disaccharides were resolved on a RPIP column. In the untreated elution profile, GlcA-GlcNS6S and GlcA2S-GlcNS6S disaccharide peaks were observed and had elution times of 18 min. and 58 min. (Figure 30, panel A). After HSulf-2 treatment, the GlcA2S-GlcNS6S disaccharide peak completely disappeared with the subsequent observance of a free sulfate peak at 8 min. (Figure 30, panel B). In addition, there was a decrease in the GlcA-GlcNS6S disaccharide peak that contributed to the free sulfate peak. The observance of the free sulfate peak was indicative of

HSulf-2 activity against this compound removing 6-*O*-sulfo groups from the material. This evidence further proves HSulf-2 has broad substrate specificity against HS, and is able to de-sulfate disaccharide motifs that can be found in moderately sulfated domains of HP/HS structures.

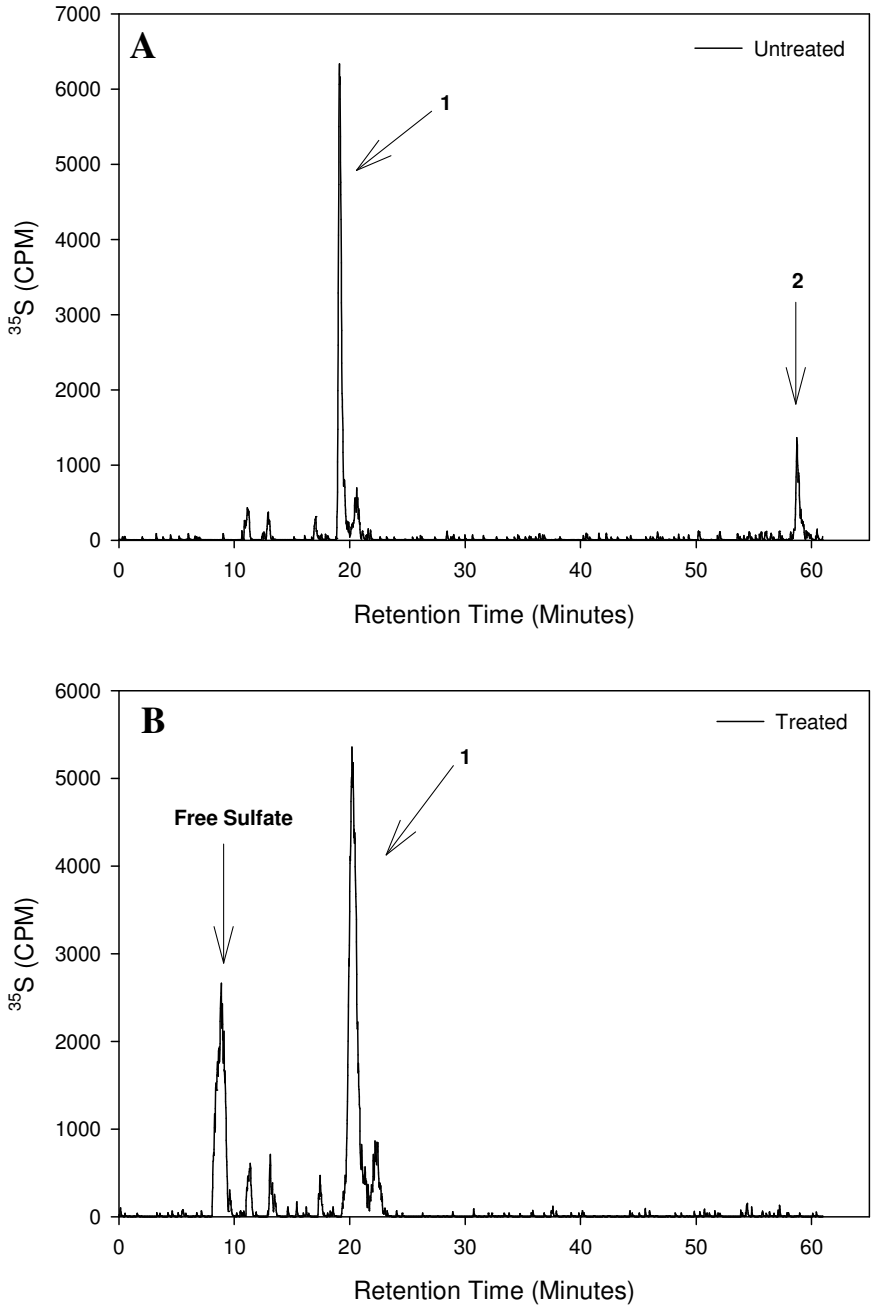

Figure 30. HSulf-2 activity against compound 2. Treated and untreated compound 2 was subjected to heparin lyase degradation into ^{35}S-labeled disaccharides. Approximately 50,000 cpm of the digested material was subjected to RPIP chromatography. (1) GlcA-GlcNS6S; (2) represents GlcA2S-GlcNS6S. The *x-axis* shows the retention time in minutes, and the *y axis* monitors [^{35}S] using online detection.

	Free Sulfate (mol %)	(1) GlcA-GlcNS6S (mol %)	(2) GlcA2S-GlcNS6S (mol %)
Untreated	0.0	81.3	18.7
Treated	32.6	67.4	0.0

Table 7. Summary of compound 2 disaccharide analysis. Untreated and treated polysaccharide was degraded with heparin lyase I, II, and III to generate ^{35}S-labeled disaccharides. Disaccharides were resolved on RPIP-HPLC for analysis. Results represented as mol-percent of specific disaccharide products.

Determination of Whether 2-O-Sulfation is Necessary for HSulf-2 Activity

Once we were able to show that HSulf-2 had activity against GlcA2S residues, it was important to determine whether 2-*O*-sulfation was critical for activity. Therefore, we synthesized structures containing either IdoA- or GlcA-[6-*O*-^{35}S] GlcNS6S disaccharide motifs within the polysaccharide. For the synthesis of compound 3, *N*-sulfo heparosan was subjected to [^{35}S] sulfation at the 6-OH position of GlcNS residues producing GlcA-[6-*O*-^{35}S] GlcNS6S disaccharide motifs within the polysaccharide. For compound 4, CDNS heparin was used as starting material. CDNS heparin was chosen as the starting material in order to generate compounds with a high IdoA/GlcA residue content. Therefore, CDNS heparin was subjected to [^{35}S] sulfation at the 6-OH position of GlcNS residues producing IdoA-[6-*O*-^{35}S] GlcNS6S disaccharide motifs within the polysaccharide.

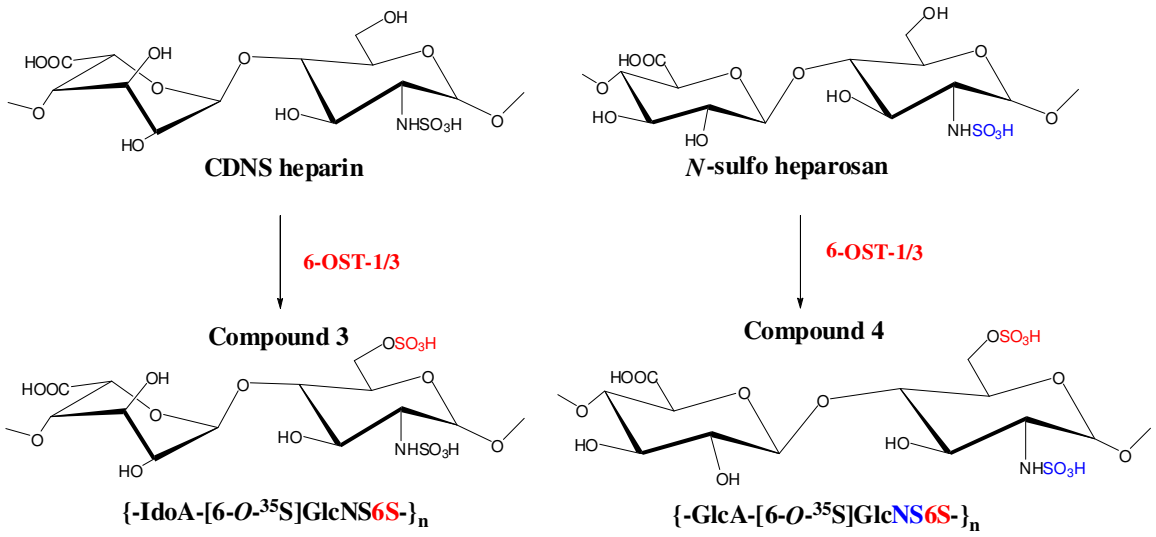

Figure 31. Generation of compound 3 and 4. For compound 3 CDNS heparin is used as the starting material, and for compound 4 *N*-sulfo heparosan is used as the starting material. After subsequent modifications using sulfotransferases, sulfo groups were placed on the polysaccharide to produce the desired product. Sulfotransferases depicted in *blue* add sulfo groups colored *blue*. Sulfotransferases depicted in *red* add sulfo groups colored in *red*. The color *blue* represents modification using nonradioactive PAPS, while the color *red* represents modifications using radioactive PAPS.

The spin column method showed compound 3 was shown to have approximately 24.3% [^{35}S] 6-*O*-sulfo group release after HSulf-2 treatment compared to 8.3% released from the control. Since this compound was a potential substrate for HSulf-2, an HPLC disaccharide analysis was performed to further investigate whether there was any activity against this compound. After degradation by a mixture of heparin lyases, disaccharides containing only a 6-*O*-[^{35}S] labeled were generated. The elution profile for this compound showed an IdoA-GlcNS6S disaccharide peak as the majority of the radiolabeled product which eluted at 15 min. (Figure 32, panel A). However, there was also a minor IdoA2S-GlcNS6S disaccharide peak observed at 31 min. The observance of the IdoA2S-GlcNS6S disaccharide peak was due to a small percentage of the starting material still containing IdoA2S residues. Upon HSulf-2 treatment there was a very small percentage of digestion

(4.9%) of the IdoA-GlcNS6S disaccharide peak, but the IdoA2S-GlcNS6S disaccharide peak was completely digested. As a result there was the appearance of a 6.5% free [^{35}S] sulfate peak (Figure 32, panel B). The combination of the sulfate removal from IdoA-GlcNS6S and IdoA2S-GlcNS6S contributed to the amount of free sulfate observed in the elution profile. After further evaluation, this data suggested that HSulf-2 may have a small amount of activity against the IdoA-GlcNS6S disaccharide peak. However, this result is inconclusive due to the presence of IdoA2S-GlcNS6S. In addition, since this compound contains approximately 10% of GlcA residues, it is possible that GlcA2S-GlcNS6S and GlcA-GlcNS6S may contribute to the data being inconclusive.

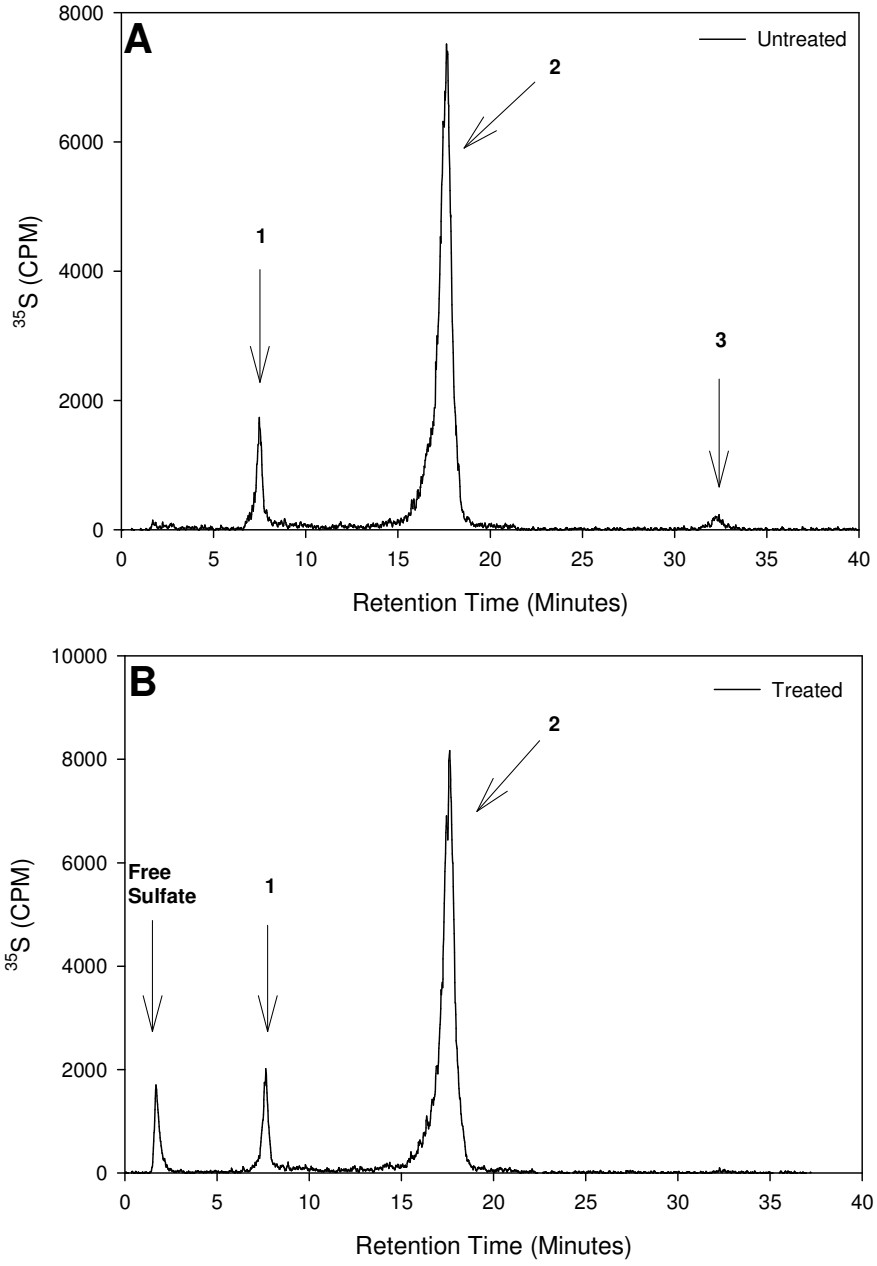

Figure 32. RPIP disaccharide analysis of compound 3. Treated and untreated compound 3 was subjected to heparin lyase degradation into ^{35}S-disaccharides. Approximately 50,000 cpm of the digested material was subjected to RPIP chromatography. (1) represents an unknown peak; (2) represents IdoA-GlcNS6S; (3) represents IdoA2S-GlcNS6S. The *x-axis* shows the retention time in minutes, and the *y-axis* monitors [^{35}S] using on-line detection.

	Free Sulfate (mol %)	(1) Unknown (mol %)	(2) IdoA-GlcNS (mol %)	(3) IdoA2S-GlcNS6S (mol%)
Untreated	0.0	9.3	89.0	1.7
Treated	6.5	9.4	84.1	0.0

Table 8. Summary of the disaccharide analysis of compound 3.

In addition, compound 4 was shown to be a substrate for this enzyme. Approximately 43.1% of [^{35}S] 6-*O*-sulfo groups were removed from the polysaccharide compared to 6.6% released from the control. Compound 4 was analyzed by HPLC to further demonstrate the material was a substrate for HSulf-2. This compound was degraded by a mixture of heparin lyases to generate disaccharides with only a 6-*O*-[^{35}S] label. The ^{35}S-labeled disaccharides were resolved on a RPIP column. The elution profile for compound 4 showed there was one major disaccharide peak, GlcA-GlcNS6S, eluted at 20 min. (Figure 33, panel A). The summary of the disaccharide analysis is shown in table 5. After HSulf-2 treatment (Figure 33, panel B) there is approximately a 22% decrease in GlcA-GlcNS6S disaccharide with the development a free sulfate peak that was approximately 22% of the peaks present in the elution profile. This result showed that HSulf-2 activity is not limited to highly sulfated domains containing repeating IdoA2S-GlcNS6S disaccharide units. The sulfatase activity extends to GlcA-GlcNS6S disaccharide motifs that contain no IdoA2S residues. These disaccharide motifs are found in moderately sulfated domains of HP/HS.

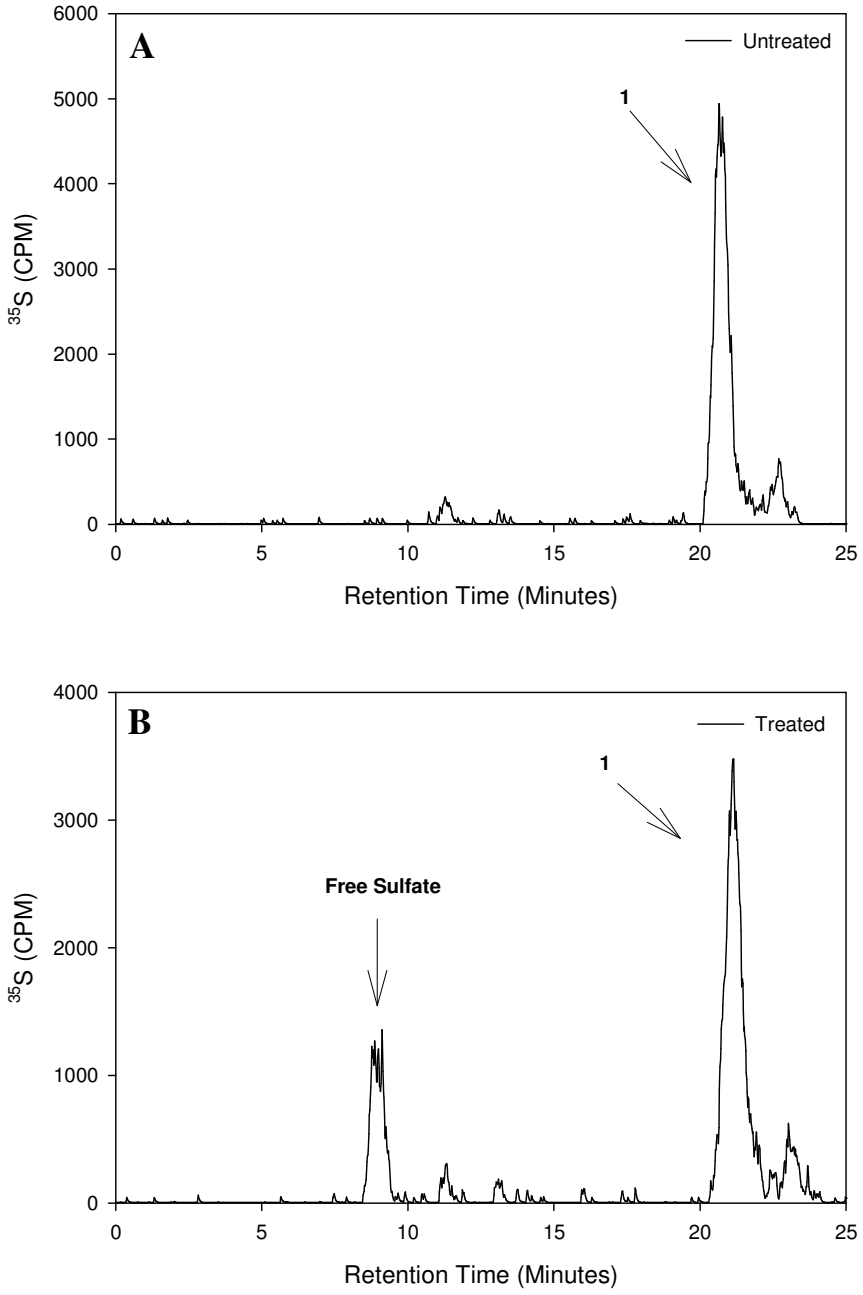

Figure 33. HSulf-2 activity against compound 4. Treated and untreated compound 4 was subjected to heparin lyase degradation into ^{35}S-labeled disaccharides. Approximately 50,000 cpm of the digested material was subjected to RPIP chromatography. (1) represents GlcA-GlcNS6S. The *x-axis* shows the retention time in minutes, and the *y axis* monitors [^{35}S] using online detection.

	Free Sulfate (mol%)	(1) GlcA-GlcNS6S (mol %)
Untreated	0.0	100.0
Treated	21.9	78.1

Table 9. Summary of compound 4 disaccharide analysis. Untreated and treated polysaccharide was degraded with heparin lyases to generate ^{35}S-labeled disaccharides. Disaccharides were resolved on RPIP-HPLC for analysis. Results represented as mol-percent of specific disaccharide products.

Determination of Whether N-Sulfation is Critical for HSulf-2 Activity

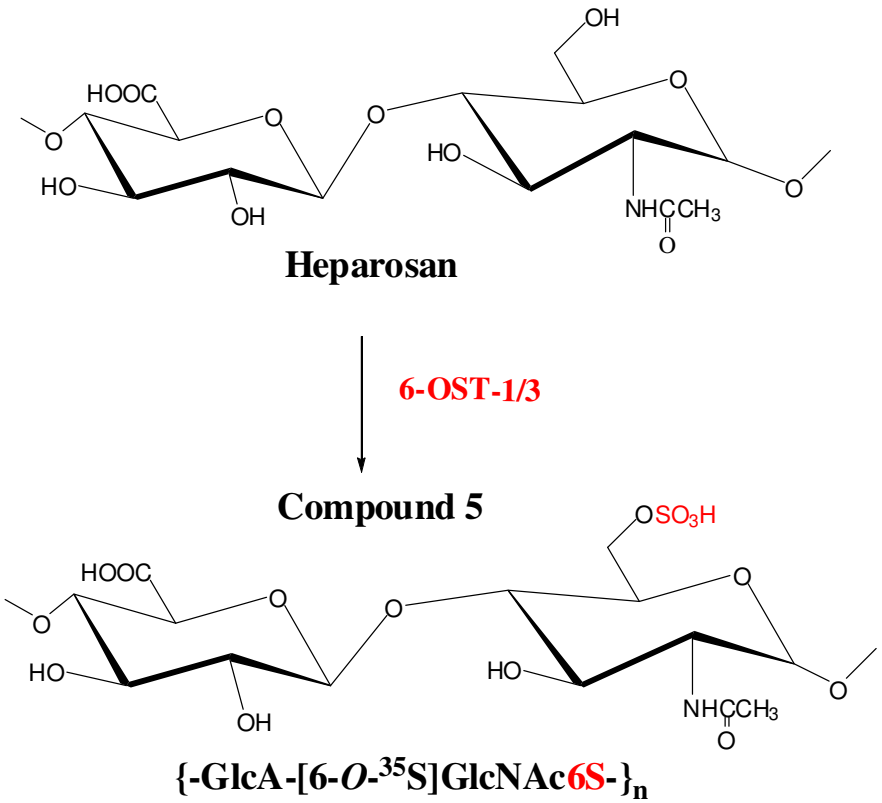

Figure 34. Generation of compound 5 Heparosan was incubated with 6-OST-1 and 6-OST-3 in the presence of [^{35}S] PAPS to place a radioactive sulfo group on GlcNAc residues in the polysaccharide chain. Sulfotransferases depicted in *blue* add sulfo groups colored *blue*. Sulfotransferases depicted in *red* add sulfo groups colored in *red*. The color *blue* represents modification using nonradioactive PAPS, while the color *red* repr-esents modifications using radioactive PAPS.

Compound 4 was shown to be a substrate for HSulf-2. Therefore, we wanted to determine whether *N*-sulfation was necessary for HSulf-2 activity. Compound 5 was synthesized from heparosan, a capsular polysaccharide from *E. coli* K5 strain, which is identical to a nonsulfated and unepimerized HS. This structure was synthesized by placing a [^{35}S]-sulfo group on the 6-OH position of GlcNAc to generate GlcA-[6-*O*-^{35}S] GlcAc6S disaccharide motifs within the polysaccharide. The GlcA-GlcAc6S disaccharide is a rare structure found in HP/HS. Therefore, it was difficult to [^{35}S] label this material since 6-OSTs prefer *N*-sulfation first placed on glucosamine residues before any *O*-sulfation occurs. For compound 5, spin column results showed there was a 28.1% release of free [^{35}S] sulfate release compared to control (14.2%). Based on the spin column method, it was difficult to determine whether this material was a substrate for HSulf-2 activity, because the amount of free [^{35}S] sulfate release after subtracting the control was comparable to other compounds that were not substrates for this enzyme. Therefore, a disaccharide analysis was performed, and the results showed HSulf-2 was not active against this substrate (data not shown).

Evaluation of HSulf-2 Activity Against 2-O-Sulfation

In order to generate compound 6 CDNS heparin was used as starting material, and was subjected to [^{35}S] labeling of the 2-OH position on the IdoA residue to create [2-*O*-^{35}S] GlcA2S-GlcNS disaccharide motifs within the polysaccharide. *N*-sulfo heparosan was used to synthesize compound 7 by using 2-OST to place [^{35}S] sulfo groups on the 2-OH position of GlcA residues. This produces a compound containing [2-*O*-^{35}S] GlcA2S-GlcNS disaccharide motifs within the polysaccharide.

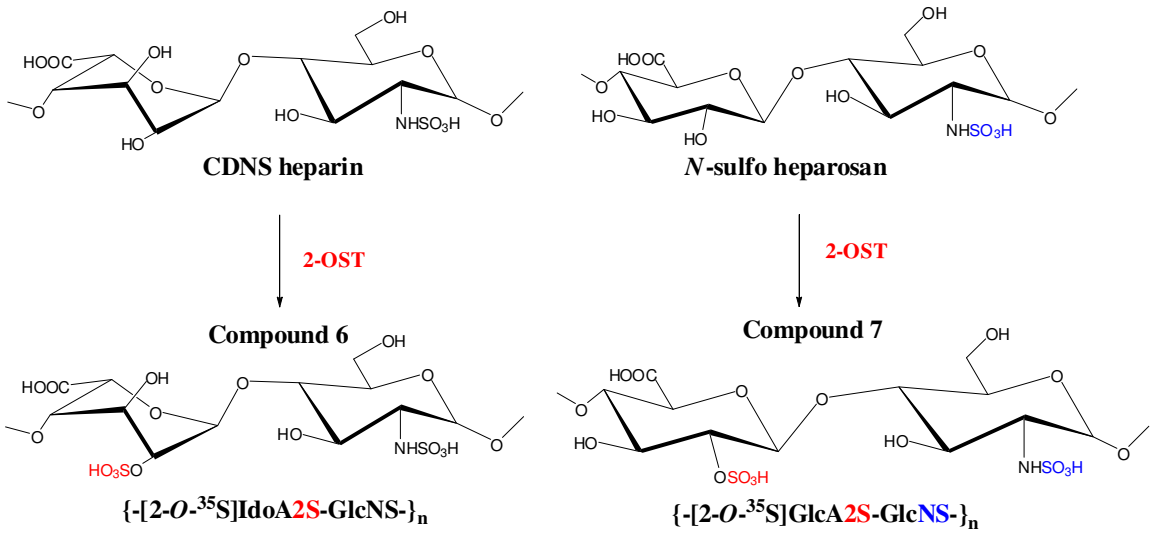

Figure 35. Generation of compound 6 and 7. For compound 6 and7, CDNS heparin and *N*-sulfo heparosan are used as the starting material. After subsequent modifications using sulfotransferases, sulfo groups were placed on the polysaccharide to produce the desired product. Sulfotransferases depicted in *blue* add sulfo groups colored *blue*. Sulfotransferases depicted in *red* add sulfo groups colored in *red*. The color *blue* represents modification using nonradioactive PAPS, while the color *red* represents modifications using radioactive PAPS.

Compounds 6 and 7 were not substrates for HSulf-2. Compound 6 released 12.6% versus 10.6% of free [^{35}S] sulfate compared to control. In addition, compound 7 released 13.7% of free [^{35}S] sulfate compared to control which released 6.7%. Therefore, minimal release of free [^{35}S] sulfate was observed, which was due to the limitations of the spin column. Therefore, Hsulf-2 does not release 2-*O*-sulfo groups from either GlcA or IdoA residues.

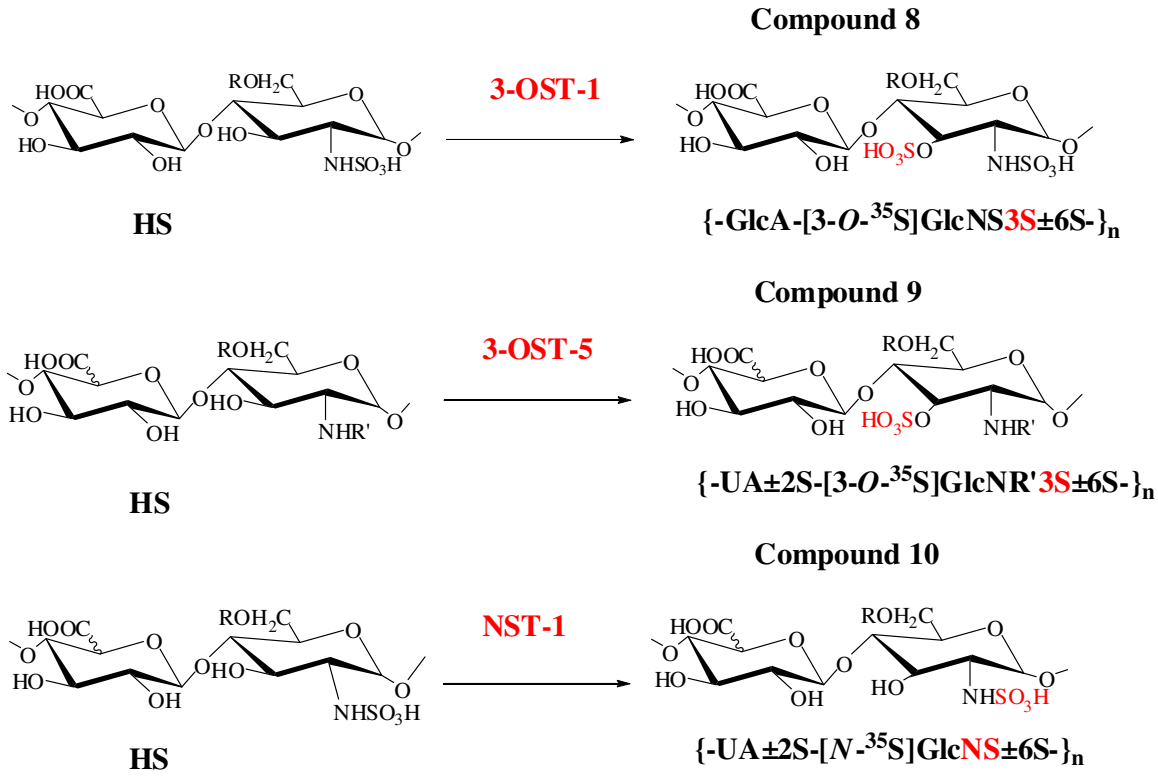

Figure 36. Scheme for synthesizing structures from HS. 3-*O*-sulfated and *N*-sulfated structures were produced by incubating the starting material with 3-OST-1, 3-OST-5, or NST-1 in the presence of [^{35}S] PAPS.

3-*O*- and *N*-sulfated positions on glucosamine were evaluated to determine if HSulf-2 could remove sulfo groups from these positions. 3-OSTs transfer sulfo groups to the 3-OH position of specific glucosamine residues within the polysaccharide. Therefore, bovine kidney heparan sulfate was modified by 3-OST-1 and 3-OST-5 separately to produce 3-*O*-[^{35}S] ICN HS which contain either GlcA-[3-*O*-^{35}S] GlcNS3S±6S or UA±2S-[3-*O*-^{35}S] GlcNR3S±6S, where R represents a proton or sulfo group, respectively. In addition, *N*-[^{35}S] sulfated HS was generated by using NST-1 to produce UA±2S-[*N*-^{35}S] GlcNS±6S disaccharide motifs within the structure. Spin column results demonstrated that compound 8, 9, and 10 were not substrates for HSulf-2 since the percentage of [^{35}S] sulfate release was

approximately the same as the control. Therefore, it was determined that HSulf-2 does not release 3-*O*-sulfo or *N*-sulfo groups from HP/HS polysaccharides. A summary of the HSulf-2 activity against the synthetic polysaccharides is shown in table 10.

Compound	Structure	Control [^{35}S] Sulfate Release (pmol)	HSulf-2 Treatment [^{35}S] Sulfate Release (pmol)
1	**[-IdoA2S-[6-*O*-^{35}S]GlcNS6S-]$_n$**	**2.7±1.0**	**97.5±0.8**
2	**[-GlcA2S-[6-*O*-^{35}S]GlcNS6S-]$_n$**	**N.D**	**N.D.**
3	**[-IdoA-[6-*O*-^{35}S]GlcNS6S-]$_n$**	**8.3±0.1**	**24.3±2.7**
4	**[-GlcA-[6-*O*-^{35}S]GlcNS6S-]$_n$**	**6.6±1.6**	**43.1±2.4**
5	**[-GlcA-[6-*O*-^{35}S]GlcAc6S-]$_n$**	**14.2±3.5**	**28.1±1.3**
6	**[-[2-*O*-^{35}S]IdoA2S-GlcNS-]$_n$**	**10.4±2.6**	**12.6±1.3**
7	**[-2-*O*-^{35}S]GlcA2S-GlcNS-]$_n$**	**6.7±1.9**	**13.7±3.0**
8	**[-GlcA-[3-*O*-^{35}S]GlcNS3S±6S-]$_n$**	**13.6**	**12.2**
9	**[-UA±2S-[3-*O*-^{35}S]GlcNR3S±6S-]$_n$**	**10.1**	**13.9**
10	**[-UA±2S-[*N*-^{35}S]GlcNS±6S-]$_n$**	**11.7**	**13.2**

Table 10. Evaluation of HSulf-2 substrate specificity against synthetic polysaccharides.
N.D. Not determined

Conclusions

HSulf-2 cDNA was introduced into and expressed by CHO cells to study the substrate specificity of this enzyme. Results of the disaccharide analysis of HS collected from CHO cells expressing HSulf-2 showed approximately a 2-fold reduction of ΔUA2S-GlcNS6S disaccharide, a known substrate for HSulf-2, and approximately a 2-fold reduction of ΔUA2S-GlcNS disaccharide. This demonstrated that HSulf-2 expressed by CHO cells was active *in vivo*. Western blotting analysis produced a 138 kDa band for HSulf-2 found in the cell extract. This was consistent with the glycosylated protein containing a *myc*-His tag and no signal sequence. HSulf-2 cell extract was then used to treat HS from nontransfected CHO cells. The disaccharide analysis showed HSulf-2 was active in the cell extract by

reducing the ΔUA2S-GlcNS6S disaccharide in the elution profile while increasing the amount of ΔUA2S-GlcNS disaccharide found in the treated HS. In addition, testing was performed for the activity in the CM of CHO cells expressing HSulf-2. The disaccharide analysis demonstrated that active HSulf-2 was present in the CM of CHO cells. However, the presence of HSulf-2 in the CM of CHO cells could not be demonstrated by Western blotting. This led us to believe the *myc*-His tag found on the *C*-terminus of the protein was cleaved during post-translational processing.

Synthetic polysaccharides were prepared and used to probe the substrate specificity of HSulf-2. These synthesized structures contained specific disaccharide motifs and sulfation patterns. A [^{35}S] label was placed on the 2-*O*-, 3-*O*-, 6-*O*-, or *N*-sulfation positions of uronic acid and glucosamine residues to investigate whether HSulf-2 could remove sulfo groups at different positions of variable sulfated structures. As expected, HSulf-2 had the highest activity against compound 1. For compound 3, data was inconclusive as to whether HSulf-2 had activity against IdoA residues containing no 2-*O*-sulfation due to the impurity of the starting material. However, HSulf-2 had activity against compound 4, a structure containing GlcA-GlcNS6S disaccharide motifs, and activity against compound 2, which contains GlcA2S-GlcNS6S disaccharide motifs in its structure. HSulf-2 did not remove 2-*O*-, 3-*O*-, or *N*-sulfo groups from structures, which showed that HSulf-2 is specific toward 6-*O*-sulfo groups on GlcNS residues. In addition, HSulf-2 substrate specificity extends to other disaccharide motifs not found in highly sulfated domains of HP/HS structures. Furthermore, HSulf-2 activity did not discriminate against which 2-*O*-sulfated hexuronic acid was present, even though HSulf-2 had a preference for IdoA2S residues since HSulf-2 had the highest activity against compound 1. GlcA residues devoid of 2-O-sulfation were shown to be

substrates, but the activity against this substrate was lower. Taken together, the data suggests that 2-*O*-sulfation is important for HSulf-2 activity. In addition, *N*-sulfation is critical for activity, since HSulf-2 had not activity against compound 5, which contained GlcNAc residues.

In summary, this study has provided valuable information about the substrate specificity of this member of the Sulf family. These results indicate HSulf-2 has broad substrate specificity, and is active against nonsulfated and 2-*O*-sulfated glucuronic acid residues linked to *N*-sulfated glucosamine residues. Understanding the HSulf-2 substrate specificity can be an important tool to provide further characterization of HS structures that can offer insight into its physiological roles and perhaps the design of new approaches toward synthesis of important HS oligosaccharides.

Chapter IV

THE EFFECT OF HSULF-2 ON THE BIOSYNTHESIS OF ANTICOAGULANT HS

Introduction

Heparin's anticoagulant properties have led to heparin's clinical use in the treatment of thrombolytic conditions and preventative measures during surgery. Heparin-induced thrombocytopenia (HIT) is a serious and major side effect of heparin treatment due to platelet factor 4 (PF4) binding to heparin causing an adverse immunological response. In this chapter, we wanted to employ HSulf-2 as an editing enzyme by tailoring the fine structure of anticoagulant structures. After enzymatic editing of the fine structure we wanted to evaluate the tailored structure's anticoagulant properties. In addition, we wanted to explore whether HSulf-2 tailoring of the fine structure of the anticoagulant drug, lovenox, would affect its anticoagulant properties and could maintain its anticoagulant activity in the presence of PF4. Finally, we wanted to develop a fast and cost effective way to produce large quantities of sulfatase for editing purposes by the expression of HSulf-2, MSulf-1, and MSulf-2 in a bacterial system.

Determination of 3-O-[^{35}S] HS Binding to AT

The AT binding assay is a method for determining the relative percentage of heparan sulfate that binds to this protein. This assay is a proven method to demonstrate biological function of 3-*O*-sulfated HS (i.e. thrombin and factor Xa deactivation). From the previous

chapter, HS was ^{35}S- labeled by 3-OST-1 and 3-OST-5 separately to produce material capable of binding to AT. It was demonstrated that HSulf-2 had no activity against 3-*O*-sulfo groups since it did not remove [^{35}S] 3-*O*-sulfo groups from these polysaccharides. The binding of 3-*O*- [^{35}S] sulfated ICN HS to AT was determined to evaluate the effect of HSulf-2 treatment. The results are shown in Figure 37. For 3-*O*-[^{35}S] HS generated by 3-OST-1, 43.6% of treated HS bound to AT, which was very comparable to the 51.2% of untreated HS that bound to AT. Results were similar to 3-*O*-[^{35}S] HS generated by 3-OST-5. Therefore, the data suggests that HSulf-2 does not remove critical 6-*O*-sulfo groups from the AT-binding pentasaccharide within the polysaccharide which would affect the binding to AT.

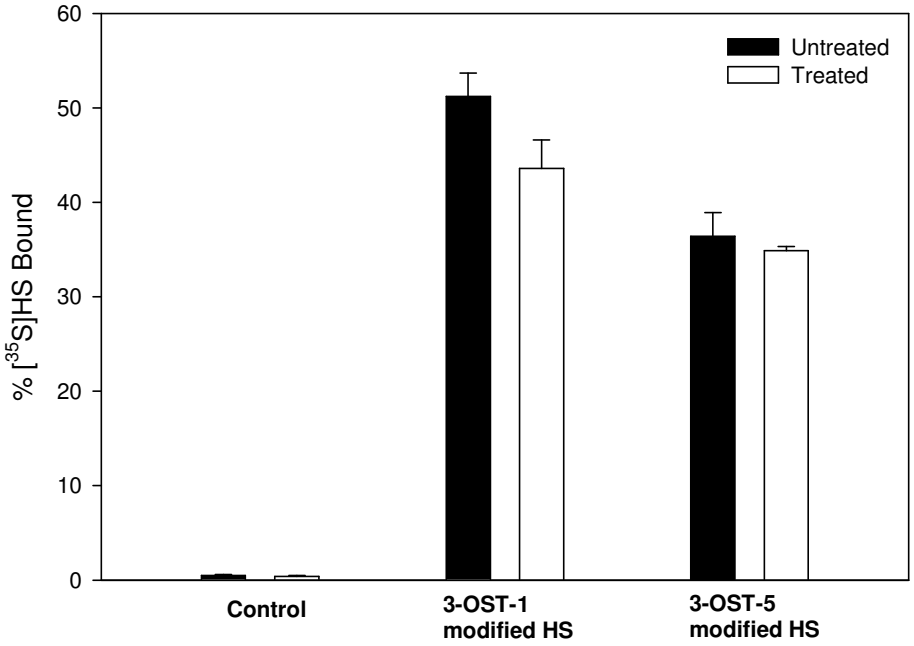

Figure 37. AT binding of 3-O-[^{35}S] HS. The binding of 3-*O*-[^{35}S] HS to AT was determined by incubating HS and AT/ConA-Sepharose beads. The control was *N*-[^{35}S] HS by NST-1, which does not bind to AT considerably. Results represented from two independent experiments as the relative-percentage of polysaccharide bound to AT after elution with buffer containing 1M NaCl.

Since binding to AT was maintained after HSulf-2 treatment, it was speculated that HSulf-2 may be removing nonradioactive 6-*O*-sulfo groups from these structures. The critical structural features of the pentasaccharide required for the anticoagulant function are 6-*O* and 3-*O* sulfates on 1 and 3 residues (Figure 38), and the two residues are thermodynamically linked for accelerating coagulation enzyme inactivation by induction of the required conformational change in AT (214-218) (figure 2). Our hypothesis was that HSulf-2 could remove 6-*O*-sulfo groups from anticoagulatant HS structures, but not remove 6-*O*-sulfo groups in the critical pentasaccharide region.

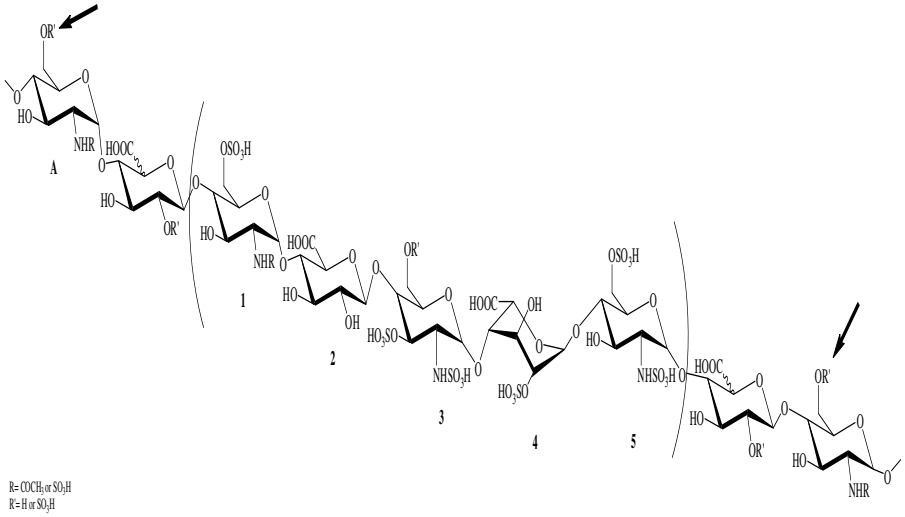

Figure 38. The AT binding HS pentasaccharide. Residue 3 contains a critical 6-*O*-sulfo group on glucosamine. The R represents an acetyl (-$COCH_3$) group or a sulfo (-OSO_3H) group. R' represents hydrogen (-H) or a sulfo (-OSO_3H) group. Arrows point to positions outside of the pentasaccharide region where potential HSulf-2 activity could take place.

In order to determine whether HSulf-2 was removing 6-*O*-sulfo groups from anticoagulant structure, we decided to metabolically label CHO cells as described in chapter II. [^{35}S] HS was isolated from the CHO cells, and subjected to addition of 3-*O*-sulfo groups by 3-OST-1 and 3-OST-5 separately using nonradioactive PAPS as a donor. In addition,

nonradioactive labeled 3-*O*-[^{35}S] HS from CHO cells were subjected to AT binding to determine the effects of HSulf-2 treatment on these polysaccharides. In Figure 39, 14.4% and 10.6% treated nonradioactive labeled 3-OST-1 and 3-OST-5 modified [^{35}S] HS from CHO cells bound to AT comparably to untreated 3-OST-1 and 3-OST-5 modified [^{35}S] HS from CHO cells, 16.1% and 11.0%, respectively. This showed that AT binding was maintained, which suggested that HSulf-2 does not remove 6-*O*-sulfo groups from within the critical AT pentasaccharide sequence needed for anticoagulant activity.

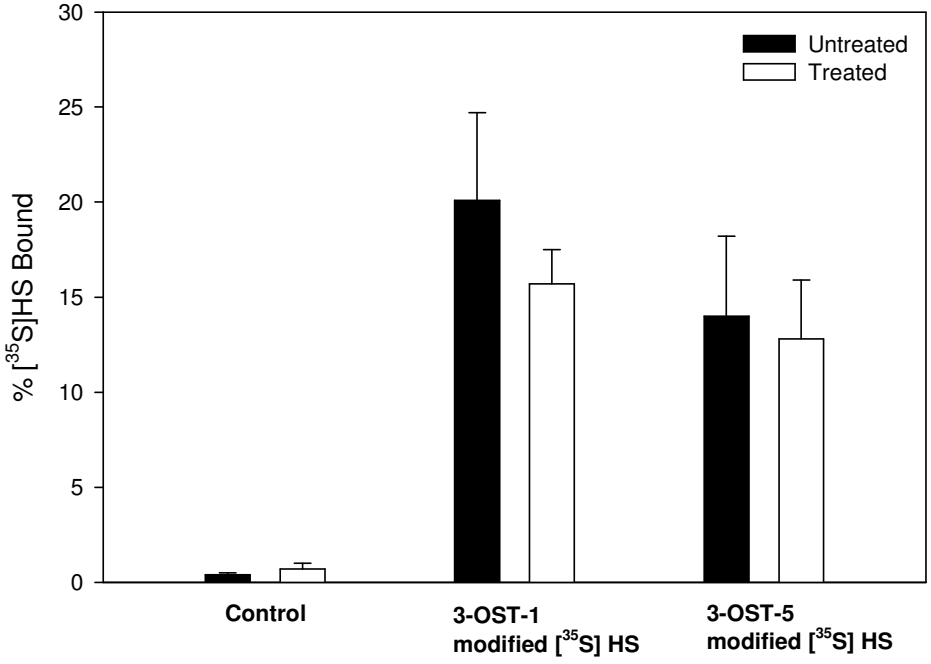

Figure 39. AT binding of 3-*O*-[^{35}S] HS from CHO cells. The binding of 3-*O*-[^{35}S] HS to AT was determined by incubating HS and AT/ConA-Sepharose beads. The control was unmodified [^{35}S] HS from CHO cells, which does not bind to AT considerably. Results represented from two independent experiments as the relative-percentage of polysaccharide bound to AT after elution with buffer containing 1M NaCl.

Determination of sulfatase activity on 3-O-sulfated structures

To further investigate whether HSulf-2 was removing 6-*O*-sulfo groups from the nonradiolabeled 3-*O*-sulfated [^{35}S] HS from CHO cells, the same material used for the AT binding assay was degraded to disaccharides by a mixture of heparin lyases. The ^{35}S-labeled disaccharides were subjected to RPIP chromatography. In figure 40, panel A and B display the chromatograms of the disaccharide analysis of untreated and treated nonradiolabeled 3-*O*-labeled [^{35}S] HS from CHO cells by 3-OST-1. After treatment with HSulf-2, there is a 15% decrease in peak 4, which was a ΔUA2S-GlcNS6S disaccharide. There is also a 15% increase in peak 3, which was identified as a ΔUA2S-GlcNS disaccharide. Panels A and B in figure 41 display the chromatograms of nonradiolabled 3-*O*-labeled [^{35}S] HS from CHO cells by 3-OST-5. In the chromatogram, a 4% decrease of peak 4 with a subsequent 4% increase in peak 3 is observed. However, in both figures 40 and 41, peak 4 does not completely disappear. This ΔUA-GlcNS3S6S disaccharide motif within the polysaccharide is part of the AT pentasaccharide necessary for anticoagulant activity. In the pentasaccharide, 6-*O*-sulfation at this position is not necessary for anticoagulant activity, but the presence of 3-*O*-sulfation may hinder HSulf-2 activity against this disaccharide or other disaccharides within the vicinity. This seems to be more prevalent in the 3-OST-5 modified structure. This is due to more 3-*O*-sulfated positions within the polysaccharide since 3-OST-5 can create an AT binding site and a gD binding site. Thus, this structure could generate more HSulf-2 resistant motifs within the polysaccharide. The summary of the disaccharide analysis is shown in table 11. Taken as a whole, there is observable HSulf-2 activity against this anticoagulant structure which does not affect binding to AT.

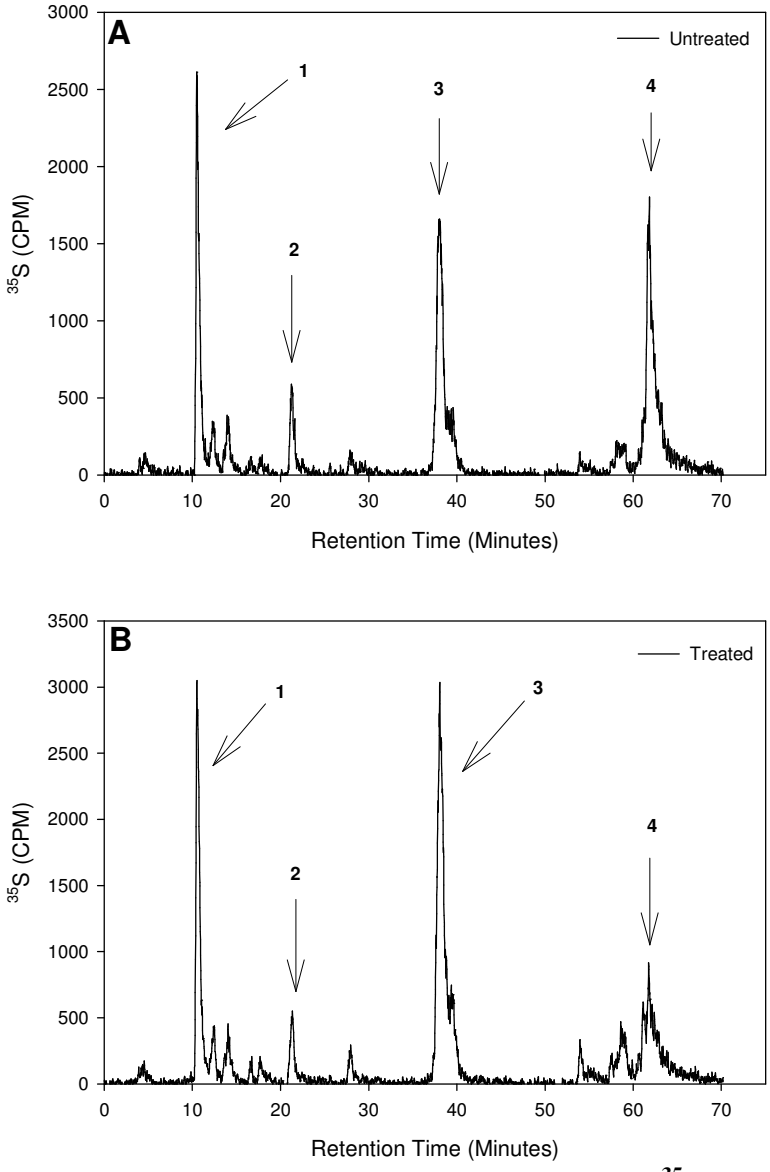

Figure 40. Disaccharide analysis of nonradiolabled 3-*O*-sulfated [^{35}S] HS from CHO cells by 3-OST-1. Panel A represents the disaccharide analysis of untreated 3-*O*-[^{35}S] HS nonradioactive labeled by 3-OST-1. Panel B represents the disaccharide analysis of HSulf-2 treated 3-*O*-[^{35}S] HS nonradioactive labeled by 3-OST-1. Treated and untreated nonradioactive labeled 3-*O*-[^{35}S] HS from CHO cells was subjected to heparin lyase I, II, and III degradation into ^{35}S-labeled disaccharides. Approximately 100,000 cpm of the digested material was subjected to RPIP chromatography. (1) represents ΔUA-GlcNS; (2) represents UA-GlcNS6S; (3) represents ΔUA2S-GlcNS; (4) represents ΔUA2S-GlcNS6S. The *x-axis* shows the retention time in minutes, the *y axis* monitors [^{35}S] using online detection.

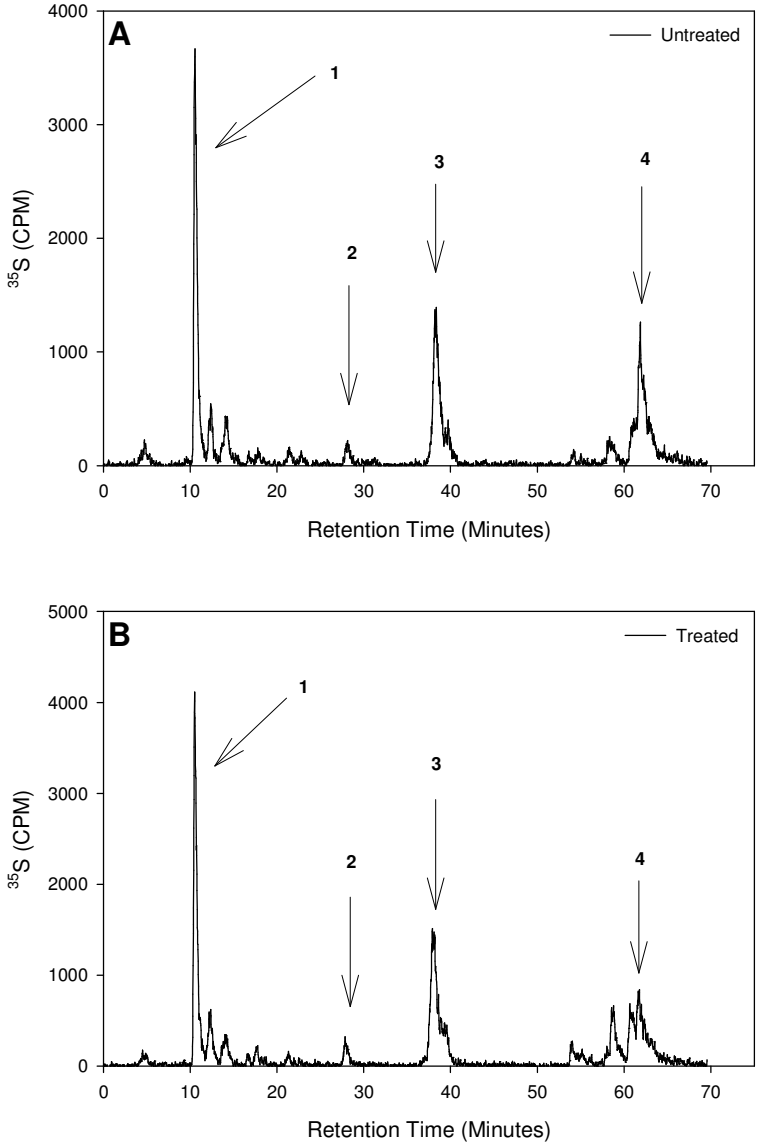

Figure 41. Disaccharide analysis of nonradioactive labeled 3-*O*-[^{35}S] HS from CHO cells by 3-OST-5. Panel A represents the disaccharide analysis of untreated 3-*O*-[^{35}S] HS nonradioactive labeled by 3-OST-5. Panel B represents the disaccharide analysis of HSulf-2 treated 3-*O*-[^{35}S] HS nonradioactive labeled by 3-OST-5. Treated and untreated nonradioactive labeled 3-*O*-[^{35}S] HS from CHO cells was subjected to heparin lyase I, II, and III degradation into ^{35}S-labeled disaccharides. Approximately 100,000 cpm of the digested material was subjected to RPIP chromatography. (1) represents ΔUA-GlcNS; (2) represents UA-GlcNS6S; (3) represents ΔUA2S-GlcNS; (4) represents a mixture of ΔUA2S-GlcNS6S and ΔUA-GlcNS3S6S. The *x-axis* shows the retention time in minutes, the *y axis* monitors [^{35}S] using online detection.

	(1) ΔUA-GlcNS (mol %)	(2) ΔUA-GlcNS6S (mol %)	(3) ΔUA2S-GlcNS (mol %)	(4) ΔUA2S-GlcNS6S (mol %)
3OST-1				
Untreated	22	6	33	39
Treated	23	5	48	24
3OST-5				
Untreated	35	2	29	34
Treated	35	2	33	30

Table 11. Summary of the disaccharide analysis of non-radioactive labeled 3-*O*-[^{35}S] HS. Untreated and treated polysaccharide was degraded with heparin lyase I, II, and III to generate ^{35}S-labeled disaccharides. Disaccharides were resolved on RPIP-HPLC for analysis. Results represented as mol-percent of specific disaccharide products.

Determination of AT binding by Affinity Co-Electrophoresis

The dissociation constant (K_d) for AT binding nonradiolabeled 3-*O*-sulfated [^{35}S] HS from CHO cells was established by affinity co-electrophoresis (ACE). ACE is a method that has been in several studies evaluating HS/protein interactions in both high and low affinities. (*3, 210, 211*) The advantage of employing this method is that GAGs such as HS have high mobility under the electrophoretic conditions, and ACE requires a small amount of HS to determine the K_d. The nonradiolabeled 3-*O*-sulfated [^{35}S] HS from CHO cells was purified after elution from the AT/ConA-Sepharose beads. The purified nonradiolabeled 3-*O*-sulfated [^{35}S] HS was separated under electrophoresis conditions through agarose gel zones containing AT concentrations ranging from 0 to 60nM. The migration profile of the nonradiolabeled 3-*O*-sulfated [^{35}S] HS was visualized using a Phosphor-Imager (not shown).

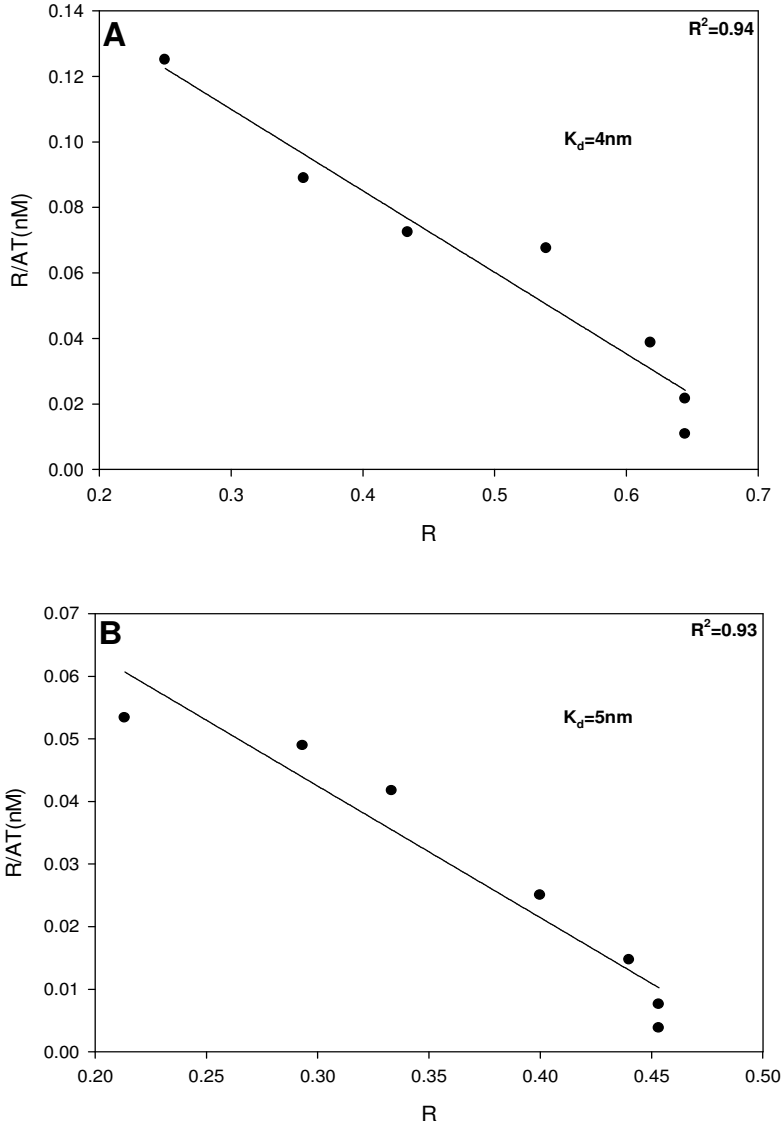

Figure 42. Determination of the K_d by affinity co-electrophoresis. An agarose gel in which 10,000cpm per lane of AT-binding nonradiolabeled 3-*O*-sulfated [^{35}S] HS by 3-OST-1 was subjected to electrophoresis through zones containing AT at the concentrations indicated. The Scatchard plot of data was obtained through autoradiograph. Panel A represents the Scatchard plot of untreated nonradiolabeled 3-*O*-sulfated [^{35}S] HS, and panel B represents the Scatchard plot of HSulf-2 treated nonradiolabeled 3-*O*-sulfated [^{35}S] HS. A plot of R/[AT] verses R, where the retardation coefficient $R=(M_0-M)/M_0$. M_0 is the migration of free 3-*O*-sulfated [^{35}S] HS, and M is the observed migration of 3-*O*-sulfated [^{35}S] HS in the presence of AT. Assuming 3-*O*-sulfated [^{35}S] HS and AT form a 1:1 complex and AT is in great excess, this plot will yield a straight line with a slope of $-1/K_d$ according to the Scatchard equation.

The nonradiolabeled 3-*O*-sulfated [^{35}S] HS was retarded by AT in a concentration dependent manner, and the relative migration distances of nonradiolabled 3-*O*-sulfated [^{35}S] HS in combination with the Scatchard equation, were used to determine the K_d value to be 4nM for the untreated nonradiolabled 3-*O*-sulfated [^{35}S] HS (figure 42, panel A) and 5nM for HSulf-2 treated nonradiolabled 3-*O*-sulfated [^{35}S] HS (figure 42, panel B). For the untreated and treated nonradiolabeled 3-*O*-sulfated [^{35}S] HS, the K_d values were comparable suggesting that removal of 6-*O*-sulfo groups from this material by HSulf-2 did not adversely affect the binding affinity to AT. In addition, the results suggest that HSulf-2 treatment is not removing 6-*O*-sulfo groups from the critical pentasaccharide motif necessary for AT binding. The concentration of nonradiolabeled 3-*O*-sulfated [^{35}S] HS was considerable lower than the AT contained in the separation zones, which allowed for the determination of the K_d value. In addition, nonradiolabeled 3-*O*-sulfated [^{35}S] HS was nearly fully retarded at high concentrations of AT suggesting the preparation was pure in terms of AT binding affinity. It is important to note that the binding affinity of heparin and AT was determined to be 9nM (211) showing there is a similar binding affinity for AT by untreated and treated nonradiolabeled 3-*O*-sulfated [^{35}S] HS that relates to previously characterized anticoagulant HS.

Determination of HSulf-2 Activity Against Lovenox®

Since the previous data suggested that HSulf-2 treated anticoagulant structures maintained binding to AT, we wanted to investigate the effects of HSulf-2 treatment on the anticoagulant, LMWH drug lovenox. Therefore, lovenox was treated with HSulf-2 described in Chapter II. The material was quantified by using an alcian blue assay. In the assay,

negatively charged groups on HS interact with the positively charged dye leading to HS binding to the dye in a concentration dependent manner as shown in figure 43. Figure 43 shows the standard curve using the alcian blue assay with untreated lovenox in order to demonstrate this method could be used to quantify the amount of treated lovenox that was purified. It also demonstrated that there is a linear correlation between the amount of lovenox and $O.D._{600nm}$, which is maintained up to 2 ug of lovenox. Therefore, once the standard curve for untreated lovenox was generated, the concentration of purified treated lovenox was determined, giving a standard curve with similar results to figure 8.

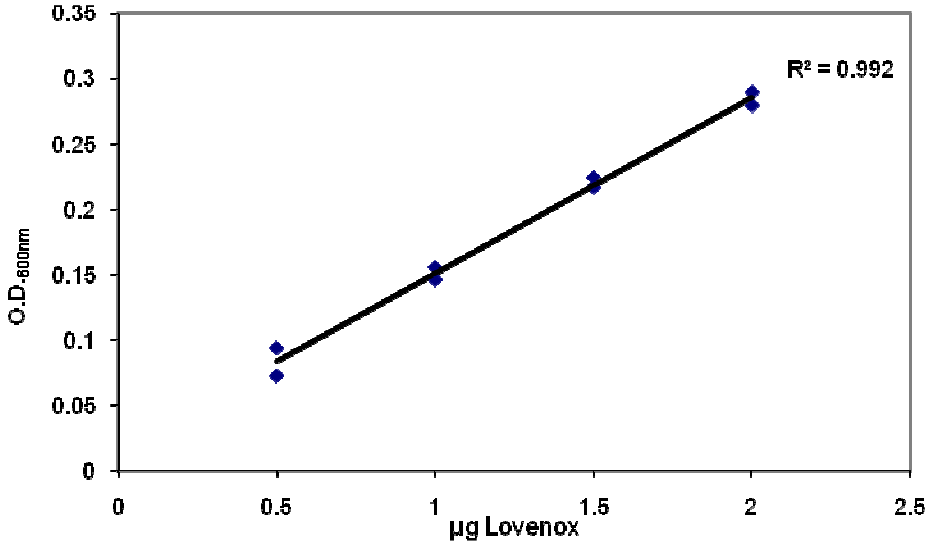

Figure 43. Alcian blue assay for the quantification of treated lovenox. The standard curve was prepared in duplicate with untreated lovenox. The assay was performed as explained in "materials and methods" section. The linear regression and R^2 value are present in the graph. The purified treated lovenox was prepared in duplicate at various concentrations to fall on the standard curve.

It was important to determine whether HSulf-2 treatment yielded a reduction of 6-*O*-sulfo groups within lovenox. After treatment of lovenox with HSulf-2, a mixture of heparin lyases was used to degrade 5µg of untreated and treated lovenox separately into

disaccharides. The disaccharides were resolved by RPIP chromatography. The elution profile for untreated lovenox contained a major disaccharide peak, ΔUA2S-GlcNS6S, which eluted at 59 min represented as peak 2 (figure 44, panel A). For the elution profile of HSulf-2 treated lovenox, peak 2 decreases with a subsequent increase in another major disaccharide peak identified as ΔUA2S-GlcNS, which eluted at 30 min and is represented as peak 1(figure 44, panel B). In figure 44, panel B, peak 2 did not completely disappear from the chromatogram due to incomplete digestion by HSulf-2. In the elution profile of untreated lovenox the ratio of peak 1 compared to peak 2 is approximately 1:8. After treatment with HSulf-2, this ratio becomes approximately 1:1. This suggested that HSulf-2 treatment of lovenox reduced 6-*O*-sulfo groups with this structure, but again there may be some resistant motifs that are not susceptible to HSulf-2 activity due to the presence of 3-*O*-sulfation as previously seen in other treated anticoagulant structures.

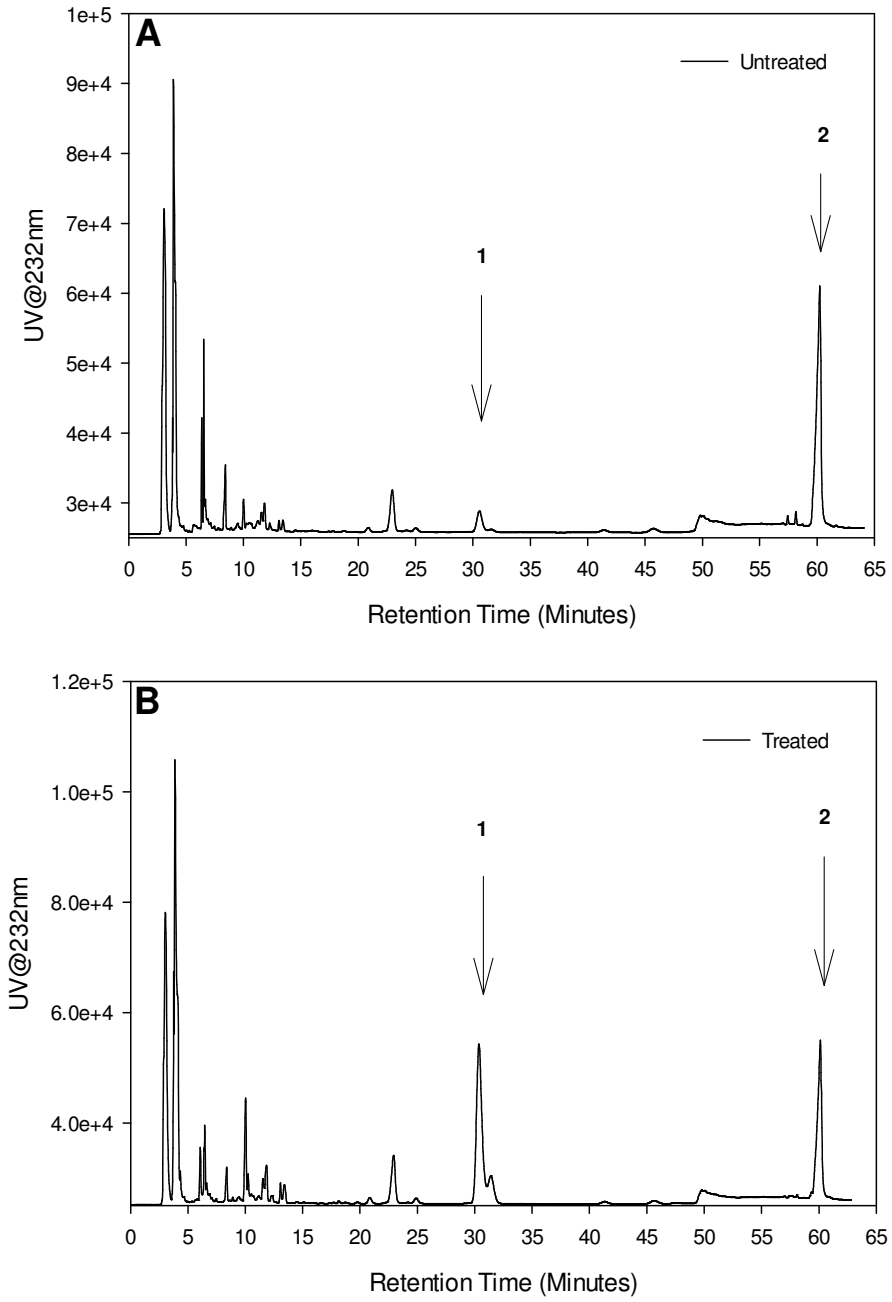

Figure 44. Disaccharide analysis of lovenox. Panel A represents untreated lovenox, and panel B represents HSulf-2 treated lovenox. Both untreated and treated lovenox were subjected to degradation by heparin lyase I, II, III into nonradioactive disaccharides, and resolved on an RPIP column. The procedure is described in chapter II. Peak 1 represents ΔUA2S-GlcNS disaccharide, and peak 2 represents ΔUA2S-GlcNS6S disaccharide. The *x-axis* shows the retention time in minutes, and the *y-axis* monitors the UV at 232nm.

AT-Mediated Inhibition of Factor Xa

Factor Xa is a serine protease that plays a critical role in blood coagulation by regulating the formation of a major constituent of blood clots, fibrin. In blood vessels, the interaction of HS and AT prevents blood from clotting by inhibiting Factor Xa activity and other serine proteases. AT-mediated inhibition of Factor Xa was used to investigate whether HSulf-2 treated lovenox bound to AT would inhibit Factor Xa comparably to untreated lovenox. Figure 45 shows the inhibition curve of the activity of Factor Xa by untreated and treated lovenox .The IC_{50} values were determined to be 100ng/ml for both untreated and treated lovenox, where approximately 15% of the Factor Xa activity remained in the presence of 400ng/ml from untreated and treated lovenox. The inhibition curve for treated lovenox still maintained anti-Factor Xa activity after binding to AT compared to the inhibition curve for untreated lovenox.

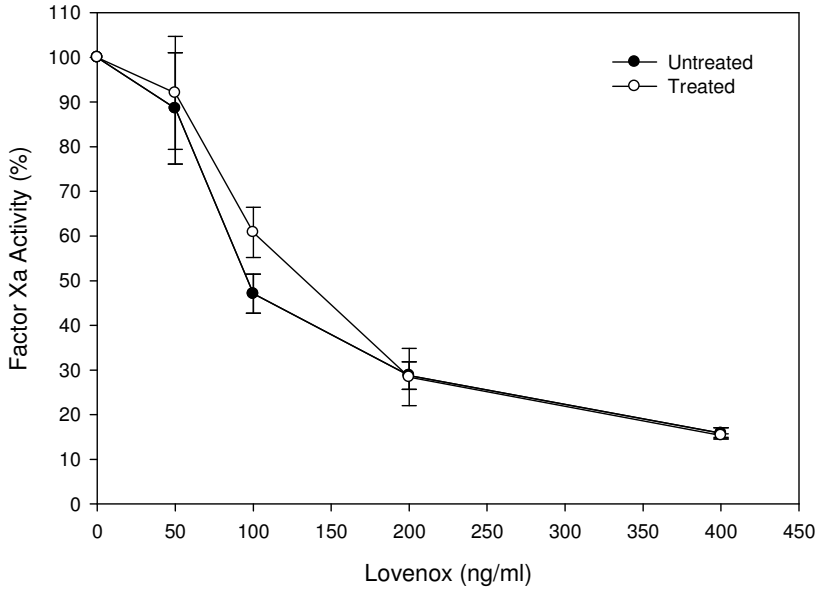

Figure 45. Inhibition curve of Factor Xa activity. Untreated lovenox (filled circle) and HSulf-2 treated lovenox (open circle) at varying concentrations as described in chapter II. The activity of Factor Xa was determined by monitoring the increase of the absorbance at 405nm after the addition of S-2764 chromogenic substrate. Each data point represents the average of two independent experiments.

Effects of HSulf-2 treatment on restoration of factor xa activity

Platelet factor 4 (PF4) is known to interfere with anticoagulation by binding to the polysaccharide and reducing the ability of the polysaccharide/AT complex to inhibit Factor Xa activity. The activity of PF4 is a side effect of anticoagulant heparins that causes heparin induced thrombocytopenia (HIT), and many studies have been devoted to understanding and preventing this issue with anticoagulant drugs. Therefore, we wanted to determine whether HSulf-2 treatment of lovenox would reduce PF4 binding and inhibit the restoration of Factor Xa activity. PF4 was expressed in bacteria and purified in our laboratory. Various amounts of PF4 were pre-incubated with 400ng/ml of untreated and treated lovenox. At this concentration, there is only approximately 15% Factor Xa activity remaining in the presence of lovenox and AT. After pre-incubation, anti-Factor Xa activities of the untreated and treated lovenox were examined by determining the remaining activity of Factor Xa. In figure 46, addition of increasing amounts of PF4 progressively neutralized the anti-Factor Xa activity of 400ng/ml of untreated lovenox, with an IC_{50} approximately 8µg. Total inhibition required approximately 20µg of PF4. Pre-incubation with treated lovenox produced an IC_{50} of approximately 5 µg, which was comparable to untreated lovenox. However, HSulf-2 treated lovenox was able to prevent the total restoration of Factor Xa activity with a total inhibition at 10µg of PF4. The results show that PF4 binds approximately the same to untreated and treated lovenox, but there is a population of treated lovenox that is not binding to PF4 since the restoration of Factor Xa activity by untreated lovenox is approximately 2-fold higher than treated lovenox.

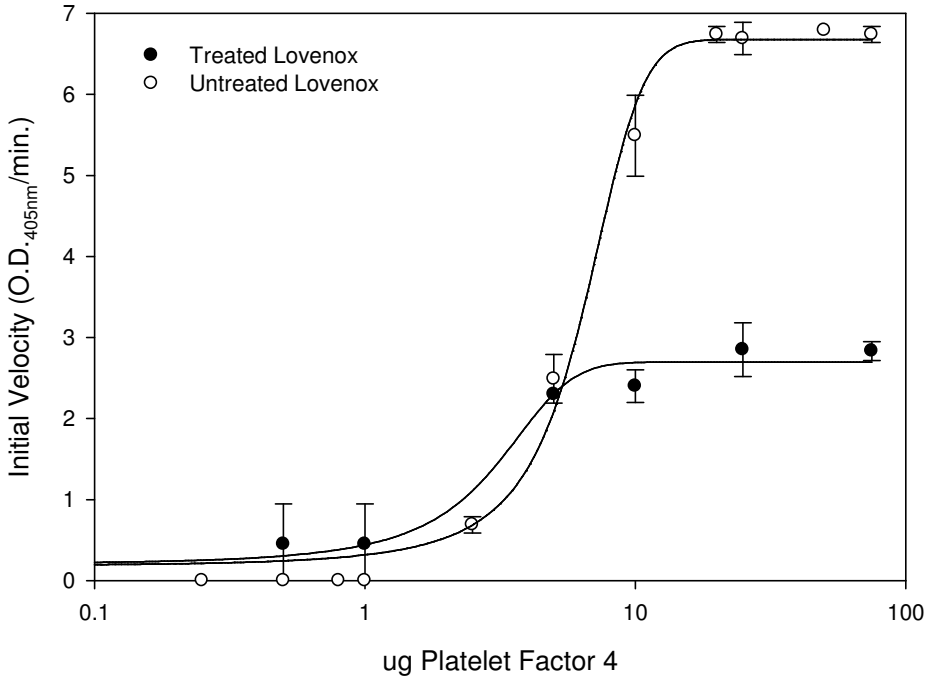

Figure 46. Restoration of Factor Xa activity with platelet factor 4. HSulf-2 treated and untreated lovenox (400ng/ml) and different concentrations of PF4 were preincubated together before the addition of AT and factor Xa. Chromogenic substrate S2765 was added to determine the initial velocity of factor Xa activities at 405nm.

Effects of HSulf-2 Treatment on PF4 Binding

Once it was shown that PF4 could not bind to a population of lovenox and restore Factor Xa activity after HSulf-2 treatment, we wanted to further demonstrate whether HSulf-2 treatment was affecting PF4 binding to HS polysaccharides. Therefore, a filter binding assay was performed by incubating various amounts of PF4 with [^{35}S] HS from CHO cells, and applying the reaction mixture to a nitrocellulose membrane. This membrane is capable of binding to proteins and will not bind to the radioactive polysaccharide. Therefore, if PF4 forms a complex with the radioactive polysaccharide, it will remain bound to the membrane after washing the membrane several times. [^{35}S] HS complexed with PF4 was determined using a scintillation counter. Figure 47 show the results of the filter binding assay. In the

figure, increasing amounts of PF4 bound significantly less to [^{35}S] HS after HSulf-2 treatment compared to control. This data demonstrated that HSulf-2 treatment can affect PF4 binding and forming a complex with HS polysaccharides.

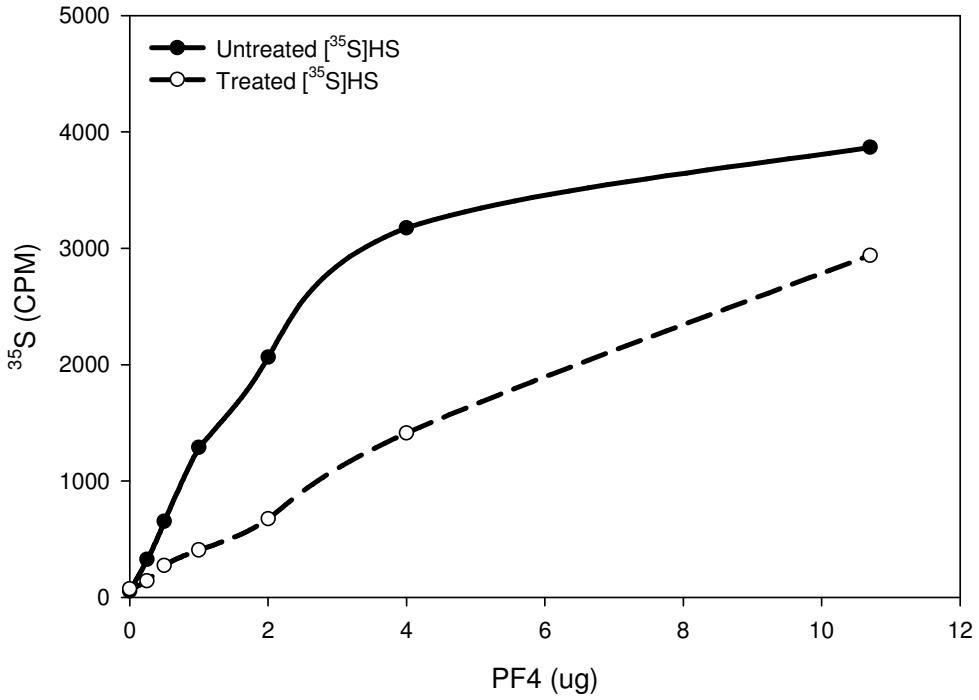

Figure 47. Filter binding assay of PF4 before and after HSulf-2 treatment. 10,000 cpm [^{35}S] HS was incubated with increasing amounts of PF4, and placed on a nitrocellulose membrane. The membrane was washed and the bound material was detected using a scintillation counter. S.D. < ±1%.

Reduction in FGF Mediated Proliferation

BaF3 cells expressing the FGFR1c receptor are dependent on IL-3 supplemented in the medium for growth. In the absence of IL-3, the BaF3/FRGR1c cells depend on the addition of both FGF and HP/HS for cell proliferation. We wanted to determine the effect on FGF mediated proliferation in the presence of HSulf-2 treated lovenox. Therefore, the activity was measured for heparin, untreated lovenox, and HSulf-2 treated lovenox in promoting cell mitogenesis using FGF-2/FGFR1c system in BaF3 cells at different

concentrations. The cells receiving untreated lovenox showed an increase in [^{3}H]-thymidine incorporation, which was about 30% of that of heparin, respectively, demonstrating that both 2-*O*- and 6-*O*-sulfation confer the activity in promoting cell proliferation (figure 48). HSulf-2 treated lovenox exhibited no activity in promoting cell proliferation. This showed that HSulf-2 was able to edit lovenox by removing 6-*O*-sulfo groups altering the original structure of lovenox carrying a specific sequence and order of 2-*O*- and 6-*O*-sulfation necessary for the moderate signal given by untreated lovenox as suggested by previous literature (219). These results also demonstrate that HSulf-2 treated lovenox can separate anticoagulant activity from mitogenic activity, which would be beneficial to patients on long-term anticoagulation therapy.

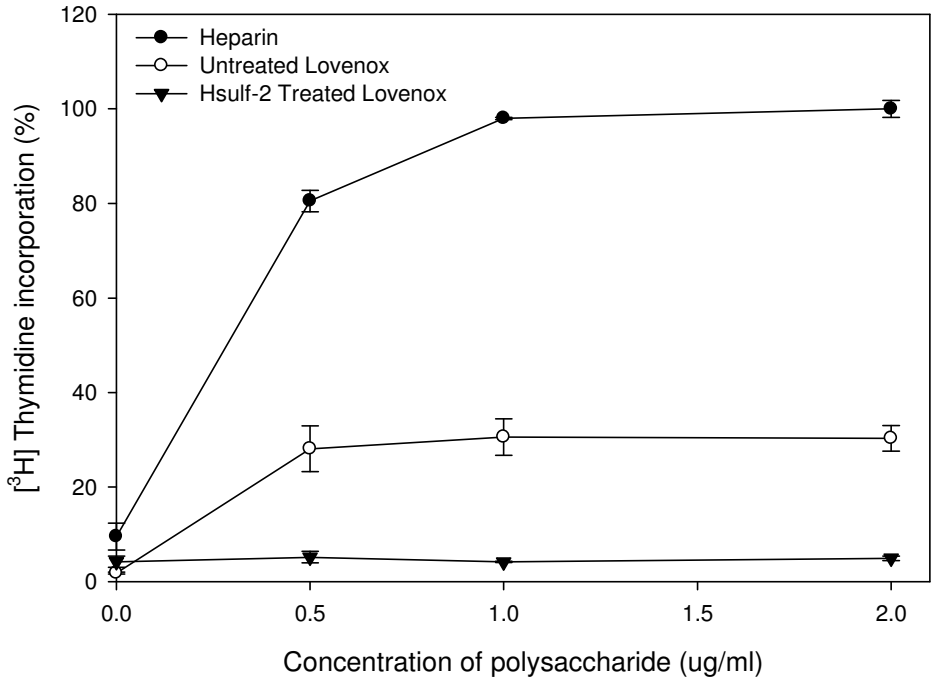

Figure 48. The effects of lovenox on FGF2-dependent BaF3 FGFR1c cell proliferation. BaF3 FGFR1c cells were seeded in 48-well plates with 2 nM FGF2 for control and 2 nM FGF2 plus various concentrations untreated and treated lovenox and heparin. Cells were cultured for 40 hr, followed by incubation in the media containing [^{3}H]thymidine for 4 hr. The cellular proliferation was determined by [^{3}H]thymidine incorporation into the DNA.

Chaperone Assisted Expression of Mammalian Sulfs in E. coli

In order to be capable of tailoring milligram amounts of lovenox or other anticoagulant heparins for future animal studies, HSulf-2 had to be produced in large quantities. Therefore, HSulf-2 was cloned into pMAL-c2x vector designed to express a maltose binding protein (MBP) fused to the *N*-terminus of the recombinant protein. The advantage of using the MBP fusion protein is that it helps generate a large amount of soluble protein. The procedure for the expression of MBP-HSulf-2 is described in Chapter II, which was carried out in E. coli co-expressing the chaperone proteins GroEL and GroES. Cloning and expression of mouse sulf isoforms one and two were also prepared in the same manner along with another version of HSulf-2 in which the signal sequence was truncated. The cell supernatant of each construct was purified by amylose chromatography. The Sulf proteins after amylose column purification were analyzed by SDS-PAGE and the gel is shown in figure 49. Figure 50 represents the standard curve of the molecular weight of the protein standards and their migration distance used to calculate the molecular weight of the bands observed in the gel. The purified Sulf migrated at a calculated molecular weight of 143kDa, which was consistent with the size of the protein fused to the maltose binding protein. The results suggest that the recombinant MBP-Sulfs were approximately 10% pure, since the eluent contained a large amount of chaperone and lower molecular weight fragments which could be the result of proteolytic degradation during the purification.

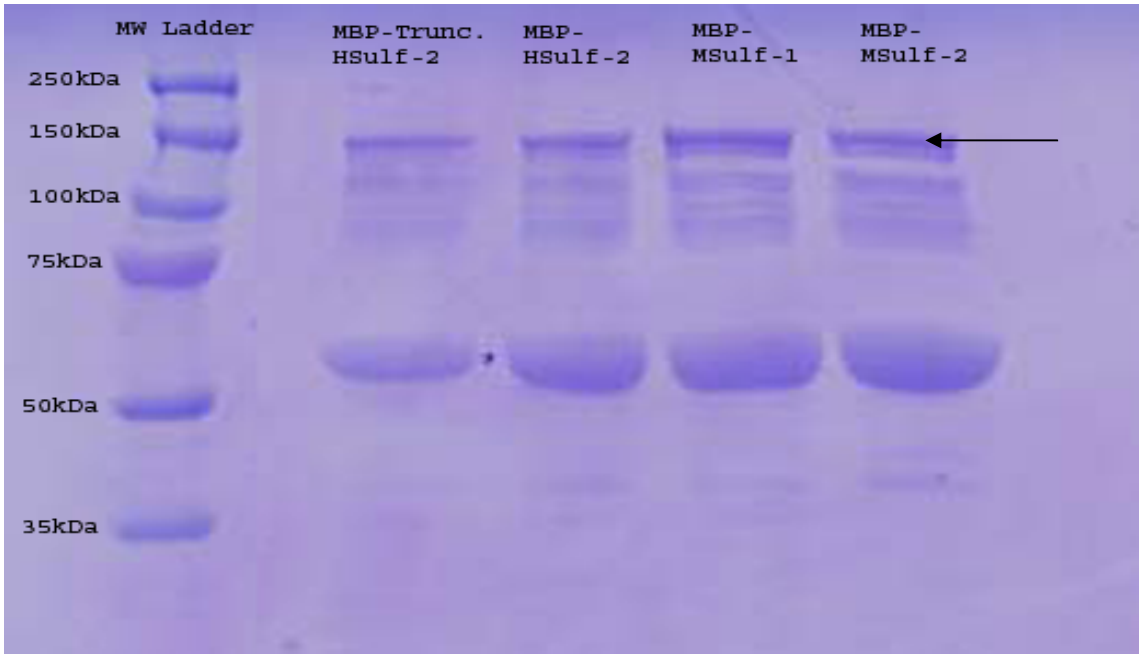

Figure 49. SDS-PAGE analysis of purified bacterial expressed mammalian Sulfs. SDS-PAGE analysis was performed on the purified MBP-Sulf proteins as described in chapter II. Lane 1 represents the molecular weight ladder; lane 2 represents MBP-truncated HSulf-2, which does not contain the signal sequence; lane 3 represents full length MBP-HSulf-2; lane 4 represents MBP-MSulf-1; lane 5 represents MBP-MSulf-2. Each MBP-Sulf yielded between 27-75mg per liter of culture.

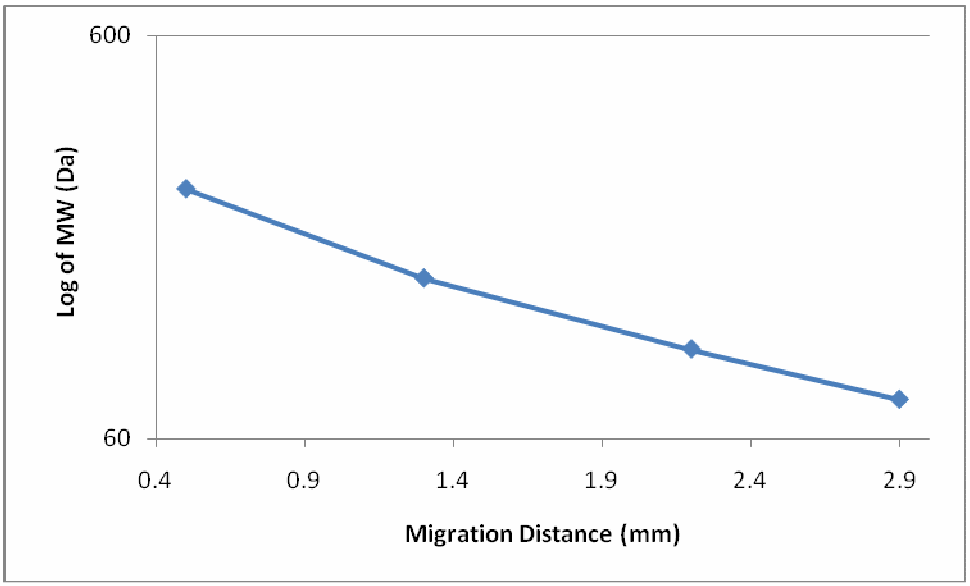

Figure 50. Molecular weight standard curve of MBP-Sulfs. The standard curve was prepared by comparing the molecular weight markers within the molecular weight ladder with their migration distances within the Western blot. The migration distance of the band of interest was measured and the resultant molecular weight was determined from the standard curve.

Determination of the Activity of MBP-HSulf-2 from E.coli

To determine whether the bacterial expressed maltose binding protein (MBP)-HSulf-2 fusion protein had activity, human embryonic kidney (HEK) cells were metabolically labeled with $Na_2{}^{35}SO_4$, and the [^{35}S] HS was isolated. The [^{35}S] HS was treated with MBP-HSulf-2, and the resultant was subjected degradation by a mixture of heparin lyases which generated ^{35}S-labeled disaccharides. The ^{35}S-labeled disaccharides were resolved on a PAMN column. The disaccharide analysis did not demonstrate HSulf-2 activity (data not shown). A disaccharide analysis was performed in the same manner for MBP-truncated HSulf-2, MBP-MSulf-1, and MBP-MSulf-2. This also showed no activity was present.

Therefore, we had to use an alternative method to determine the activity of the bacterial expressed Sulfs. The spin column method was used to evaluate sulfatase activity. Compound 1 was to investigate whether these bacterial expressed Sulfs had activity. Results

showed minimal activity against compound 1 (data not shown). Since the activity of the bacterial expressed mammalian Sulfs was low, we decided to increase the amount of sulfatase present in the reaction by growing and expressing six liters of each sulfatase, and then treating the sulfatase as described in chapter II for CHO cell cultured HSulf-2 before testing the activity. This yielded an increase in activity against compound 1 that was comparable to HSulf-2 found in the CM of CHO cells (figure 51). Both the truncated and the full length version of MBP-HSulf-2 released approximately 92.8% of [^{35}S] sulfate from compound 1 compared to control (12%), which was comparable the 97.5% release from HSulf-2 CM. MBP-MSulf-1 released approximately 94.5%, and MBP-MSulf-2 removed 63.6% of [^{35}S] sulfate from compound 1.

Overall, these results demonstrated HSulf-2, MSulf-1, and MSulf-2 expressed in bacteria removed 6-*O*-sulfo groups from compound 1. However, this process was laborious and not very efficient for the amount of enzyme expressed versus the low specific activity. Therefore, the bacterial expression and activity of these mammalian Sulfs needed to be improved. In order to utilize a considerable smaller amount of enzyme with comparable activity to HSulf-2 expressed from CHO cells, the enzymes were subjected to furin cleavage to try to create truncated proteins with potentially higher activity. After furin cleavage, an SDS-PAGE was run to determine whether the cleavage of the proteins was successful. The gel showed there was no furin cleavage of any of the Sulf proteins (data not shown). This could have been due to the bacterial expressed Sulfs having resistance to cleavage, interference of other proteins since the purity is low, or a component of the cleavage process missing in the *in vitro* reaction.

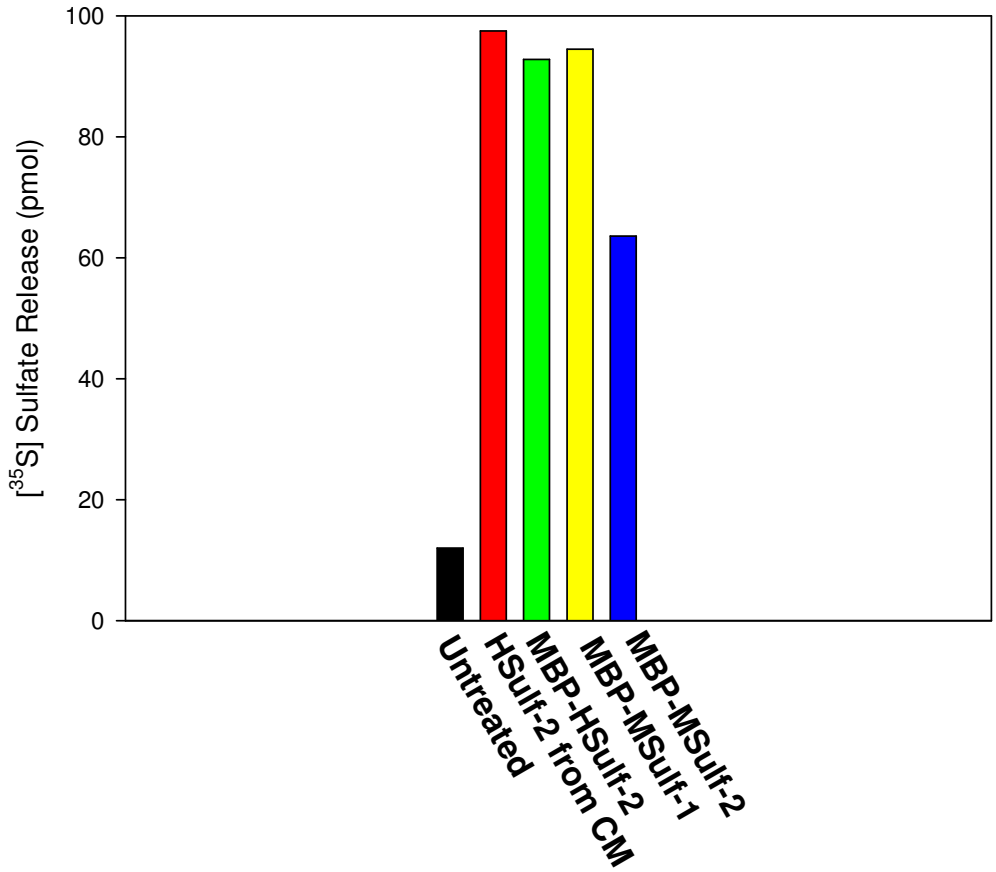

Figure 51. MBP-Sulf activity against compound 1. Each Sulf was prepared and incubated with compound 1 as described in chapter II. The reaction was subjected to the spin column method, and [^{35}S] sulfated release was determined by calculating the amount of pmols remaining after centrifugation and scintillation counting. The negative control represents the untreated substrate. The positive control represents the treatment of the substrate with mammalian expressed HSulf-2 CM. MBP-HSulf-2 represents the full length bacterial expressed maltose binding fusion protein construct. MBP-MSulf-1 represents the full length bacterial expressed maltose binding fusion protein. MBP-MSulf-2 represents the full length bacterial expressed maltose binding fusion protein.

Conclusions

HSulf-2 was utilized as an editing enzyme to evaluate whether the enzyme could tailor the fine structure of anticoagulant structures, and whether the tailoring of the fine structure had any effect of their anticoagulant properties. Results showed that AT binding was still maintained after HSulf-2 treatment. This implied that HSulf-2 was removing 6-*O*-

sulfo groups from the anticoagulant structures outside of the critical pentasaccharide sequence necessary for AT binding and anticoagulant activity. The disaccharide analysis of nonradiolabeled 3-*O*-sulfated [^{35}S] HS from CHO cells by 3-OST-1 and 3-OST-5 separately demonstrated that HSulf-2 could remove 6-*O*-sulfo groups from these structures but to a lesser extent with structures modified by 3-OST-5. This could be due to the generation of more HSulf-2 resistant structures found within the structure. In addition, the binding affinity to AT for untreated and HSulf-2 treated nonradiolabeled 3-*O*-sulfated [^{35}S] HS from CHO cells by 3-OST-1 were comparable suggesting HSulf-2 does not affect the anticoagulant structure binding to AT.

Since the data suggested HSulf-2 treated anticoagulant structures maintained anticoagulant properties, we decided to evaluate HSulf-2 treatment on the LMWH anticoagulant heparin, lovenox. The disaccharide analysis of HSulf-2 treated lovenox showed the enzyme was active against this compound removing 6-*O* sulfo groups from the compound. HSulf-2 activity against lovenox did not adversely affect the inhibition of Factor Xa by lovenox, but did effect the restoration of the Factor Xa activity by the introduction of PF4. Data suggested that PF4 was unable to bind to a population of HSulf-2 treated lovenox, which lead to a 2-fold reduction in the neutralization of anti-Factor Xa activity. In addition, a filter binding assay involving PF4 and [^{35}S] HS from CHO cells demonstrated that HSulf-2 treated affected PF4 ability to bind and form a complex with HS polysaccharides. Moreover, the FGF-2 dependent Baf3 FGFR1c cell proliferation assay demonstrated HSulf-2 treated lovenox showed basal levels of [^{3}H] thymidine incorporation into cells suggesting the tailored compound does not induce cell growth.

In order to perform a tailoring of anticoagulant structures in an efficient and cost effect manner on a large scale, large quantities of Sulf enzyme had to be produced. HSulf-2, MSulf-1, and MSulf-2 were cloned and expressed in large quantities in *E. coli* with a yield of 27-75mg per liter of culture. This expression was accomplished by co-expressing bacterial chaperone proteins. Bacterial expression of MBP- mammalian Sulf fusion proteins demonstrated they contained sulfatase activity by removing 6-*O*-sulfo groups from compound 1. To our knowledge, using a bacterial expression system to produce mammalian Sulf proteins has not been reported previously, and contradicts the notion that glycoslyation of Sulfs is necessary for activity. In summary, the utilization of Sulfs as an editing enzyme to tailor the fine structure of HP/HS structures has the potential to be an important tool in activities involving biological and therapeutic aims. However, improvement of the expression and activity is necessary for large scale Sulf tailoring of HP/HS structures.

CHAPTER V

EXPRESSION AND CHARACTERIZATION OF A PUTATIVE SULFATASE

Introduction

Characterization of sulfate enzymes may prove to be very beneficial in determining the sulfation state of GAGS under physiological and pathophysiological conditions. In addition, they could become a valuable tool in drug discovery and design. A potential iduronate-2-sulfatase (IDS) was identified. This protein was designated as x-sulfatase. In this study we sought to determine whether this potential sulfatase was active, to understand the substrate specificity, and the potential biological function of x-sulfatase. Iduronate-2-sulfatase has been identified as lysosomal storage enzyme involved in the catabolism of sulfate bearing GAGs. IDS has been found in mouse and human as well as bacteria with only one isoform (125). IDS catalyzes the hydrolysis of 2-*O*-sulfo groups from L-iduronic acid residues of HP, HS, and DS as depicted in Figure 52.

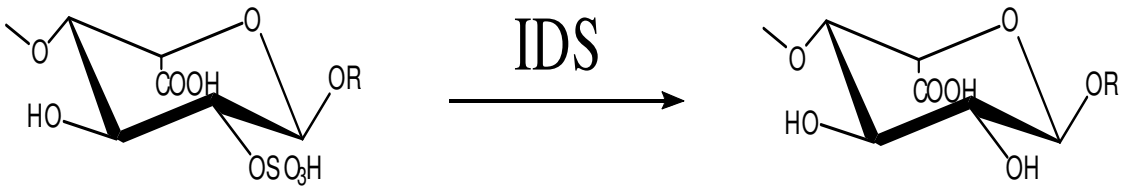

Figure 52. Reaction with iduronate-2-sulfatase. Iduronate-2-sulfatase catalyzes the hydrolysis of 2 sulfated groups of L-iduronate-2-sulfate units of heparan sulfate, dermatan sulfate, and heparin.

Identification of a Potential a IDS from S.typhimurium

Screening the nonredundant database of the National Center for Biotechnology Information with the deduced amino acid sequence of human IDS (accession number AF050145), a putative sulfatase was identified from the Salmonella Typhimurium LT2 (S. typhimurium) genome (accession number NC_003197). In addition, the complete open reading frame for the protein was found containing 495 amino acid residues. The sequence alignment of human IDS and x-sulfatase revealed the protein had a 24% similarity to human IDS in addition to containing an overall 20-39% similarity to the sulfatase family of proteins (Figure 53). The sulfatase family of proteins contains highly conserved sequential, structural, and mechanistic characteristics. All sulfatases contain a highly homologous amino acid motif found within the *N*-terminal sequence comprised of 12 amino acids. The sequence alignment revealed that x-sulfatase carries this signature sulfatase sequence of amino acids. This signature sulfatase sequence is necessary for enzymatic activity. Therefore, this suggests that x-sulfatase has the sequential feature needed to be a sulfatase.

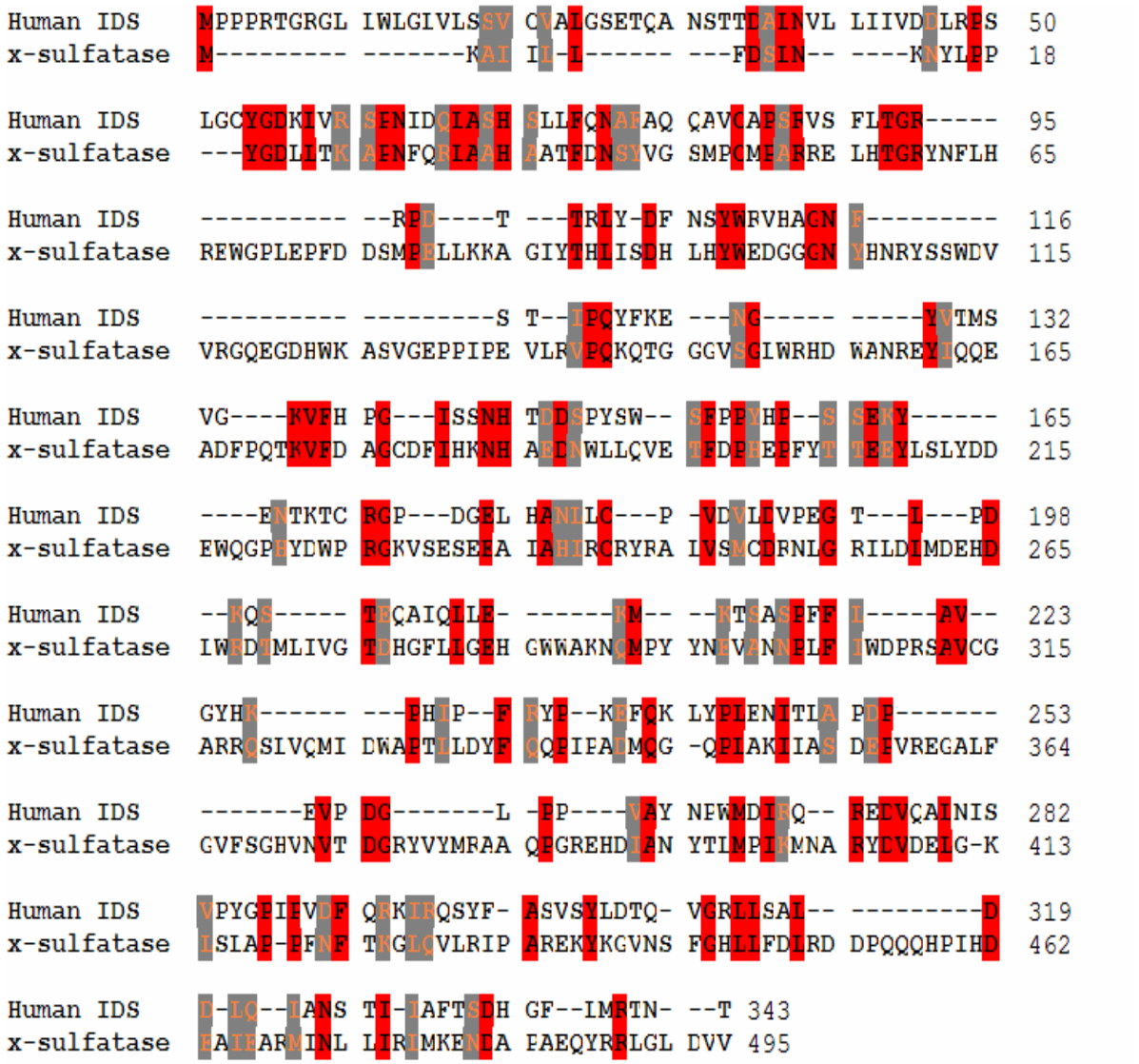

Figure 53. Amino acid sequence alignment of human iduronate 2-sulfatase and the putative x-sulfatase. The alignment was performed by using the program BioEdit. Introduced gaps are shown as hyphens, and aligned amino acids are boxed and shaded with red for identical residues and dark gray for similar residues.

Cloning and expression of x-sulfatase from S. typhimurium LT2

Blunt-ended PCR was used to clone x-sulfatase directly from the S.typhimurium LT2 genome. A resultant 1.4kb band was resolved on an agaraose gel to confirm the correct size

of the PCR product (figure 54). Once the correct size of the PCR product was obtained, the putative sulfatase gene was subcloned into the pPCR Script Amp SK (+) vector. This vector was chosen for its efficiency in cloning of PCR fragments with a high yield and a low rate of false positives. The pPCR-Script Amp SK(+) cloning vector works ideally with blunt-ended PCR products. The cloning vector also allows for an easy screening for recombinants determined by blue-white color selection of colonies (the white colonies being true positives).

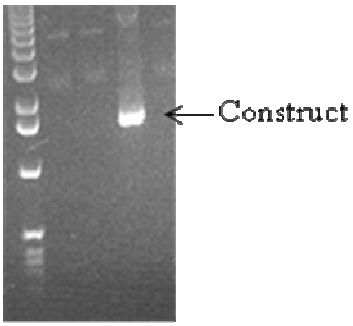

Figure 54. X-sulfatase PCR product cloned from the *S.typhimurium* genome. PCR was run on the S. typhimurium genome with the appropriate primers. The resultant PCR product was resolved on a 1% agaraose gel. The 1.4kb fragment is shown in lane 3. Lane 1 contains the molecular weight ladder.

Subsequently, the gene was cloned into the bacterial expression plasmid, pET28a(+), which would provide the recombinant protein with a 6×His tag at the *N*-terminus for purification purposes. Figure 55 shows the verification of the insert after being excised out of the plasmid after restriction enzyme digestion. The higher molecular weight band represents the vector while the lower molecular weight band represents the x-sulfatase gene insert. The procedure for the expression of x-sulfatase was carried out in *E. coli*. The cells were lysed by sonification, and the supernatant was applied to a nickel column. The protein was eluted from the column with a buffer containing imidazole. The eluted protein was

subjected to SDS-PAGE analysis. The SDS-PAGE results showed a highly expressed a 60 kDa protein (Figure. 56). The resultant protein was approximately 90% pure.

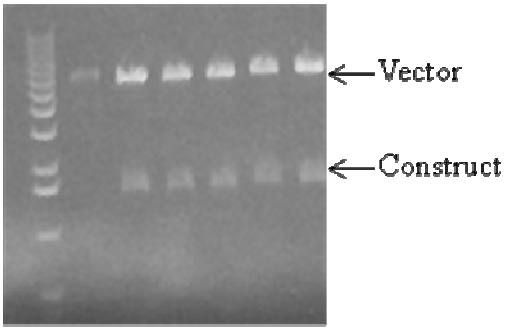

Figure 55. Verification of x-sulfatase gene insert. The 1.4kb x-sulfatase gene was cloned into the pET28a(+) vector. To verify whether the purified plasmid contained the gene of interest, the insert was digested with NdeI and BamHI. The restriction enzyme digestion yielded two bands present in the gel. The higher molecular weight band is the vector while the lower molecular weight band is the x-sulfatase gene.

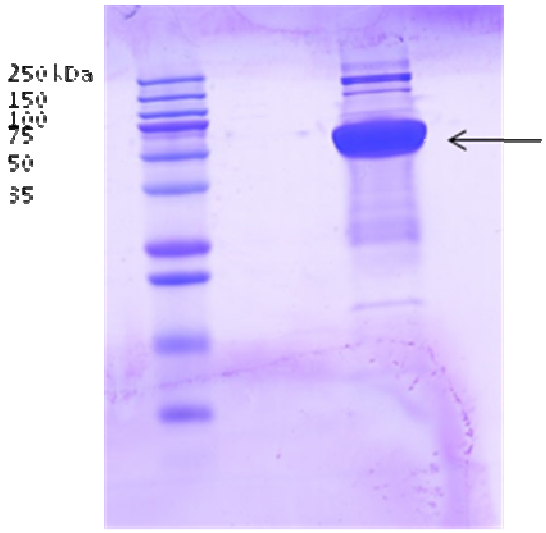

Figure 56. SDS-PAGE of x-sulfatase expression. Lane 1 contains the MW marker. Lane 2 contains expressed x-sulfatase protein. 5µl of x-sulfatase protein was loaded onto the gel.

IDS is a 2-*O*-sulfatase considered to have exolytic activity, meaning it removes 2-*O*-sulfo groups from disaccharide motifs at the reducing end of a polysaccharides and oligosaccharides as small as a disaccharide (Figure 57). It was important to determine whether this highly expressed protein indeed has enzymatic activity. Since x-sulfatase could potentially have IDS activity, we decided to use disaccharide standards to determine whether

sulfatase activity was present. In addition, we employed a commercially available 2-*O*-sulfatase as a control to monitor activity.

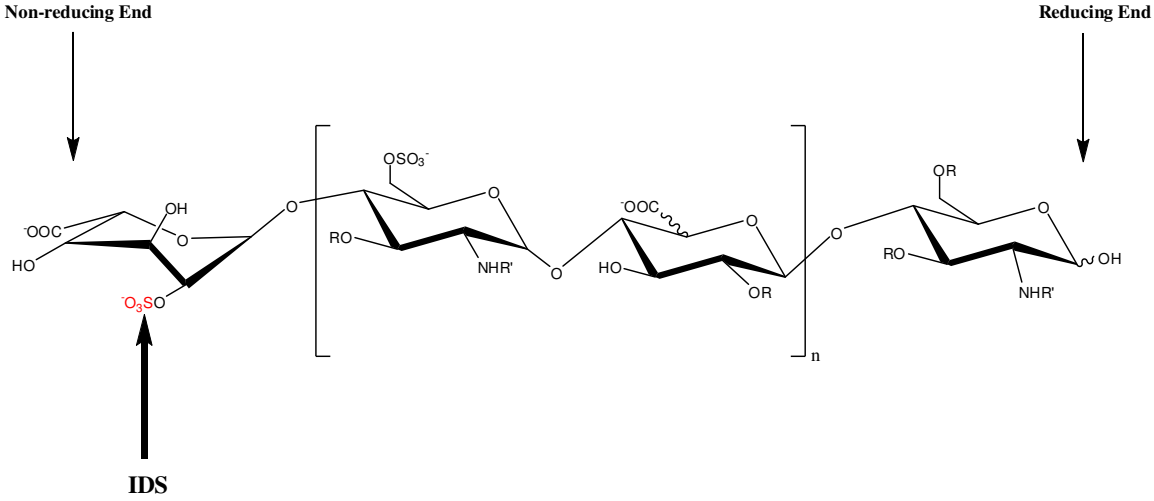

Figure 57. Scheme of exolytic activity of IDS. IDS removes 2-O-sulfo groups from the non-reducing end of polysaccharides and oligosaccharides as small as a disaccharide. R represents a proton or sulfate. R' represents a proton, acetyl, or sulfate.

The disaccharide standard, ΔUA2S-GlcNS6S, was resolved on a PAMN column. The elution profile showed this disaccharide standard eluted at 28 min (Figure 58, panel A). After treatment with the commercially available 2-*O*-sulfatase, the peak representing the ΔUA2S-GlcNS6S disaccharide standard was completely digested, and consequently a peak representing ΔUA-GlcNS6S disaccharide was observed at 23 min. (Figure 58, panel B).

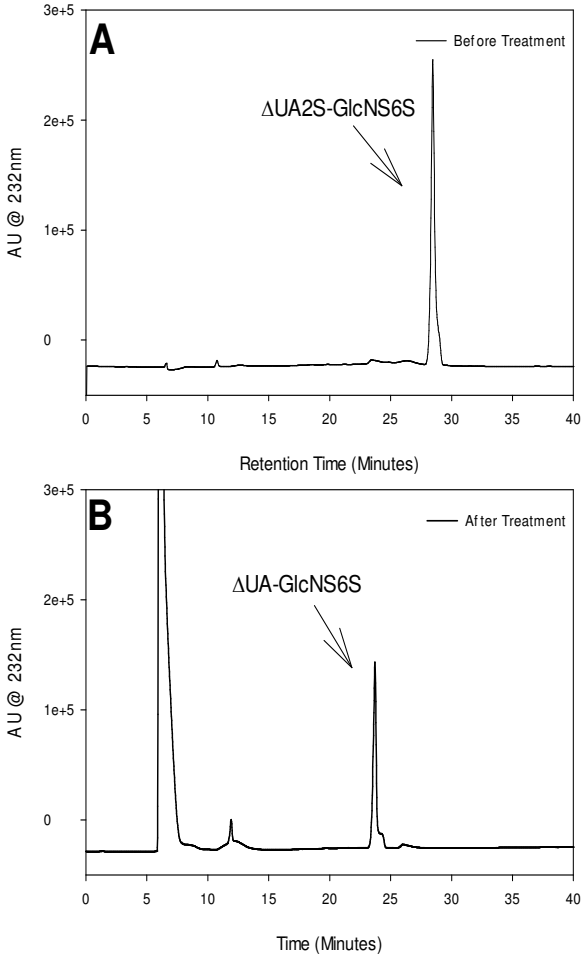

Figure 58. Disaccharide analysis of 2-*O*-sulfatase activity. Treated and untreated ΔUA2S-GlcNS6S disaccharides were resolved on a PAMN column. Panel A represents the disaccharide analysis before 2-*O*-sulfatase treatment. Panel B represents the disaccharide analysis after 2-*O*-sulfatase treatment. The elution profiles were monitored at an absorbance of 232nm.

This demonstrated that the commercially available 2-*O*-sulfatase was active under standard conditions, and was able to remove 2-*O*-sulfo groups from the disaccharide standard. Therefore, this information provided us with a control for the enzymatic activity of x-sulfatase against the ΔUA2S-GlcNS6S disaccharide standard. ΔUA2S-GlcNS6S was incubated with x-sulfatase. ΔUA2S-GlcNS6S eluted at the same position for the elution profile before x-sulfatase treatment (Figure 59, panel A). However, the elution profile after

treatment with x-sulfatase did not demonstrate that the enzyme was active against this substrate. ΔUA2S-GlcNS6S disaccharide peak did not diminish in stature and a subsequent ΔUA-GlcNS6S disaccharide peak did not develop in the elution profile (Figure 59, panel B).

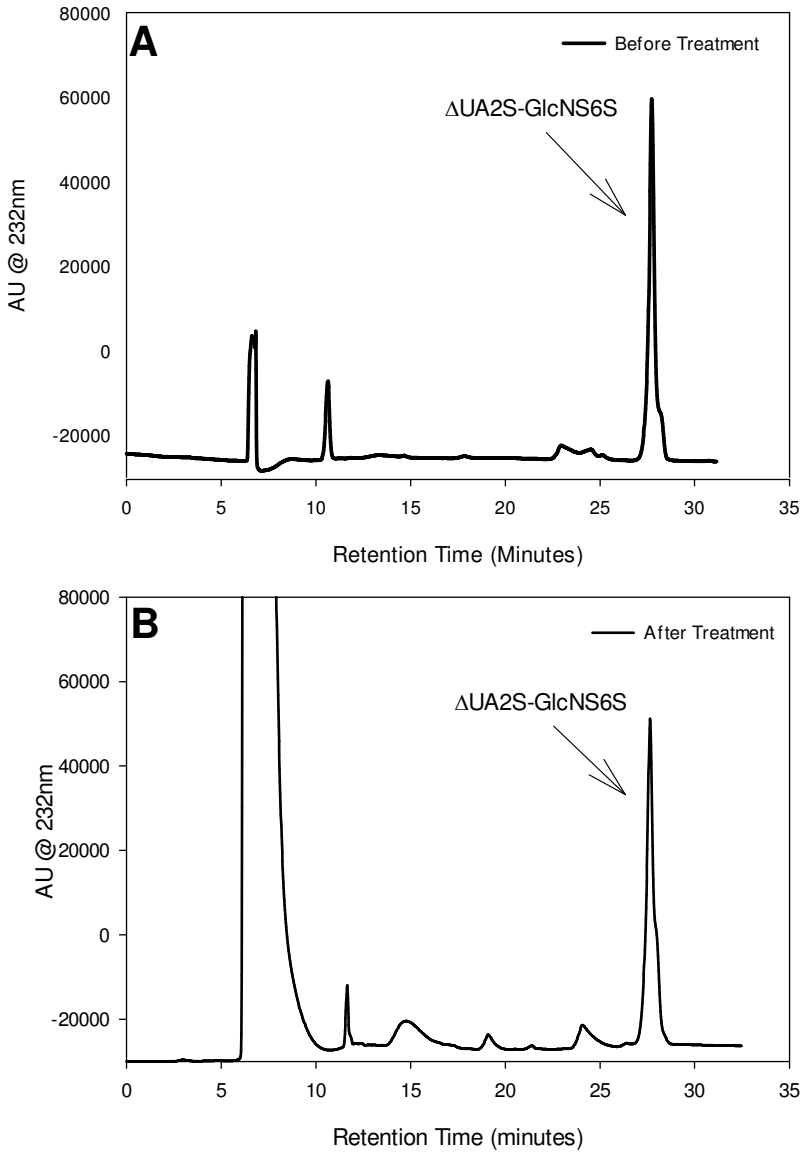

Figure 59. Disaccharide analysis for the determination of x-sulfatase activity. Treated and untreated ΔUA2S-GlcNS6S disaccharides were resolved on a PAMN column. Panel A represents the disaccharide analysis before x-sulfatase treatment. Panel B represents the disaccharide analysis after x-sulfatase treatment. The elution profiles were monitored at an absorbance of 232nm.

Various disaccharide standards and polysaccharides for HS and CS were used as substrates along with modifying the reaction conditions (i.e. pH, salt concentration, divalent metals), but no combination of substrate and conditions yielded any observable sulfatase activity. Interestingly, under acidic conditions, this protein precipitated out of solution. This could have been due to the *N*-terminal His tag on the protein, to components in the buffer at the acidic pH not generating a favorable environment for the protein, or it is an indication that x-sulfatase may not be an lysosomal sulfatase since the optimal activity of lysosomal sulfatases is in an acidic pH range.

Since activity could not be detected with known disaccharides, an alternative method needed to be utilized in order to determine whether x-sulfatase had activity. The sulfatase family of proteins is known to have a broad substrate specificity accommodating one or more natural substrates along with one or more generic substrates (125). Therefore, we hypothesized that active x-sulfatase would have activity against one or more of the generic substrates reported. We decided to use 4-MUS as a generic substrate to test for sulfatase activity for x-sulfatase, because 4-MUS is a generic substrate for known sulfatases. In addition, potassium 4-nitrophenyl sulfate (pNPS) and 4-nitrocatechol sulfate (pNCS) were also used as generic substrates to test for sulfatase activity since they are more specific for arylsulfatase activity. Fluorescence and chromogenic studies using generic substrates were used to test for the sulfatase activity. X-sulfatase did not demonstrate activity against any of the generic substrates.

Fluorescence Assay

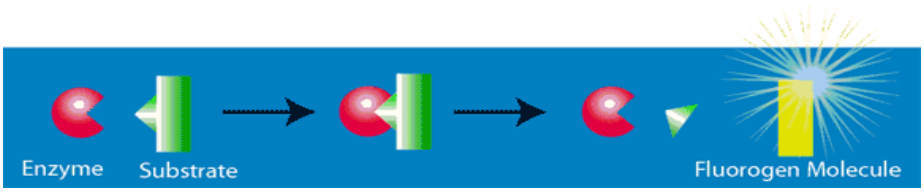

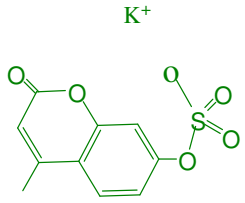

4-Methylumbelliferyl sulfate potassium salt (4-MUS)

Chromogenic Assay

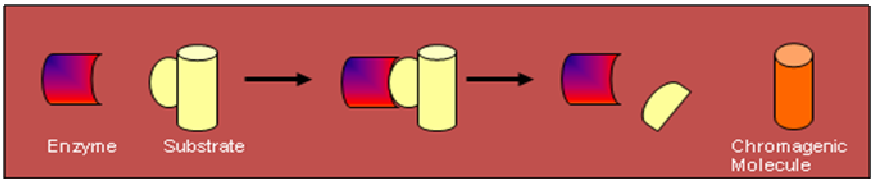

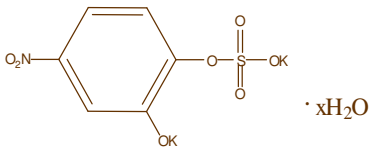

4-Nitrocatechol sulfate dipotassium salt (pNCS)

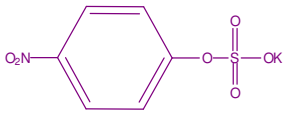

Potassium 4-nitrophenyl sulfate (pNPS)

Figure 60. Scheme for testing activity with generic substrates. 4-MUS, pNPS, and pNCS were used to test for sulfatase activity. Fluorescence studies would be used for 4-MUS, since the release of sulfate from this molecule would fluoresce at 435nm. pNPS and pNCS would be used for chromogenic studies since the reaction would change color once sulfate is released allowing the absorbance to be taken.

Conclusions

X-sulfatase was identified as a sulfatase and potentially an iduronate-2-sulfatase. Therefore, x-sulfatase was cloned and expressed in bacteria. As a result, a 65 kDa protein was observed. Exolytic activity for x-sulfatase was tested by using various HS and CS disaccharides. However, x-sulfatase activity was not observed with any of these disaccharides. In addition, oligosaccharides and polysaccharides were tested, but there was not activity present. In an effort to determine whether x-sulfatase had activity, generic substrates known to show activity in other sulfatases were used to test whether this putative sulfatase had activity. Again, no activity was observed for any of these generic substrates. Expression of active sulfatases has been reported in previous literature and in chapter IV (220). Therefore, bacterial expression contains the machinery to produce an active sulfatase. However, it is our consensus that x-sulfatase may not be an active sulfatase.

CHAPTER VI

CONCLUSIONS

The discovery of a novel class of enzymes called Sulfs, which can modulate the structure and function of HS in the ECM after intracellular biosynthesis, has proved to be a very important in many biological contexts. As a result, there has been intense investigation into evaluating their role in biological activities ranging from embryonic development to cancer within almost a decade. Therefore, it is vital to understand the substrate specificity of this enzyme to harness its potential as a tool for understanding structure-function relationships of physiological processes in addition to designing new HP/HS based drug therapies.

Consequently, we investigated the substrate specificity of HSulf-2 by synthesizing polysaccharides to evaluate their potential as substrates. However, first we had to demonstrate HSulf-2 had activity against HS. After the cloning and expression of HSulf-2 in CHO cells, it was determined through disaccharide analysis that HSulf-2 was active. Next, specific polysaccharides were generated by placing a [^{35}S] label on the 2-*O*-, 3-*O*-, 6-*O*-, or *N*-sulfation positions of uronic acid and glucosamine residues to investigate whether HSulf-2 could remove sulfo groups at different positions of variable sulfated structures.

First, we wanted to determine whether HSulf-2 had a preference for polysaccharides containing either IdoA2S or GlcA2S residues. Compound 1, a synthetic polysaccharide containing IdoA2S-GlcNS6S disaccharide motifs was shown to be a substrate for HSulf-2.

Compound 2 containing GlcA2S-GlcNS6S disaccharides motifs was also shown to be a substrate for HSulf-2. Therefore, HSulf-2 activity did not discriminate against which 2-*O*-sulfated uronic acid was present within the HS polysaccharide. Next, we wanted to determine whether 2-*O*-sulfation was important for HSulf-2 activity. Compounds containing IdoA and GlcA residues devoid of 2-*O*-sulfation were generated. This study showed that 2-*O*-sulfation was important for activity but was not essential, since compound 4 containing GlcA residues devoid of 2-*O*-sulfation was shown to be substrate. However, this could not be demonstrated for compound 3 containing IdoA residues devoid of 2-*O*-sulfation, because the data was inconclusive due to an impurity in the starting material. Furthermore, we wanted to determine whether *N*-sulfation was critical for activity. Results showed that HSulf-2 was inactive against compound 5, which contained only GlcNAc residues. After evaluating all of the synthetic polysaccharides, it was determined that HSulf-2 was selective toward 6-*O*-sulfo groups on glucosamine residues. Overall, this portion of the project demonstrated that HSulf-2 substrate specificity extends to other disaccharide motifs not found in only highly sulfated domains of HP/HS structures, which may be helpful in evaluating biological functions concerning moderately sulfated HS domains.

This study further extended to utilizing HSulf-2 as an editing enzyme to evaluate whether this enzyme could tailor the fine structure of anticoagulant structures, and whether the tailoring of the fine structure had any effect of their anticoagulant properties. AT binding assays and disaccharide analysis demonstrated that HSulf-2 could tailor and remove 6-*O*-sulfo groups from anticoagulant structures. In addition, HSulf-2 activity against these anticoagulant structures did not have a detrimental effect on AT binding. This showed that

HSulf-2 was removing 6-*O*-sulfo groups from the anticoagulant structures outside of the critical pentasaccharide sequence necessary for AT binding and anticoagulant activity. HSulf-2 treated anticoagulant structures maintained anticoagulant properties. Therefore, we wanted to investigate HSulf-2 treatment on the LMWH anticoagulant heparin, lovenox. Our results demonstrated that HSulf-2 could edit this FDA approved anticoagulant drug, and did not have adverse effects on anticoagulant activity against Factor Xa. The tailoring of this drug showed it reduced the ability of PF4 to neutralize anti-Factor Xa activities. In addition, filter binding assay results demonstrated that HSulf-2 treatment can reduce PF4 binding and forming a complex with HS polysaccharides. Moreover, a cell based assay demonstrated that HSulf-2 treated lovenox had anti-proliferative activity, which further enhanced this tailored anticoagulant drug's potential for prolonged administration to patients without promoting other biological activities.

Furthermore, in order to provide a large quantity of tailored anticoagulant drugs for animal testing, HSulf-2, MSulf-1, and MSulf-2 were cloned and expressed in large quantities in *E. coli*. Bacterial expression of MBP- mammalian Sulf fusion proteins demonstrated they contained sulfatase activity by removing 6-*O*-sulfo groups from compound 1. To our knowledge, bacterial expression of Sulfs has not been previously reported, and the ability to express active Sulf in bacteria contradicts previously reported data suggesting glycosylation was critical for Sulf activity.

Nonetheless, further exploration into the activities and role of Sulfs is needed in order to fully take advantage of the potential of this enzyme. Herein we have reported the biochemical characterization of a 6-*O*-endosulfatase by evaluating the enzyme's substrate specificity and demonstrating its activities on substrates that are not solely contained in

highly sulfated domains. In addition, this project further extended Sulf activity in a novel manner by utilizing its HS tailoring properties, which proved to have potential in tailoring anticoagulant drugs containing reduced side effects.

Appendix 1:

Curriculum Vitae

Tanya Catherine Burch
Division of Medicinal Chemistry and Natural Products
University of North Carolina at Chapel Hill
Chapel Hill, NC 27599
Work: (919) 962-0065
Fax: (919) 843-5432
Tanya_burch@ymail.com

Home Address: 1432 Willow Pointe Court, Virginia Beach, VA 23464

Hometown: Cherry Hill, New Jersey

Education:
University of North Carolina at Chapel Hill 2002-present
Ph.D. Candidate, Division of Medicinal Chemistry and Natural Products

Norfolk State University, 1998-2002
B.S. in Chemistry with Honors
Norfolk State University CMR Graduate, 2002

Current Research Interests:
Molecular and Chemical Biology
Carbohydrate and Protein Biochemistry
Drug Development

Publications:
Tiwari, V., O'donnell, C., Copeland, R.J., Scarlett, T., Liu, J., and Shukla D. Soluble 3-O-sulfated heparan sulfate can trigger simplex virus type 1 entry into resistant Chinese hamster ovary (CHO-K1) cells. (2007) *J. Gen. Virol.* 88: 1075-1079.

Evans, M.A., Smith, D.C, Holub, J.M., Argenti, A., Hoff, M., Dalglish, G.A, Berkowitz, J.D., Burnham, B.S., Krumpe, K., Gupton, J.T, Scarlett, T.C., Durham, Jr., R.W., and Hal, I.H. Synthesis and Cytotoxicity of Substituted Ethyl 2-phenacyl-3-phenylpyrrole-4-carboxylates. (2003) *Arc der Pharm. Med. Chem.* 336:181-90.

Scarlett, T.C., Durham, Jr., R.W., and Hall, I.H. Synthesis and Cytotoxicity of Cyanoborane Adducts of N^6-Benzoyladenine and 6-Triphenylphosphonylpurine. (2002) *Metal-Based Drugs* 9: 19-32.

Awards:
Scholar, University of North Carolina at Chapel Hill, 2002-present
American Chemical Society Hampton Roads Local Section Award for Outstanding Achievement in Chemistry, Norfolk, VA, 2002
Scholar, Center for Materials Research, Norfolk State University, 1998-2002

Undergraduate Research Experience:
Participant, Research Education Support (RES) Pre-Entry Program, University of North Carolina, Chapel Hill, NC, Summer 2002
Advisor: Dr. Harold Kohn (Medicinal Chemistry and Natural Products)
Project: Evaluation of the Rho-Dependent ATP Hydrolysis
The *Escherichia coli* rho transcription termination factor terminates select transcripts and rho activity requires Mg^{2+}. We investigated whether divalent metal ions other than Mg^{2+} catalyze Rho-dependent ATP hydrolysis to ADP and P_i *in vitro*.

Participant, Summer Pre-Graduate Research Experience (SPGRE), University of North Carolina, Chapel Hill, NC, Summer 2001
Advisor: Dr. Iris Hall (Medicinal Chemistry and Natural Products)
Project: *Synthesis and Cytotoxicity of Cyanoborane Adducts of N^6-Benzoyladenine and 6-Chloropurine* N^6-benzoyladenine-cyanoborane and 6-triphenylphosphonylpurine-cyanoborane were selected for investigation of cytotoxicity in murine and human tumor cell lines, effects on human HL-60 leukemic metabolism and DNA strand scission to determine the feasibility of these compounds as clinical antineoplastic agents.

Participant, Summer Research Internship, Hampton University, Hampton, VA, Summer 2000
Advisor: Dr. Uwe Hommerich (Physics)
Project: Study of Transition Metal Ion Doped Solids for Applications as Solid-State Laser Materials and Phosphors
The optical properties of rare earth and/or transition metal ion doped solids for applications as solid-state laser materials and phosphors were tested. This projected focused on the study of rare earth ions (Er^{3+}, Eu^{3+}, etc.) in wide-gap semiconductor hosts (e.g. AlN, GaN) with the goal of combining the favorable luminescence properties of rare earth ions with the electronic properties of semiconductors.

Student Research Assistant, Norfolk State University, Norfolk, VA, 2001-2002
Advisor: Dr. Harold Alan Rowe (Chemistry)
Project: Kinetic Parameters and Effectors of Polyphenoloxidase from Homobasidiomycetes
Polyphenoloxidase was isolated from different varieties of mushroom and kinetic studies conducted on the crude extract as well as the partially purified material. The enzyme purification scheme was optimized. Using catechol as a substrate, various kinetic parameters were determined and the response of the enzyme to different effectors was examined.

Work Experience:
Graduate Research Assistant, Division of Medicinal Chemistry and Natural Products, School of Pharmacy, University of North Carolina, Chapel Hill, NC, 2002-present
Thesis advisor: Dr. Jian Liu, Associate Professor
Dissertation Title: Biochemical Characterization of Human Heparan Sulfate 6-*O*-Endosulfatase
Human and mouse heparan sulfate 6-*O*-endosulfatases (Sulfs) were cloned and expressed in mammalian and/or bacterial systems. Potential substrates were developed to evaluate the substrate specificity. In addition, human Sulf was utilized to tailor low molecular weight heparin to improve its pharmacological efficacy and reduce side effects.

Database Manager, Division of Gastroenterology and Hepatology, School of Medicine, University of North Carolina, Chapel Hill, NC, 2005-2007
Supervisor: Dr. Donna Evon, Ph.D.
Managed the database for a clinical trial which provided psychological evaluation of patients being considered for antiviral therapy and evaluated the neuropsychiatric side effects of interferon-based therapy.

Rotation Student Training, Division of Medicinal Chemistry and Natural Products, University of North Carolina, Chapel Hill, NC, 2004-present
Advisor: Dr. Jian Liu
Assist in the training of rotating graduate students working in the laboratory.

Program Assistant, Summer Enrichment Program (SEP), University of North Carolina, Chapel Hill, NC, Summer 2005 and 2006
Supervisor: Denise Belle
This is an eight week, honors-level academic enrichment program for disadvantaged undergraduate students who seek admissions into graduate or health professional programs. Served as a group leader and tutored organic chemistry. I gave weekly review sessions, created homework assignments, proctored exams, and graded all material. Duties also included assisting in weekly seminars and a variety of administrative tasks.

Committees/Organizations:
Member, UNC-School of Pharmacy Graduate Student Organization (GSO), 2002-present
Member, American Chemistry Society Scholar, Norfolk State University, 2002-2004
Member, Alpha Kappa Mu Honor Society, Norfolk State University, 2002

Skills/Techniques:
Computer
-All Microsoft Office software suites
-SPSS
-Sigma Plot
-Chem Draw

Molecular Biology
-PCR

-Agarose gel electrophoresis
-Various aspects of molecular cloning--Primer design, plasmid amplification/purification, and DNA sequencing data analysis

Biochemical/Bio-Analytical

-Bioassay development-*in vitro*
-Affinity co-electrophoresis
-Western Blotting
-Recombinant protein expression/purification (bacterial and mammalian systems)
-SDS-PAGE
-HPLC-ion exchange, size exclusion, reverse phase ion pairing
-FPLC-ion exchange, size exclusion, affinity
-Chemical and enzymatic degradation of carbohydrates for structural analysis
-UV Spectrophotometry-quantitative analysis of carbohydrates, nucleic acids, and proteins
-Mammalian cell culture-DNA transfection, radioactive metabolic labeling of proteoglycans

REFERENCES

(1) Liu, J., Thorp, S. (2002) Cell surface heparan sulfate and its roles in assisting viral infections. *Med. Res. Rev. 22*, 1-25.

(2) Rosenberg, R. D., Shworak, N. W., Liu, J., Schwartz, J. J., and Zhang, L. (1997) Heparan sulfate proteoglycans of the cardiovascular system. Specific structures emerge but how is synthesis regulated? *J. Clin. Invest. 99*, 2062-2070.

(3) Liu, J., Shriver, Z., Pope, R. M., Thorp, S. C., Duncan, M. B., Copeland, R. J., Raska, C. S., Yoshida, K., Eisenberg, R. J., Cohen, G., Linhardt, R. J., and Sasisekharan, R. (2002) Characterization of a Heparan Sulfate Octasaccharide That Binds to Herpes Simplex Virus Type 1 Glycoprotein D. *J. Biol. Chem. 277*, 33456-33467.

(4) Almond, A. (2007) Hyaluronan. *Cell. Mol. Life Sci. 64*, 1591-1596.

(5) Tengblad, A., Laurent, U. B., Lilja, K., Cahill, R. N., Engstrom-Laurent, A., Fraser, J. R., Hansson, H. E., and Laurent, T. C. (1986) Concentration and relative molecular mass of hyaluronate in lymph and blood. *Biochem J.;236, 521-5.*

(6) Toole, B. P., Wight, T. N., and Tammi, M. I. (2002) Hyaluronan-Cell Interactions in Cancer and Vascular Disease. *J. Biol. Chem. 277*, 4593-4596.

(7) Allison, D. D., and Grande-Allen, K. J. (2006) Review. Hyaluronan: A Powerful Tissue Engineering Tool. *Tissue Engin. 12*, 2131-2140.

(8) W. Y. John Chen, G. A. (1999) Functions of hyaluronan in wound repair. *Wound Repair and Regen. 7*, 79-89.

(9) Laurent, T. C., and Fraser, J. R. (1992) Hyaluronan. *FASEB J. 6*, 2397-2404.

(10) Funderburgh, J. L. (2000) MINI REVIEW Keratan sulfate: structure, biosynthesis, and function. *Glycobiology 10*, 951-958.

(11) Hemming, F. J., and Saxod, R. (1998) Regulated expression of keratan sulphate and peanut agglutinin binding sites during organogenesis in the developing chick. *Histochem. Cell Biol. 110*, 189-200.

(12) Badcock, G., Pigott, C., Goepel, J., and Andrews, P. W. (1999) The Human Embryonal Carcinoma Marker Antigen TRA-1-60 Is a Sialylated Keratan Sulfate Proteoglycan. *Cancer Res. 59*, 4715-4719.

(13) Pratta, M. A., Tortorella, M. D., and Arner, E. C. (2000) Age-related Changes in Aggrecan Glycosylation Affect Cleavage by Aggrecanase. *J. Biol. Chem. 275*, 39096-39102.

(14) Sugahara, K., and Mikami, T. (2007) Chondroitin/dermatan sulfate in the central nervous system. *Curr. Opin. Struct. Biol. 17*, 536-545.

(15) Kjellen, L., and Lindahl, U. (1991) Proteoglycans: Structures and Interactions. *Ann. Rev. Biochem. 60*, 443-475.

(16) Malavaki, C., Mizumoto, S., Karamanos, N., and Sugahara, K. (2008) Recent Advances in the Structural Study of Functional Chondroitin Sulfate and Dermatan Sulfate in Health and Disease. *Connective Tissue Res. 49*, 133 - 139.

(17) Sugahara, K., Mikami, T., Uyama, T., Mizuguchi, S., Nomura, K., and Kitagawa, H. (2003) Recent advances in the structural biology of chondroitin sulfate and dermatan sulfate. *Curr. Opin. Struct. Biol. 13*, 612-620.

(18) Conrad, H. E. (1998) *Heparin-Binding Proteins* Academic Press, San Diego.

(19) Hileman, R. E., Fromm, J. R., Weiler, J. M., and Linhardt, R. J. (1998) Glycosaminoglycan-protein interactions: definition of consensus sites in glycosaminoglycan binding proteins. *Bioessays. 20, 156-67.*

(20) Toida, T., Yoshida, H., Toyoda, H., Koshiishi, I., Imanari, T., Hileman, R. E., Fromm, J. R., and Linhardt, R. J. (1997) Structural differences and the presence of unsubstituted amino groups in heparan sulphates from different tissues and species. *Biochem J. 322*, 499-506.

(21) Lindahl, U., Kusche-Gullberg, M., and Kjellen, L. (1998) Regulated diversity of heparan sulfate. *J. Biol. Chem. 273*, 24979-82.

(22) Mulloy, B., Forster,M.J., Jones,C. and Davies,D.B. (1993) N.m.r. and molecular-modeling studies of the solution conformation of heparin. *Biochem. J. 293*, 849-858.

(23) Mulloy, B., and Forster, M. J. (2000) Conformation and dynamics of heparin and heparan sulfate. *Glycobiology 10*, 1147-1156.

(24) Faham, S., Hileman, R. E., Fromm, J. R., Linhardt, R. J., and Rees, D. C. (1996) Heparin Structure and Interactions with Basic Fibroblast Growth Factor. *Science 271*, 1116-1120.

(25) Hricovíni M, G. M., Bisio A, Torri G, Petitou M, Casu B. (2001) Conformation of heparin pentasaccharide bound to antithrombin III. *Biochem J 359*, 265-272.

(26) van Boeckel, C. A., van Aelst,S.F., Wagenaars,G. N., Mellema,J. R., Paulsen,H., Peters,T., Pollex,A. and Sinnwell,V. (1987) Conformational analysis of synthetic heparin-like oligosaccharides containing {alpha}-L-idopyranosyluronic acid. *Recl. Trav. Pays-Bas 106*, 19-29.

(27) Murphy, K. J., McLay, N., and Pye, D. A. (2008) Structural Studies of Heparan Sulfate Hexasaccharides: New Insights into Iduronate Conformational Behavior. *J. Am. Chem. Soc. 130*, 12435-12444.

(28) Rabenstein, D. L. (2002) Heparin and heparan sulfate: structure and function. *Nat. Prod. Reports 19*, 312 - 331.

(29) Liu, J., and Pedersen, L. (2007) Anticoagulant heparan sulfate: structural specificity and biosynthesis. *App. Micro. Biotech. 74*, 263-272.

(30) Hacker, U., Nybakken, K., and Perrimon, N. (2005) Heparan sulphate proteoglycans: the sweet side of development. *Nat. Rev. Mol. Cell Biol. 6*, 530-541.

(31) Bernfield, M., Kokenyesi, R., Kato, M., Hinkes, M. T., Spring, J., Gallo, R. L., and Lose, E. J. (1992) Biology of the Syndecans: A Family of Transmembrane Heparan Sulfate Proteoglycans. *Ann. Rev. Cell Biol. 8*, 365-393.

(32) Lopes, C. C., Dietrich, C. P., and Nader, H. B. (2006) Specific structural features of syndecans and heparan sulfate chains are needed for cell signaling. *Braz. J. Med. Biol. Res. 39*, 157-167.

(33) Bernfield M, G. M., Park PW. (1999) Functions of cell surface heparan sulfate proteoglycans. *Ann. Rev. Biochem.*, 729-777.

(34) De Cat, B., and David, G. (2001) Developmental roles of the glypicans. *Seminar Cell Dev. Biol. 12*, 117-125.

(35) Filmus, J. (2001) Glypicans in growth control and cancer. *Glycobiology 11*, 19R-23.

(36) Bandtlow, C. E., and Zimmermann, D. R. (2000) Proteoglycans in the Developing Brain: New Conceptual Insights for Old Proteins. *Physiological Rev. 80*, 1267.

(37) Jeong-Soo, L., and Chi-Bin, C. (2004) When sugars guide axons: insights from heparan sulphate proteoglycan mutants. *Nat. Rev. Gen. 5*, 923-935.

(38) Saunders, S., Paine-Saunders, S., and Lander, A. D. (1997) Expression of the Cell Surface Proteoglycan Glypican-5 Is Developmentally Regulated in Kidney, Limb, and Brain. *Dev. Biol. 190*, 78-93.

(39) Iozzo, R. V. (1998) MATRIX PROTEOGLYCANS: From Molecular Design to Cellular Function. *Ann. Rev. Biochem. 67*, 609.

(40) Hagen, S. G., Michael, A. F., and Butkowski, R. J. (1993) Immunochemical and biochemical evidence for distinct basement membrane heparan sulfate proteoglycans. *J Biol Chem. 268, 7261-9.*

(41) Tsen, G., Halfter, W., Kröger, S., and Cole, G. J. (1995) Agrin Is a Heparan Sulfate Proteoglycan. *J. Biol. Chem. 270*, 3392-3399.

(42) Gingras, J., Rassadi, S., Cooper, E., and Ferns, M. (2002) Agrin plays an organizing role in the formation of sympathetic synapses. *J. Cell Biol. 158*, 1109-1118.

(43) Zhang, J., Wang, Y., Chu, Y., Su, L., Gong, Y., Zhang, R., and Xiong, S. (2006) Agrin is involved in lymphocytes activation that is mediated by {alpha}-dystroglycan. *FASEB J. 20*, 50-58.

(44) Denzer, A. J., Gesemann, M., Schumacher, B., and Ruegg, M. A. (1995) An amino-terminal extension is required for the secretion of chick agrin and its binding to extracellular matrix. *J. Cell Biol. 131*, 1547-1560.

(45) Dolan, M., Horchar, T., Rigatti, B., and Hassell, J. R. (1997) Identification of Sites in Domain I of Perlecan That Regulate Heparan Sulfate Synthesis. *J. Biol. Chem. 272*, 4316-4322.

(46) Friedrich, M. V. K., Göhring, W., Mörgelin, M., Brancaccio, A., David, G., and Timpl, R. (1999) Structural basis of glycosaminoglycan modification and of heterotypic interactions of perlecan domain V. *J. Mol. Biol. 294*, 259-270.

(47) Govindraj, P., West, L., Koob, T. J., Neame, P., Doege, K., and Hassell, J. R. (2002) Isolation and Identification of the Major Heparan Sulfate Proteoglycans in the Developing Bovine Rib Growth Plate. *J. Biol. Chem. 277*, 19461-19469.

(48) Iozzo, R. V. (2005) Basement membrane proteoglycans: from cellar to ceiling. *Nat. Rev. Mol. Cell. Biol. 6*, 646-656.

(49) SundarRaj, N., Fite, D., Ledbetter, S., Chakravarti, S., and Hassell, J. R. (1995) Perlecan is a component of cartilage matrix and promotes chondrocyte attachment. *J. Cell. Sci. 108*, 2663-2672.

(50) Melissa Handler, P. D. Y. R. V. I. (1997) Developmental expression of perlecan during murine embryogenesis. *Dev. Dyn. 210*, 130-145.

(51) French, M. M., Smith, S. E., Akanbi, K., Sanford, T., Hecht, J., Farach-Carson, M. C., and Carson, D. D. (1999) Expression of the Heparan Sulfate Proteoglycan, Perlecan, during Mouse Embryogenesis and Perlecan Chondrogenic Activity In Vitro. *J. Cell Biol. 145*, 1103-1115.

(52) Lauder, R. M., Huckerby, T N, Brown, G M, Bayliss, M T, Nieduszynski, I A. (2001) Age-related changes in the sulphation of the chondroitin sulphate linkage region from human articular cartilage aggrecan. *Biochem. J. 358*, 523-528.

(53) Yamada, S., Oyama, M., Yuki, Y., Kato, K., and Sugahara, K. (1995) The Uniform Galactose 4-Sulfate Structure in the Carbohydrate-Protein Linkage Region of Human Urinary Trypsin Inhibitor. *Euro. J. Biochem. 233*, 687-693.

(54) Yamada, S., Oyama, M., Kinugasa, H., Nakagawa, T., Kawasaki, T., Nagasawa, S., Khoo, K.-H., Morris, H. R., Dell, A., and Sugahara, K. (1995) The sulphated carbohydrate-protein linkage region isolated from chondroitin 4-sulphate chains of inter-{alpha}-trypsin inhibitor in human plasma. *Glycobiology 5*, 335-341.

(55) Sugahara, K., and Kitagawa, H. (2000) Recent advances in the study of the biosynthesis and functions of sulfated glycosaminoglycans. *Curr. Opin. Struct. Biol. 10*, 518-527.

(56) Sugahara, K., and Kitagawa, H. (2002) Heparin and Heparan Sulfate Biosynthesis. *IUBMB Life 54*, 163-175.

(57) Gulberti, S., Lattard, V., Fondeur, M., Jacquinet, J.-C., Mulliert, G., Netter, P., Magdalou, J., Ouzzine, M., and Fournel-Gigleux, S. (2005) Phosphorylation and Sulfation of Oligosaccharide Substrates Critically Influence the Activity of Human {beta}1,4-Galactosyltransferase 7 (GalT-I) and {beta}1,3-Glucuronosyltransferase I (GlcAT-I) Involved in the Biosynthesis of the Glycosaminoglycan-Protein Linkage Region of Proteoglycans. *J. Biol. Chem. 280*, 1417-1425.

(58) Bourdon, M. A., Krusius, T., Campbell, S., Schwartz, N. B., and Ruoslahti, E. (1987) Identification and synthesis of a recognition signal for the attachment of glycosaminoglycans to proteins. *Proc. Natl. Acad. Sci. 84*, 3194-3198.

(59) Bourdon, M. A., Oldberg, A., Pierschbacher, M., and Ruoslahti, E. (1985) Molecular cloning and sequence analysis of a chondroitin sulfate proteoglycan cDNA. *Proc. Natl. Acad. Sci. 82*, 1321-1325.

(60) Seo, N.-S., Hocking, A. M., Hook, M., and McQuillan, D. J. (2005) Decorin Core Protein Secretion Is Regulated by N-Linked Oligosaccharide and Glycosaminoglycan Additions. *J. Biol. Chem. 280*, 42774-42784.

(61) Esko, J. D., Stewart, T. E., and Taylor, W. H. (1985) Animal cell mutants defective in glycosaminoglycan biosynthesis. *Proc. Nat. Acad. Sci. 82*, 3197-3201.

(62) Ponighaus, C., Ambrosius, M., Casanova, J. C., Prante, C., Kuhn, J., Esko, J. D., Kleesiek, K., and Gotting, C. (2007) Human Xylosyltransferase II Is Involved in the Biosynthesis of the Uniform Tetrasaccharide Linkage Region in Chondroitin Sulfate and Heparan Sulfate Proteoglycans. *J. Biol. Chem. 282*, 5201-5206.

(63) Götting, C., Kuhn, J., Zahn, R., Brinkmann, T., and Kleesiek, K. (2000) Molecular Cloning and Expression of Human UDP--Xylose:Proteoglycan Core Protein [beta]--Xylosyltransferase and its First Isoform XT-II. *J. Mol. Biol. 304*, 517-528.

(64) Kuhn, J., Gotting, C., Schnolzer, M., Kempf, T., Brinkmann, T., and Kleesiek, K. (2001) First Isolation of Human UDP-D-Xylose: Proteoglycan Core Protein beta -D-Xylosyltransferase Secreted from Cultured JAR Choriocarcinoma Cells. *J. Biol. Chem. 276*, 4940-4947.

(65) Voglmeir, J., Voglauer, R., and Wilson, I. B. H. (2007) XT-II, the Second Isoform of Human Peptide-O-xylosyltransferase, Displays Enzymatic Activity. *J. Biol. Chem. 282*, 5984-5990.

(66) Gotting, C., Sollberg, S., Kuhn, J., Weilke, C., Huerkamp, C., Brinkmann, T., Krieg, T., and Kleesiek, K. (1999) Serum Xylosyltransferase: a New Biochemical Marker of the Sclerotic Process in Systemic Sclerosis. *112*, 919-924.

(67) Götting, C., Hendig, D., Adam, A., Schön, S., Schulz, V., Szliska, C., Kuhn, J., and Kleesiek, K. (2005) Elevated xylosyltransferase I activities in pseudoxanthoma elasticum (PXE) patients as a marker of stimulated proteoglycan biosynthesis. *J. Mol. Med. 83*, 984-992.

(68) Bai, X., Zhou, D., Brown, J. R., Crawford, B. E., Hennet, T., and Esko, J. D. (2001) Biosynthesis of the Linkage Region of Glycosaminoglycans. Cloning and Activity of Galactosyltransferase II, The Sixth Member of the beta 1,3-Galactosyltransferase Family (beta 3GalT6). *J. Biol. Chem. 276*, 48189-48195.

(69) Almeida, R., Levery, S. B., Mandel, U., Kresse, H., Schwientek, T., Bennett, E. P., and Clausen, H. (1999) Cloning and Expression of a Proteoglycan UDP-Galactose:beta -Xylose beta 1,4-Galactosyltransferase I. A Seventh Member of The Human beta 4-Galactosyltransferase Gene Family. *J. Biol. Chem. 274*, 26165-26171.

(70) Okajima, T., Yoshida, K., Kondo, T., and Furukawa, K. (1999) Human Homolog of Caenorhabditis elegans sqv-3 Gene Is Galactosyltransferase I Involved in the Biosynthesis of the Glycosaminoglycan-Protein Linkage Region of Proteoglycans. *J. Biol. Chem. 274*, 22915-22918.

(71) Furukawa, K., and Okajima, T. (2002) Galactosyltransferase I is a gene responsible for progeroid variant of Ehlers-Danlos syndrome: molecular cloning and identification of mutations. *Biochimica et Biophysica Acta (BBA) - Gen. Subj. 1573*, 377-381.

(72) Gotte, M., Spillmann, D., Yip, G. W., Versteeg, E., Echtermeyer, F. G., van Kuppevelt, T. H., and Kiesel, L. (2008) Changes in heparan sulfate are associated with delayed wound repair, altered cell migration, adhesion and contractility in the galactosyltransferase I (ss4GalT-7) deficient form of Ehlers-Danlos syndrome. *Hum. Mol. Genet. 17*, 996-1009.

(73) Bai, X., Wei, G., Sinha, A., and Esko, J. D. (1999) Chinese Hamster Ovary Cell Mutants Defective in Glycosaminoglycan Assembly and Glucuronosyltransferase I. *J. Biol. Chem. 274*, 13017-13024.

(74) Pedersen, L. C., Tsuchida, K., Kitagawa, H., Sugahara, K., Darden, T. A., and Negishi, M. (2000) Heparan/Chondroitin Sulfate Biosynthesis. Structure and Mechanism of Human Glycuronyltransferase I. *J. Biol. Chem. 275*, 34580-34585.

(75) Gulberti, S., Lattard, V., Fondeur, M., Jacquinet, J.-C., Mulliert, G., Netter, P., Magdalou, J., Ouzzine, M., and Fournel-Gigleux, S. (2005) Modifications of the Glycosaminoglycan-Linkage Region of Proteoglycans: Phosphorylation and Sulfation Determine the Activity of the Human ß1,4-Galactosyltransferase 7 and ß1,3-Glucuronosyltransferase I. *Sci. World J. 5*, 510-514.

(76) Tone, Y., Pedersen, L. C., Yamamoto, T., Izumikawa, T., Kitagawa, H., Nishihara, J., Tamura, J.-i., Negishi, M., and Sugahara, K. (2008) 2-O-Phosphorylation of Xylose and 6-O-Sulfation of Galactose in the Protein Linkage Region of Glycosaminoglycans Influence the Glucuronyltransferase-I Activity Involved in the Linkage Region Synthesis. *J. Biol. Chem. 283*, 16801-16807.

(77) Lattard, V., Fondeur-Gelinotte, M., Gulberti, S., Jacquinet, J.-C., Boudrant, J., Netter, P., Magdalou, J., Ouzzine, M., and Fournel-Gigleux, S. (2006) Purification and characterization of a soluble form of the recombinant human galactose-[beta]1,3-glucuronosyltransferase I expressed in the yeast Pichia pastoris. *Protein Exp. Pur. 47*, 137-143.

(78) Venkatesan, N., Barr, Ã., L., Benani, A., Netter, P., Magdalou, J., Fournel-Gigleux, S., and Ouzzine, M. (2004) Stimulation of proteoglycan synthesis by glucuronosyltransferase-I gene delivery: A strategy to promote cartilage repair. *Proc. Natl. Acad. Sci. 101*, 18087-18092.

(79) Lindholt, K., Lindahl, U. (1992) Biosynthesis of heparin. The D-glucuronosyl- and N-acetyl-D-glucosaminyltransferase reactions and their relation to polymer modification. *Biochem. J. 287*, 21-29.

(80) Kim, B.-T., Kitagawa, H., Tamura, J.-i., Saito, T., Kusche-Gullberg, M., Lindahl, U., and Sugahara, K. (2001) Human tumor suppressor EXT gene family members EXTL1 and EXTL3 encode Î±1,4- N-acetylglucosaminyltransferases that likely are involved in heparan sulfate/ heparin biosynthesis. *Proc. Natl. Acad. Sci. 98*, 7176-7181.

(81) McCormick, C., Duncan, G., Goutsos, K. T., and Tufaro, F. (2000) The putative tumor suppressors EXT1 and EXT2 form a stable complex that accumulates in the Golgi apparatus and catalyzes the synthesis of heparan sulfate. *Proc. Natl. Acad. Sci. 97*, 668-673.

(82) Fritz, T. A., Gabb, M. M., Wei, G., and Esko, J. D. (1994) Two N-acetylglucosaminyltransferases catalyze the biosynthesis of heparan sulfate. *J. Biol. Chem. 269*, 28809-28814.

(83) Busse, M., Feta, A., Presto, J., Wilen, M., Gronning, M., Kjellen, L., and Kusche-Gullberg, M. (2007) Contribution of EXT1, EXT2, and EXTL3 to Heparan Sulfate Chain Elongation. *J. Biol. Chem. 282*, 32802-32810.

(84) Kitagawa, H., Shimakawa, H., and Sugahara, K. (1999) The Tumor Suppressor EXT-like Gene EXTL2 Encodes an alpha 1, 4-N-Acetylhexosaminyltransferase That Transfers N-Acetylgalactosamine and N-Acetylglucosamine to the Common Glycosaminoglycan-Protein Linkage Region. The Key Enzyme for the Chain Initiation of Heparan Sulfate. *J. Biol. Chem. 274*, 13933-13937.

(85) Busse, M., and Kusche-Gullberg, M. (2003) In Vitro Polymerization of Heparan Sulfate Backbone by the EXT Proteins. *J. Biol. Chem. 278*, 41333-41337.

(86) Lind, T., Tufaro, F., McCormick, C., Lindahl, U., and Lidholt, K. (1998) The Putative Tumor Suppressors EXT1 and EXT2 Are Glycosyltransferases Required for the Biosynthesis of Heparan Sulfate. *J. Biol. Chem. 273*, 26265-26268.

(87) Gorsi, B., and Stringer, S. E. (2007) Tinkering with heparan sulfate sulfation to steer development. *Trends Cell Biol. 17*, 173-177.

(88) Aikawa, J.-i., Grobe, K., Tsujimoto, M., and Esko, J. D. (2001) Multiple Isozymes of Heparan Sulfate/Heparin GlcNAc N-Deacetylase/GlcN N-Sulfotransferase. Structure And Activity of the Fourth Member, NDST4. *J. Biol. Chem. 276*, 5876-5882.

(89) Forsberg, E. a. K., L. (2001) Heparan sulfate: lessons from knockout mice. *J. Clin. Invest. 108*, 175-180.

(90) Humphries, D. E., Wong, G. W., Friend, D. S., Gurish, M. F., Qiu, W.-T., Huang, C., Sharpe, A. H., and Stevens, R. L. (1999) Heparin is essential for the storage of specific granule proteases in mast cells. *Nature 400*, 769-772.

(91) Carlsson, P., Presto, J., Spillmann, D., Lindahl, U., and Kjellen, L. (2008) Heparin/Heparan Sulfate Biosynthesis: Processive Formation of N-Sulfated Domains. *J. Biol. Chem. 283*, 20008-20014.

(92) Presto, J., Thuveson, M., Carlsson, P., Busse, M., WilÃ©n, M., Eriksson, I., Kusche-Gullberg, M., and KjellÃ©n, L. (2008) Heparan sulfate biosynthesis enzymes EXT1 and EXT2 affect NDST1 expression and heparan sulfate sulfation. *Proc. Natl. Acad. Sci. 105*, 4751-4756.

(93) Kakuta, Y., Sueyoshi, T., Negishi, M., and Pedersen, L. C. (1999) Crystal Structure of the Sulfotransferase Domain of Human Heparan Sulfate N-Deacetylase/ N-Sulfotransferase 1. *J. Biol. Chem. 274*, 10673-10676.

(94) Kakuta, Y., Pedersen, L. G., Pedersen, L. C., and Negishi, M. (1998) Conserved structural motifs in the sulfotransferase family. *Trends Biochem. Sci. 23*, 129-130.

(95) Tatsuya, S., Yoshimitsu, K., Lars, C. P., Frances, E. W., Lee, G. P., and Masahiko, N. (1998) A role of Lys614 in the sulfotransferase activity of human heparan sulfate N-deacetylase/N-sulfotransferase. *FEBS letters 433*, 211-214.

(96) Hagner-Mcwhirter, A., Lindahl, U, Li, J p. (2000) Biosynthesis of heparin/heparan sulphate: mechanism of epimerization of glucuronyl C-5. *Biochem. J. 347*, 69-75.

(97) Jacobsson, I., Lindahl, U., Jensen, J. W., Roden, L., Prihar, H., and Feingold, D. S. (1984) Biosynthesis of heparin. Substrate specificity of heparosan N-sulfate D- glucuronosyl 5-epimerase. *J. Biol. Chem. 259*, 1056-1063.

(98) Hagner-McWhirter, A., Li, J.-P., Oscarson, S., and Lindahl, U. (2004) Irreversible Glucuronyl C5-epimerization in the Biosynthesis of Heparan Sulfate. *J. Biol. Chem. 279*, 14631-14638.

(99) Pinhal, M. A. S., Smith, B., Olson, S., Aikawa, J.-i., Kimata, K., and Esko, J. D. (2001) Enzyme interactions in heparan sulfate biosynthesis: Uronosyl 5-epimerase and 2-O-sulfotransferase interact in vivo. *Proc. Natl. Acad. Sci. 98*, 12984-12989.

(100) Feyerabend, T. B., Li, J.-P., Lindahl, U., and Rodewald, H.-R. (2006) Heparan sulfate C5-epimerase is essential for heparin biosynthesis in mast cells. *Nat. Chem. Biol. 2*, 195-196.

(101) Kreuger, J., Salmivirta, M., Sturiale, L., Gimenez-Gallego, G., and Lindahl, U. (2001) Sequence Analysis of Heparan Sulfate Epitopes with Graded Affinities for Fibroblast Growth Factors 1 and 2. *J. Biol. Chem. 276*, 30744-30752.

(102) Turnbull, J. E., Fernig, D. G., Ke, Y., Wilkinson, M. C., and Gallagher, J. T. (1992) Identification of the basic fibroblast growth factor binding sequence in fibroblast heparan sulfate. *J. Biol. Chem. 267*, 10337-10341.

(103) Bullock, S. L., Fletcher, J. M., Beddington, R. S. P., and Wilson, V. A. (1998) Renal agenesis in mice homozygous for a gene trap mutation in the gene encoding heparan sulfate 2-sulfotransferase. *Genes Dev. 12*, 1894-1906.

(104) Kinnunen, T., Huang, Z., Townsend, J., Gatdula, M. M., Brown, J. R., Esko, J. D., and Turnbull, J. E. (2005) Heparan 2-O-sulfotransferase, hst-2, is essential for normal cell migration in Caenorhabditis elegans. *Proc. Natl. Acad. Sci. 102*, 1507-1512.

(105) Bülow, H. E., and Hobert, O. (2004) Differential Sulfations and Epimerization Define Heparan Sulfate Specificity in Nervous System Development. *Neuron 41*, 723-736.

(106) Kobayashi, T., Habuchi, H., Tamura, K., Ide, H., and Kimata, K. (2007) Essential Role of Heparan Sulfate 2-O-Sulfotransferase in Chick Limb Bud Patterning and Development. *J. Biol. Chem. 282*, 19589-19597.

(107) Habuchi, H., Tanaka, M., Habuchi, O., Yoshida, K., Suzuki, H., Ban, K., and Kimata, K. (2000) The Occurrence of Three Isoforms of Heparan Sulfate 6-O-Sulfotransferase Having Different Specificities for Hexuronic Acid Adjacent to the Targeted N-Sulfoglucosamine. *J. Biol. Chem. 275*, 2859-2868.

(108) Habuchi H, M. G., Nogami K, Kuroiwa A, Matsuda Y, Kusche-Gullberg M, Habuchi O, Tanaka M, Kimata K. (2003) Biosynthesis of heparan sulphate with diverse structures and functions: two alternatively spliced forms of human heparan sulphate 6-O-sulphotransferase-2 having different expression patterns and properties. *Biochem J. 371*, 131.

(109) Smeds, E., Habuchi, H., Do, A.-T., Hjertson, E., Grundberg, H., Kimata, K., Lindahl, U., and Kusche-Gullberg, M. (2003) Substrate specificities of mouse heparan sulphate glucosaminyl 6-O-sulphotransferases. *Biochem. J. 372*, 371-380.

(110) Nogami, K., Suzuki, H., Habuchi, H., Ishiguro, N., Iwata, H., and Kimata, K. (2004) Distinctive Expression Patterns of Heparan Sulfate O-Sulfotransferases and Regional Differences in Heparan Sulfate Structure in Chick Limb Buds. *J. Biol. Chem. 279*, 8219-8229.

(111) Jeff Sedita, K. I. W. V. C. (2004) Differential expression of heparan sulfate 6-O-sulfotransferase isoforms in the mouse embryo suggests distinctive roles during organogenesis. *Dev. Dynamics 231*, 782-794.

(112) Habuchi, H., Nagai, N., Sugaya, N., Atsumi, F., Stevens, R. L., and Kimata, K. (2007) Mice Deficient in Heparan Sulfate 6-O-Sulfotransferase-1 Exhibit Defective Heparan Sulfate Biosynthesis, Abnormal Placentation, and Late Embryonic Lethality. *J. Biol. Chem. 282*, 15578-15588.

(113) Kamimura, K., Fujise, M., Villa, F., Izumi, S., Habuchi, H., Kimata, K., and Nakato, H. (2001) Drosophila Heparan Sulfate 6-O-Sulfotransferase (dHS6ST) Gene. Structure, Expression, And Function in the Formation of the Tracheal System. *J. Biol. Chem. 276*, 17014-17021.

(114) Bink, R. J., Habuchi, H., Lele, Z., Dolk, E., Joore, J., Rauch, G.-J., Geisler, R., Wilson, S. W., den Hertog, J., Kimata, K., and Zivkovic, D. (2003) Heparan Sulfate 6-O-Sulfotransferase Is Essential for Muscle Development in Zebrafish. *J. Biol. Chem. 278*, 31118-31127.

(115) Xia, G., Chen, J., Tiwari, V., Ju, W., Li, J.-P., Malmstrom, A., Shukla, D., and Liu, J. (2002) Heparan Sulfate 3-O-Sulfotransferase Isoform 5 Generates Both an Antithrombin-binding Site and an Entry Receptor for Herpes Simplex Virus, Type 1. *J. Biol. Chem. 277*, 37912-37919.

(116) Liu J, R. R. (2002) *Heparan sulfate D-glucosaminyl 3-O-sulfotransferase* Springer, Berlin Heidelberg New York.

(117) Xu D, T. V., Xia G, Clement C, Shukla D, Liu J. (2005) Characterization of heparan sulphate 3-O-sulphotransferase isoform 6 and its role in assisting the entry of herpes simplex virus type 1. *Biochem J 385*, 451.

(118) Shworak, N. W., Liu, J., Petros, L. M., Zhang, L., Kobayashi, M., Copeland, N. G., Jenkins, N. A., and Rosenberg, R. D. (1999) Multiple Isoforms of Heparan Sulfate D-Glucosaminyl 3-O-Sulfotransferase. Isolation, Characterization, and Expression of Human cDNAs and Identification of Distinct Genomic Loci. *J. Biol. Chem. 274*, 5170-5184.

(119) Liu, J., Shworak, N. W., Sinay, P., Schwartz, J. J., Zhang, L., Fritze, L. M. S., and Rosenberg, R. D. (1999) Expression of Heparan Sulfate D-Glucosaminyl 3-O-Sulfotransferase Isoforms Reveals Novel Substrate Specificities. *J. Biol. Chem. 274*, 5185-5192.

(120) Chen, J., Duncan, M. B., Carrick, K., Pope, R. M., and Liu, J. (2003) Biosynthesis of 3-O-sulfated heparan sulfate: unique substrate specificity of heparan sulfate 3-O-sulfotransferase isoform 5. *Glycobiology 13*, 785-794.

(121) Nagai, N., Habuchi, H., Kitazume, S., Toyoda, H., Hashimoto, Y., and Kimata, K. (2007) Regulation of Heparan Sulfate 6-O-Sulfation by beta-Secretase Activity. *J. Biol. Chem. 282*, 14942-14951.

(122) Edavettal, S. C., Lee, K. A., Negishi, M., Linhardt, R. J., Liu, J., and Pedersen, L. C. (2004) Crystal Structure and Mutational Analysis of Heparan Sulfate 3-O-Sulfotransferase Isoform 1. *J. Biol. Chem. 279*, 25789-25797.

(123) Dhoot, G. K., Gustafsson, M. K., Ai, X., Sun, W., Standiford, D. M., and Emerson, C. P., Jr. (2001) Regulation of Wnt Signaling and Embryo Patterning by an Extracellular Sulfatase. *Science 293*, 1663-1666.

(124) Morimoto-Tomita, M., Uchimura, K., Werb, Z., Hemmerich, S., and Rosen, S. D. (2002) Cloning and Characterization of Two Extracellular Heparin-degrading Endosulfatases in Mice and Humans. *J. Biol. Chem. 277*, 49175-49185.

(125) Hanson, S. R., Best, M. D., Wong, C. H. (2004) Sulfatases: Structure, Mechanism, Biological Activity, Inhibition, and Synthetic Utility. *Ange. Chemie. Internatl. Ed. 43*, 5736-5763.

(126) Dierks, T., Lecca, M. R., Schlotterhose, P., Schmidt, B., and von Figura, K. (1999) Sequence determinants directing conversion of cysteine to formylglycine in eukaryotic sulfatases. *The EMBO J. 18*, 2084–2091.

(127) Ai, X., Do, A.-T., Kusche-Gullberg, M., Lindahl, U., Lu, K., and Emerson, C. P., Jr. (2006) Substrate Specificity and Domain Functions of Extracellular Heparan Sulfate 6-O-Endosulfatases, QSulf1 and QSulf2. *J. Biol. Chem. 281*, 4969-4976.

(128) Nagamine, S., Koike, S., Keino-Masu, K., and Masu, M. (2005) Expression of a heparan sulfate remodeling enzyme, heparan sulfate 6-O-endosulfatase sulfatase FP2, in the rat nervous system. *Dev. Brain Res. 159*, 135-143.

(129) Ohto, T., Uchida, H., Yamazaki, H., Keino-Masu, K., Matsui, A., and Masu, M. (2002) Identification of a novel nonlysosomal sulphatase expressed in the floor plate, choroid plexus and cartilage. *Genes to Cells 7*, 173-185.

(130) Morimoto-Tomita, M., Uchimura, K., Bistrup, A., Lum, D. H., Egeblad, M., Boudreau, N., Werb, Z., and Rosen, S. D. (2005) Sulf-2, a Proangiogenic Heparan Sulfate Endosulfatase, Is Upregulated in Breast Cancer. *Neoplasia 7*, 1001-1010.

(131) Ambasta, R. K., Ai, X., and Emerson, C. P., Jr. (2007) Quail Sulf1 Function Requires Asparagine-linked Glycosylation. *J. Biol. Chem. 282*, 34492-34499.

(132) Ai, X., Do, A.-T., Lozynska, O., Kusche-Gullberg, M., Lindahl, U., and Emerson, C. P., Jr. (2003) QSulf1 remodels the 6-O sulfation states of cell surface heparan sulfate proteoglycans to promote Wnt signaling. *J. Cell. Biol. 162*, 341-351.

(133) Viviano, B. L., Paine-Saunders, S., Gasiunas, N., Gallagher, J., and Saunders, S. (2004) Domain-specific Modification of Heparan Sulfate by Qsulf1 Modulates the Binding of the Bone Morphogenetic Protein Antagonist Noggin. *J. Biol. Chem. 279*, 5604-5611.

(134) Saad, O. M., Ebel, H., Uchimura, K., Rosen, S. D., Bertozzi, C. R., and Leary, J. A. (2005) Compositional profiling of heparin/heparan sulfate using mass spectrometry: assay for specificity of a novel extracellular human endosulfatase. *Glycobiology 15*, 818-826.

(135) Lamanna, W. C., Baldwin, R. J., Padva, M., Kalus, I., tenÂ dam, G., vanÂ kuppevelt, T. H., Gallagher, J. T., vonÂ figura, K., Dierks, T., and Merry, C. L. R. (2006) Heparan sulfate 6-O-endosulfatases: discrete in vivo activities and functional co-operativity. *Biochem. J. 400*, 63-73.

(136) Dai, Y., Yang, Y., MacLeod, V., Yue, X., Rapraeger, A. C., Shriver, Z., Venkataraman, G., Sasisekharan, R., and Sanderson, R. D. (2005) HSulf-1 and HSulf-2 Are Potent Inhibitors of Myeloma Tumor Growth in Vivo. *J. Biol. Chem. 280*, 40066-40073.

(137) Lamanna, W. C., Frese, M.-A., Balleininger, M., and Dierks, T. (2008) Sulf loss influences N-, 2O-, and 6O-sulfation of multiple heparan sulfate proteoglycans and modulates FGF signaling. *J. Biol. Chem.*, M802130200.

(138) Lamanna, W. C., Kalus, I., Padva, M., Baldwin, R. J., Merry, C. L. R., and Dierks, T. (2007) The heparanome--The enigma of encoding and decoding heparan sulfate sulfation. *J. Biotech. 129*, 290-307.

(139) Nawroth, R., van Zante, A., Cervantes, S., McManus, M., Hebrok, M., and Rosen, S. D. (2007) Extracellular Sulfatases, Elements of the Wnt Signaling Pathway, Positively Regulate Growth and Tumorigenicity of Human Pancreatic Cancer Cells. *PLoS ONE 2*, 392.

(140) Wang, S., Ai, X., Freeman, S. D., Pownall, M. E., Lu, Q., Kessler, D. S., and Emerson, C. P. (2004) QSulf1, a heparan sulfate 6-O-endosulfatase, inhibits fibroblast growth factor signaling in mesoderm induction and angiogenesis. *Proc. Natl. Acad. Sci. 101*, 4833-4838.

(141) Uchimura, K., Morimoto-Tomita, M., Bistrup, A., Li, J., Lyon, M., Gallagher, J., Werb, Z., and Rosen, S. (2006) HSulf-2, an extracellular endoglucosamine-6-sulfatase, selectively mobilizes heparin-bound growth factors and chemokines: effects on VEGF, FGF-1, and SDF-1. *BMC Biochem. 7*, 2.

(142) Otsuki, S., Taniguchi, N., Grogan, S., D'Lima, D., Kinoshita, M., and Lotz, M. (2008) Expression of novel extracellular sulfatases Sulf-1 and Sulf-2 in normal and osteoarthritic articular cartilage. *Arthritis Res. Therapy 10*, R61.

(143) Yue, X., Li, X., Nguyen, H. T., Chin, D. R., Sullivan, D. E., and Lasky, J. A. (2008) TGF-beta 1 induces heparan sulfate 6-O-endosulfatase 1 expression in vitro and in vivo. *J. Biol. Chem.*, M802850200.

(144) Langsdorf, A., Do, A.-T., Kusche-Gullberg, M., Emerson Jr, C. P., and Ai, X. (2007) Sulfs are regulators of growth factor signaling for satellite cell differentiation and muscle regeneration. *Dev. Biol. 311*, 464-477.

(145) Zhao, W., Allen, S., and Dhoot, G. K. (2007) FGF mediated Sulf1 regulation. *FEBS Letters 581*, 4960-4964.

(146) Wanfeng Zhao, G. B. S.-N. G. K. D. (2006) Sulf1 expression pattern and its role in cartilage and joint development. *Dev. Dynamics 235*, 3327-3335.

(147) Yoshihiko, K. (2004) A sulfatase regulating the migratory potency of oligodendrocyte progenitor cells through tyrosine phosphorylation of beta-catenin. *J. Neurosci. Res. 77*, 653-661.

(148) Ratzka, A., Kalus, I., Moser, M., Dierks, T., Mundlos, S., Vortkamp, A. (2008) Redundant function of the heparan sulfate 6-O-endosulfatases Sulf1 and Sulf2 during skeletal development. *Dev. Dynamics 237*, 339-353.

(149) Ai, X., Kitazawa, T., Do, A.-T., Kusche-Gullberg, M., Labosky, P. A., and Emerson, C. P., Jr. (2007) SULF1 and SULF2 regulate heparan sulfate-mediated GDNF signaling for esophageal innervation. *Development 134*, 3327-3338.

(150) Lum, D. H., Tan, J., Rosen, S. D., and Werb, Z. (2007) Gene Trap Disruption of the Mouse Heparan Sulfate 6-O-Endosulfatase Gene, Sulf2. *Mol. Cell. Biol. 27*, 678-688.

(151) Lai, J., Chien, J., Staub, J., Avula, R., Greene, E. L., Matthews, T. A., Smith, D. I., Kaufmann, S. H., Roberts, L. R., and Shridhar, V. (2003) Loss of HSulf-1 Up-regulates Heparin-binding Growth Factor Signaling in Cancer. *J. Biol. Chem. 278*, 23107-23117.

(152) Lai, J.-P., Chien, J., Strome, S. E., Staub, J., Montoya, D. P., Greene, E. L., Smith, D. I., Roberts, L. R., and Shridhar, V. (2004) HSulf-1 modulates HGF-mediated tumor cell invasion and signaling in head and neck squamous carcinoma. *Oncogene 23*, 1439-1447.

(153) Narita, K., Staub, J., Chien, J., Meyer, K., Bauer, M., Friedl, A., Ramakrishnan, S., and Shridhar, V. (2006) HSulf-1 Inhibits Angiogenesis and Tumorigenesis In vivo. *Cancer Res. 66*, 6025-6032.

(154) Morimoto-Tomita M, U. K., and Rosen SD. (2003) Novel extracellular sulfatases: potential roles in cancer. *Trends Glycosci.Glycotech. 15*, 159 – 164.

(155) Morimoto-Tomita M, U. K., Bistrup A, Lum DH, Egeblad M, Boudreau N, Werb Z, Rosen SD. (2005) Sulf-2, a proangiogenic heparan sulfate endosulfatase, is upregulated in breast cancer. *Neoplasia 11*, 1001-1010.

(156) Lai, J.-P., Yu, C., Moser, C. D., Aderca, I., Han, T., Garvey, T. D., Murphy, L. M., Garrity-Park, M. M., Shridhar, V., Adjei, A. A., and Roberts, L. R. (2006) SULF1 Inhibits Tumor Growth and Potentiates the Effects of Histone Deacetylase Inhibitors in Hepatocellular Carcinoma. *Gastroenterology 130*, 2130-2144.

(157) Lai, J.-P. et. al. (2008) Sulfatase 2 up-regulates glypican 3, promotes fibroblast growth factor signaling, and decreases survival in hepatocellular carcinoma. *Hepatology 47*, 1211-1222.

(158) Grigoriadis, A., Mackay, A., Reis-Filho, J., Steele, D., Iseli, C., Stevenson, B., Jongeneel, C. V., Valgeirsson, H., Fenwick, K., Iravani, M., Leao, M., Simpson, A., Strausberg, R., Jat, P., Ashworth, A., Neville, A. M., and O'Hare, M. (2006) Establishment of the epithelial-specific transcriptome of normal and malignant human breast cells based on MPSS and array expression data. *Breast Cancer Res. 8*, R56.

(159) Iacobuzio-Donahue, C. A., Maitra, A., Olsen, M., Lowe, A. W., Van Heek, N. T., Rosty, C., Walter, K., Sato, N., Parker, A., Ashfaq, R., Jaffee, E., Ryu, B., Jones, J., Eshleman, J. R., Yeo, C. J., Cameron, J. L., Kern, S. E., Hruban, R. H., Brown, P. O., and Goggins, M. (2003) Exploration of Global Gene Expression Patterns in Pancreatic Adenocarcinoma Using cDNA Microarrays. *Am. J. Pathol. 162*, 1151-1162.

(160) Lai, J.-p., Chien, J. R., Moser, D. R., Staub, J. K., Aderca, I., Montoya, D. P., Matthews, T. A., Nagorney, D. M., Cunningham, J. M., Smith, D. I., Greene, E. L., Shridhar, V., and Roberts, L. R. (2004) hSulf1 sulfatase promotes apoptosis of hepatocellular cancer cells by decreasing heparin-binding growth factor signaling. *Gastroenterology 126*, 231-248.

(161) Li, J., Kleeff, J., Abiatari, I., Kayed, H., Giese, N., Felix, K., Giese, T., Buchler, M., and Friess, H. (2005) Enhanced levels of Hsulf-1 interfere with heparin-binding growth factor signaling in pancreatic cancer. *Mol. Cancer 4*, 14.

(162) Bhattacharjee, A., Richards, W. G., Staunton, J., Li, C., Monti, S., Vasa, P., Ladd, C., Beheshti, J., Bueno, R., Gillette, M., Loda, M., Weber, G., Mark, E. J., Lander, E. S., Wong, W., Johnson, B. E., Golub, T. R., Sugarbaker, D. J., and Meyerson, M. (2001) Classification of human lung carcinomas by mRNA expression profiling reveals distinct adenocarcinoma subclasses. *Proc. Natl. Acad. Sci. 98*, 13790-13795.

(163) Narita, K., Chien, J., Mullany, S. A., Staub, J., Qian, X., Lingle, W. L., and Shridhar, V. (2007) Loss of HSulf-1 Expression Enhances Autocrine Signaling Mediated by Amphiregulin in Breast Cancer. *J. Biol. Chem. 282*, 14413-14420.

(164) Staub, J., Chien, J., Pan, Y., Qian, X., Narita, K., Aletti, G., Scheerer, M., Roberts, L. R., Molina, J., and Shridhar, V. (2007) Epigenetic silencing of HSulf-1 in ovarian cancer:implications in chemoresistance. *Oncogene 26*, 4969-4978.

(165) Miyamoto, K., Asada, K., Fukutomi, T., Okochi, E., Yagi, Y., Hasegawa, T., Asahara, T., Sugimura, T., and Ushijima, T. Methylation-associated silencing of heparan sulfate D-glucosaminyl 3-O-sulfotransferase-2 (3-OST-2) in human breast, colon, lung and pancreatic cancers. *Oncogene 22*, 274-280.

(166) Vlodavsky, I., Friedmann, Y., Elkin, M., Aingorn, H., Atzmon, R., Ishai-Michaeli, R., Bitan, M., Pappo, O., Peretz, T., Michal, I., Spector, L., and Pecker, I. (1999) Mammalian heparanase: Gene cloning, expression and function in tumor progression and metastasis. *Nat. Med. 5*, 793-802.

(167) Hulett, M. D., Freeman, C., Hamdorf, B. J., Baker, R. T., Harris, M. J., and Parish, C. R. (1999) Cloning of mammalian heparanase, an important enzyme in tumor invasion and metastasis. *Nat. Med. 5*, 803-809.

(168) Parish, C. R., Freeman, C., and Hulett, M. D. (2001) Heparanase: a key enzyme involved in cell invasion. *Biochimica et Biophysica Acta (BBA) - Rev. Cancer 1471*, M99-M108.

(169) Vlodavsky I Fau - Eldor, A., Eldor A Fau - Haimovitz-Friedman, A., Haimovitz-Friedman A Fau - Matzner, Y., Matzner Y Fau - Ishai-Michaeli, R., Ishai-Michaeli R Fau - Lider, O., Lider O Fau - Naparstek, Y., Naparstek Y Fau - Cohen, I. R., Cohen Ir Fau - Fuks, Z., and Fuks, Z. Expression of heparanase by platelets and circulating cells of the immune system: possible involvement in diapedesis and extravasation. (1992) Invasion Met. 12, 112-127.

(170) Levy-Adam, F., Miao, H.-Q., Heinrikson, R. L., Vlodavsky, I., and Ilan, N. (2003) Heterodimer formation is essential for heparanase enzymatic activity. *Biochem. Biophy. Res. Com. 308*, 885-891.

(171) McKenzie, E., Young, K., Hircock, M., Bennett, J., Bhaman, M., Felix, R., Turner, P., Stamps, A., McMillan, D., Saville, G., Ng, S., Mason, S., Snell, D., Schofield, D., Gong, H., Townsend, R., Gallagher, J., Page, M., Parekh, R., and Stubberfield, C. (2003) Biochemical characterization of the active heterodimer form of human heparanase (Hpa1) protein expressed in insect cells. *Biochem. J. 373*, 423-435.

(172) Pikas, D. S., Li, J.-p., Vlodavsky, I., and Lindahl, U. (1998) Substrate Specificity of Heparanases from Human Hepatoma and Platelets. *J. Biol. Chem. 273*, 18770-18777.

(173) Quiros, R. M., Rao, G., Plate, J., Harris, J. E., Brunn, G. J., Platt, J. L., Gattuso, P., Prinz, R. A., and Xu, X. (2006) Elevated serum heparanase-1 levels in patients with pancreatic carcinoma are associated with poor survival. *Cancer 106*, 532-540.

(174) Vlodavsky, I. a. F., Y. (2001) Molecular properties and involvement of heparanase in cancer metastasis and angiogenesis. *J. Clin. Invest. 108*, 341-347.

(175) Joyce, J. A., Freeman, C., Meyer-Morse, N., Parish, C. R., and Hanahan, D. (2005) A functional heparan sulfate mimetic implicates both heparanase and heparan sulfate in tumor angiogenesis and invasion in a mouse model of multistage cancer. *Oncogene 24*, 4037-4051.

(176) Chow, L., Gustafson, D., O'Bryant, C., Gore, L., Basche, M., Holden, S., Morrow, M., Grolnic, S., Creese, B., Roberts, K., Davis, K., Addison, R., and Eckhardt, S. (2008) A phase I pharmacological and biological study of PI-88 and docetaxel in patients with advanced malignancies. *Cancer Chemo. Pharm. 63*, 65-74.

(177) Liu, J., and Thorp, S. C. (2002) Cell surface heparan sulfate and its roles in assisting viral infections. *Med. Res. Rev. 22*, 1-25.

(178) Desai, U. R., Wang, H. M., and Linhardt, R. J. (1993) Substrate Specificity of the Heparin Lyases from Flavobacterium heparinum. *Arch. Biochem. Biophysics 306*, 461-468.

(179) Shively, J. E., and Conrad, H. E. (1976) Formation of anhydrosugars in the chemical depolymerization of heparin. *Biochemistry 15*, 3932-3942.

(180) Shaklee, P. N., and Conrad, H. E. (1984) Hydrazinolysis of heparin and other glycosaminoglycans. *Biochem J. 217*, 187-97.

(181) Merry, C. L. R., Lyon, M., Deakin, J. A., Hopwood, J. J., and Gallagher, J. T. (1999) Highly Sensitive Sequencing of the Sulfated Domains of Heparan Sulfate. *J. Biol. Chem. 274*, 18455-18462.

(182) Liu, J., Desai, U. R., Han, X.-J., Toida, T., and Linhardt, R. J. (1995) Strategy for the sequence analysis of heparin. *Glycobiology 5*, 765-774.

(183) Rhomberg, A. J., Ernst, S., Sasisekharan, R., and Biemann, K. (1998) Mass spectrometric and capillary electrophoretic investigation of the enzymatic degradation of heparin-like glycosaminoglycans. *Proc. Natl. Acad. Sci. 95*, 4176-4181.

(184) Pope, R. M., Raska, C. S., Thorp, S. C., and Liu, J. (2001) Analysis of heparan sulfate oligosaccharides by nano-electrospray ionization mass spectrometry. *Glycobiology 11*, 505-513.

(185) Juhasz, P., Biemann, K. (1995) Utility of non-covalent complexes in the matrix-assisted laser desorption ionization mass spectrometry of heparin-derived oligosaccharides. *Carb. Res. 270*, 131-147.

(186) Venkataraman, G., Shriver, Z., Raman, R., and Sasisekharan, R. (1999) Sequencing Complex Polysaccharides. *Science 286*, 537-542.

(187) Jin, L., Abrahams, J. P., Skinner, R., Petitou, M., Pike, R. N., and Carrell, R. W. (1997) The anticoagulant activation of antithrombin by heparin. *Proc. Natl. Acad. Sci. 94*, 14683-14688.

(188) Li, W., Johnson, D. J. D., Esmon, C. T., and Huntington, J. A. (2004) Structure of the antithrombin-thrombin-heparin ternary complex reveals the antithrombotic mechanism of heparin. *Nat. Struct. Mol. Biol. 11*, 857-862.

(189) Huntington, J. A., McCoy, A., Belzar, K. J., Pei, X. Y., Gettins, P. G. W., and Carrell, R. W. (2000) The Conformational Activation of Antithrombin. A 2.85-A Structure of a Fluorescein Derivative Reveals an Electrostatic Link Between the Hinge and Heparin Binding Regions. *J. Biol. Chem. 275*, 15377-15383.

(190) Desai, U. R., Petitou, M., Bjork, I., and Olson, S. T. (1998) Mechanism of Heparin Activation of Antithrombin: Evidence for an Induced-Fit Model of Allosteric Activation Involving Two Interaction Subsites. *Biochemistry 37*, 13033-13041.

(191) Atha, D. H., Lormeau, J. C., Petitou, M., Rosenberg, R. D., and Choay, J. (1985) Contribution of monosaccharide residues in heparin binding to antithrombin III. *Biochemistry 24*, 6723-6729.

(192) Zhang, L., Lawrence, R., Schwartz, J. J., Bai, X., Wei, G., Esko, J. D., and Rosenberg, R. D. (2001) The Effect of Precursor Structures on the Action of Glucosaminyl 3-O-Sulfotransferase-1 and the Biosynthesis of Anticoagulant Heparan Sulfate. *J. Biol. Chem. 276*, 28806-28813.

(193) Chen, J., Jones, C. L., and Liu, J. (2007) Using an Enzymatic Combinatorial Approach to Identify Anticoagulant Heparan Sulfate Structures. *Chem. Biol. 14*, 986-993.

(194) Oosta, G. M., Gardner, W. T., Beeler, D. L., and Rosenberg, R. D. (1981) Multiple functional domains of the heparin molecule. *Proc. Natl. Acad. Sci. 78*, 829-833.

(195) Becker, R. C. (2004) Optimizing Heparin Compounds: A Working Construct for Future Antithrombotic Drug Development. *J. Thrombosis and Thrombolysis 18*, 55-58.

(196) Stringer, S. E., and Gallagher, J. T. (1997) Specific Binding of the Chemokine Platelet Factor 4 to Heparan Sulfate. *J. Biol. Chem. 272*, 20508-20514.

(197) Fiore, M. M., and Kakkar, V. V. (2003) Platelet factor 4 neutralizes heparan sulfate-enhanced antithrombin inactivation of factor Xa by preventing interaction(s) of enzyme with polysaccharide. *Biochem. Biophy. Res. Com. 311*, 71-76.

(198) McKeehan, W. L., Wang, F., and Kan, M. (1998) The heparan sulfate-fibroblast growth factor family: diversity of structure and function. *Prog. Nucleic Acid Res. Mol. Biol. 59*, 135-76.

(199) Powers, C. J., McLeskey, S. W., and Wellstein, A. (2000) Fibroblast growth factors, their receptors and signaling. *Endocr. Relat. Cancer 7*, 165-197.

(200) Ornitz, D. M., and Marie, P. J. (2002) FGF signaling pathways in endochondral and intramembranous bone development and human genetic disease. *Genes Dev. 16*, 1446-1465.

(201) Yayon, A., Klagsbrun, M., Esko, J. D., Leder, P., and Ornitz, D. M. (1991) Cell surface, heparin-like molecules are required for binding of basic fibroblast growth factor to its high affinity receptor. *Cell 64*, 841-848.

(202) Rapraeger, A. C., Krufka, A., and Olwin, B.B. (1991) Requirement of heparan sulfate for bFGF-mediated fibroblast growth and myoblast differentiation. *Science 252*, 1705–1708.

(203) Inatani, M., Irie, F., Plump, A. S., Tessier-Lavigne, M., and Yamaguchi, Y. (2003) Mammalian Brain Morphogenesis and Midline Axon Guidance Require Heparan Sulfate. *Science 302*, 1044-1046.

(204) Lin X., B. E. M., Perrimon N., Michelson A.M. (1999) Heparan sulfate proteoglycans are essential for FGF receptor signaling during Drosophila embryonic development. *Development 126*, 3715-3723.

(205) Guerrini, M., Agulles, T., Bisio, A., Hricovini, M., Lay, L., Naggi, A., Poletti, L., Sturiale, L., Torri, G., and Casu, B. (2002) Minimal Heparin/Heparan Sulfate Sequences for Binding to Fibroblast Growth Factor-1. *Biochem. Biophy.Res.Com. 292*, 222-230.

(206) Mohammadi, M., Olsen, S. K., and Ibrahimi, O. A. (2005) Structural basis for fibroblast growth factor receptor activation. *Cytokine & Growth Factor Rev. 16*, 107-137.

(207) Pellegrini, L., Burke, D. F., von Delft, F., Mulloy, B., and Blundell, T. L. (2000) Crystal structure of fibroblast growth factor receptor ectodomain bound to ligand and heparin. *Nature 407*, 1029-1034.

(208) Schlessinger, J., Plotnikov, A. N., Ibrahimi, O. A., Eliseenkova, A. V., Yeh, B. K., Yayon, A., Linhardt, R. J., and Mohammadi, M. (2000) Crystal Structure of a Ternary FGF-FGFR-Heparin Complex Reveals a Dual Role for Heparin in FGFR Binding and Dimerization. *Mol. Cell 6*, 743-750.

(209) Bjornsson, S. (1993) Simultaneous Preparation and Quantitation of Proteoglycans by Precipitation with Alcian Blue. *Anal. Biochem. 210*, 282-291.

(210) Shukla, D., Liu, J., Blaiklock, P., Shworak, N. W., Bai, X., Esko, J. D., Cohen, G. H., Eisenberg, R. J., Rosenberg, R. D., and Spear, P. G. (1999) A Novel Role for 3-O-Sulfated Heparan Sulfate in Herpes Simplex Virus 1 Entry. *Cell 99*, 13-22.

(211) Lee, M. K., and Lander, A. D. (1991) Analysis of affinity and structural selectivity in the binding of proteins to glycosaminoglycans: development of a sensitive electrophoretic approach. *Proc. Natl. Acad. Sci. 88*, 2768-2772.

(212) Zhang, L., Yoshida, K., Liu, J., and Rosenberg, R. D. (1999) Anticoagulant Heparan Sulfate Precursor Structures in F9 Embryonal Carcinoma Cells. *J. Biol. Chem. 274*, 5681-5691.

(213) Moon, A. F., Edavettal, S. C., Krahn, J. M., Munoz, E. M., Negishi, M., Linhardt, R. J., Liu, J., and Pedersen, L. C. (2004) Structural Analysis of the Sulfotransferase (3-O-Sulfotransferase Isoform 3) Involved in the Biosynthesis of an Entry Receptor for Herpes Simplex Virus 1. *J. Biol. Chem. 279*, 45185-45193.

(214) Hernaiz, M., Liu, J., Rosenberg, R. D., and Linhardt, R. J. (2000) Enzymatic Modification of Heparan Sulfate on a Biochip Promotes Its Interaction with Antithrombin III. *Biochem. Biophy. Res. Com. 276*, 292-297.

(215) Atha, D. H., Stephens, A. W., and Rosenberg, R. D. (1984) Evaluation of critical groups required for the binding of heparin to antithrombin. *Proc. Natl. Acad. Sci. 81*, 1030-1034.

(216) Wu, Z. L., Zhang, L., Beeler, D. L., Kuberan, B., and Rosenberg, R. D. (2002) A new strategy for defining critical functional groups on heparan sulfate. *FASEB J. 16*, 539-545.

(217) Desai, U. R., Petitou, M., Bjork, I., and Olson, S. T. (1998) Mechanism of Heparin Activation of Antithrombin. Role of Individual Residues of the Pentasaccharide Activating Sequence in the Recognition of Native abd Activated States of Antithrombin. *J. Biol. Chem. 273*, 7478-7487.

(218) Atha, D. H., Lormeau, J. C., Petitou, M., Rosenberg, R. D., and Choay, J. (1987) Contribution of 3-O- and 6-O-sulfated glucosamine residues in the heparin-induced conformational change in antithrombin III. *Biochemistry 26*, 6454-6461.

(219) Jacobsson, I., and Lindahl, U. (1980) Biosynthesis of heparin. Concerted action of late polymer-modification reactions. *J. Biol. Chem. 255*, 5094-5100.

(220) Myette, J. R., Shriver, Z., Claycamp, C., McLean, M. W., Venkataraman, G., and Sasisekharan, R. (2003) The Heparin/Heparan Sulfate 2-O-Sulfatase from Flavobacterium heparinum. Molecular Cloning, Recombinant Expression, and Biochemical Characterization. *J. Biol. Chem. 278*, 12157-12166.